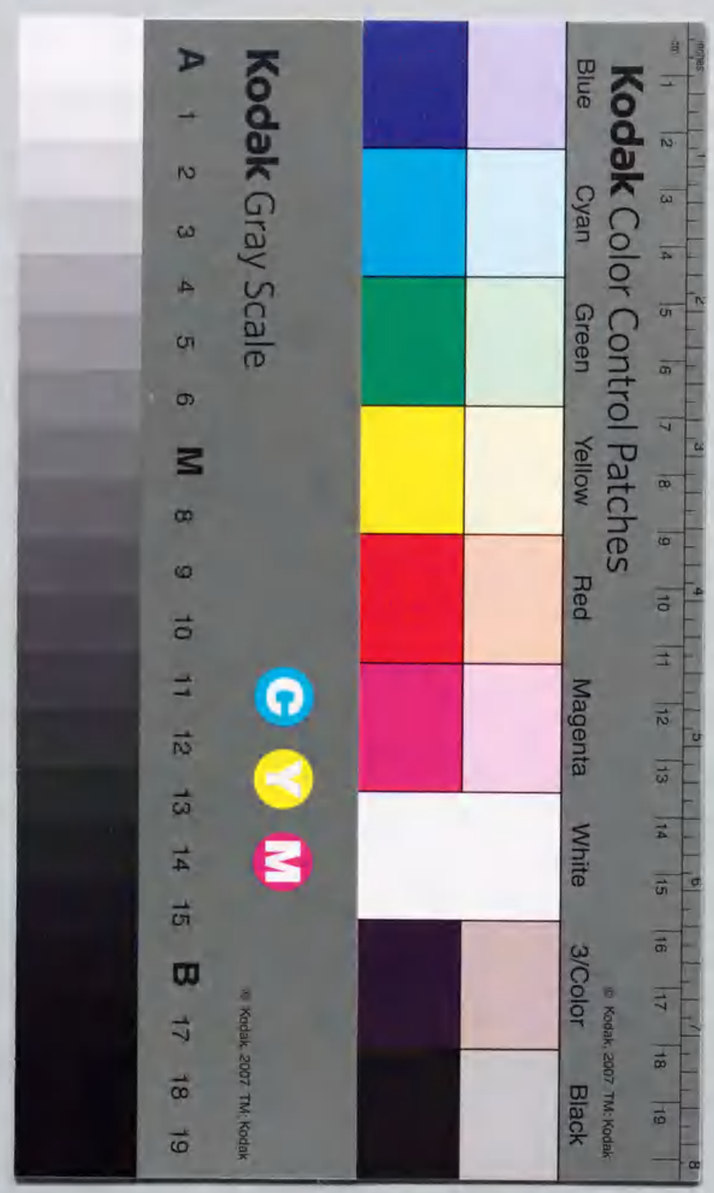

ゼブラフィッシュ中枢神経系における前後・背腹軸に沿った領域特異性の獲得機構

Analysis of regional specification along the anteroposterior and dorsoventral axes in zebrafish central nervous system

新屋みのり

Minori Shinya

名古屋大学大学院理学研究科
生命理学専攻

2001年2月

ゼブラフィッシュ中枢神経系における
前後・背腹軸に沿った領域特異性の獲得機構

Analysis of regional specification along the anteroposterior and dorsoventral axes in zebrafish central nervous system

新屋みのり

Minori Shinya

名古屋大学大学院理学研究科

生命理学専攻

2001 年 2 月

Contents

Summary

The central nervous system in vertebrates is patterned in early developmental stages. According to a classical model, the axial mesoderm is a major player in the patterning the neuroectoderm along both anteroposterior and dorsoventral axes. In this thesis, using zebrafish mutants and transplantation techniques, I addressed the following three important questions in neural development. First, how and when floor-plate cells, which are present in the most ventral part of the neural tube, are specified. Second, what the function of the prechordal plate (axial mesoderm in head region) is in head formation. Finally, what factor(s) are responsible for patterning the telencephalon. In these studies, I show that the initial induction of the floor-plate precursor cells occurs in the organizer region, before the fates of axial mesoderm and neural cells are separated, and, then, the floor-plate precursors colonize into the ventral part of the neural tube. The functional analysis of zebrafish *dickkopf-1* gene reveals that the prechordal plate functions to maintain the anterior forebrain. Furthermore, I show that in addition to Shh secreted from the prechordal plate and/or ventral diencephalon, Fgfs expressed in the anterior neural boundary is required for the development of the ventral telencephalon. These findings demonstrate that patterning of the neuroectoderm in vertebrates consists of multi-step inductive events in which early organizer, axial mesoderm (notochord and prechordal mesoderm) and the anterior edge of the neural plate function as a source of inducing factors.

General introduction

The central nervous system (CNS) which is a tube-shaped organ on the dorsal side of the body in vertebrates, can be partitioned into the several domains along the anteroposterior (AP) and dorsoventral (DV) axes. Along the AP axis, forebrain, midbrain, hindbrain, and spinal cord are lined, and the forebrain is further subdivided into the telencephalon and diencephalon. Along the DV axis, the CNS is roughly divided into four domains:, from the ventral, the floor plate, basal plate, alar plate and roof plate.

The CNS arises from the neural plate, a cytologically homogeneous sheet of epithelial cells that forms the dorsal surface of the gastrula embryo. The neural plate subsequently rolls up on its AP axis to form the tube, and then, the specific domains can be recognized from their morphology. Development of the CNS represents a multi-step process that involves: first, induction of the neural plate; second, patterning or regionalization of the neural tissue along the two axes; third, differentiation of neuron subpopulations along the newly formed patterns, and, fourth, extension of axons to correct targets. Neurons have been suggested to extend the axons depending on the boundary of regional specific gene expressions (Macdonald et al., 1994). Thus, regional specification at early stages would be a fundamental event for later development and function.

The mechanisms for neural patterning have long been studied well as one of the basic questions in the field of developmental biology. These studies have shown that regional specification of the neural tissue starts at as early as gastrulation stage and that the underlying axial mesoderm plays an important role in this process. For example, the Spemann organizer, which gives rise to the axial mesoderm, has been shown to be responsible for induction and AP patterning of the neural during the development of amphibians (Spemann, 1938). Further transplantation studies have proposed a two-signal model to account for induction of different type of neural tissues by the organizer (Toivonen and Saxon, 1968; Nieuwkoop, 1985). According to the model, the first signal, referred to as the activator, initiates neural development, inducing neural tissue of an anterior type, and the second signal, the transformer converts the neural tissue induced by the first signal

into progressively more posterior types of neural tissue. The axial mesoderm is also thought to be crucial in the DV patterning of the CNS. *In vitro* and *in vivo* tissue-grafting assays in chick and rat embryos have shown that the notochord, axial mesoderm in the trunk derived from the organizer, is a source of two inductive signals: a local signal that induces floor-plate differentiation in midline neural plate cells and a longer-range signal that induces motor neurons in the basal plate (Hirano et al., 1991; Yamada et al., 1991; Placzek et al., 1991, 1993). Sonic hedgehog (Shh), one of the Hedgehog-related proteins, secreted from the axial mesoderm is found to be a major responsive molecule for both short- and long-range induction (Marti *et al.*, 1995; Roelink *et al.*, 1995). The function of the axial mesoderm and Shh in the DV patterning has been further supported by the analysis of mutant mice and zebrafish (Hatta et al., 1991; Ang and Rossant, 1994; Weinstein et al., 1994). Thus, until recently, the organizer and its derivative, the axial mesoderm, were thought to be only source of patterning activities in neural development.

However, recent studies reveal that various other tissues function as an organizing center for each region. For example, the cells in the anterior neural boundary (ANB) located in the anterior neural and non-neural border (Shimamura and Rubenstein, 1997; Houart et al., 1998), midbrain-hindbrain boundary (MHB) (reviewed in Joyner, 1996), non-axial mesoderm in gastrula embryos (Woo and Fraser, 1997; Koshida et al., 1998), and the anterior visceral endoderm (AVE), an extraembryonic tissue, in mouse pre-gastrula embryos (Thomas and Beddington, 1996). These tissues exhibit various abilities to pattern the nearby neural tissues at different stages, from pregastrula to segmentation stages.

Catala et al. (1996), by fate-mapping experiments in chicken embryos, demonstrated that the floor plate derives from the Hensen's node (Spemann organizer in chick) and shares common precursors with the notochord, raising a question as to when and how those precursors are induced. Based on the fate map, it is possible that induction of floor-plate precursors could occur within the organizer region at much earlier stages than expected. This contrasted the previous notion that the floor plate is induced from the neural ectoderm by the notochord when the neural tube is underlined by the notochord (reviewed in Tanabe and Jessell, 1996).

When I started the experiments, many questions remained unanswered. Although BMP antagonists, Chordin and Noggin, were found to be major neural inducers expressed in Spemann organizer (reviewed in Hemmati-Brivanlou and Melton, 1997), molecular mechanisms for patterning activities of various organizing tissues were largely unknown. To address these questions, I used zebrafish as a model system, in which genetic and embryological analyses can be applied. The thesis consists of three chapters. In the first chapter, I examined when and how the floor-plate precursors are specified, using *one-eyed pinhead* (*oep*) mutants which are devoid of floor-plate cells (Brand *et al.*, 1996; Hammerschmidt *et al.*, 1996; Schier *et al.*, 1996, 1997; Strähle et al., 1998). The experiments reveal that Oep is cell-autonomously necessary in the cells which become floor-plate cells, and that the floor-plate precursors may be determined in the shield region (the equivalent tissue to the *Xenopus* organizer in zebrafish) and selectively incorporated into the ventral neural tube. Furthermore, careful examination indicates that non-floor-plate cells in the ventral neural tube may have an activity to inhibit differentiation of the floor-plate cells. In the second chapter, I analyzed the function of a secreted factor, Dickkopf-1 (Dkk-1), expressed in the prechordal plate. Overexpression studies of zebrafish *dkk-1* in whole embryo or in the prechordal plate indicate that Dkk-1 secreted from the prechordal plate may function to maintain the size of the anterior forebrain region. In the third chapter, I examined a role of Fgf signaling in development of the telencephalon. Fate-mapping studies have shown that the ventral telencephalon arises from the cells in the ANB (Houart et al., 1998; Whitlock and Westerfield, 2000). Fgf8 is expressed in the ANB, and its mutant, *acerebellar* (*ace*) shows some defects in the ventral telencephalon (Shanmugalingam et al., 2000). Inhibition of Fgf signaling indicates that the establishment of the ventral telencephalon requires Fgf signaling at a certain period of development.

Chapter 1: Analysis of floor-plate development using *oep* mutant

Introduction

The developing floor-plate cells located at the ventral midline of the CNS participate in a signal cascade that establishes DV patterning of the neural tube (For a review, see Placzek and Furley, 1996). The differentiation of floor-plate cells requires signals from the axial mesoderm (Yamada *et al.*, 1991; Placzek *et al.*, 1991, 1993). The signaling molecule, Shh has been implicated in this process since it is expressed in the notochord (Echelard *et al.*, 1993; Krauss *et al.*, 1993; Riddle *et al.*, 1993) and it induces the development of a floor-plate when exogenously applied (Marti *et al.*, 1995; Roelink *et al.*, 1995). This was further supported by the results of the analysis of *shh* knock-out mice; in *shh* mutant embryos, the ventral neural tube loses the gene expression pattern characteristic of normal basal-plate and floor-plate cells, but acquires alar-plate characteristics (Chiang *et al.*, 1996). In addition to signals from the notochord, homeogenetic induction between floor-plate cells appears to be involved in the maintenance and propagation of the floor-plate region (Hatta *et al.*, 1991; Placzek *et al.*, 1993).

Even though the notochord and floor plate develop into distinct structures, recent fate-mapping studies in avian embryo have shown that the notochord and floor-plate derive from a common population of cells in Hensen's node (Catala *et al.*, 1996). This observation raises the question as to how floor-plate precursors are segregated and incorporated into a narrow stripe in the ventral part of the neural tube. Genetic analysis of zebrafish embryos may provide a means of understanding this process. The zebrafish *oep* gene is essential for the development of several regions of the embryo including the prechordal plate, endoderm and ventral neuroectoderm (Brand *et al.*, 1996; Hammerschmidt *et al.*, 1996; Schier *et al.*, 1996, 1997; Strähle et al., 1998). In the mutants, the number of floor-plate cells is greatly reduced although *shh* is expressed in the

notochord (Schier *et al.*, 1997). Strähle *et al.* (1998) have demonstrated that wild-type cells, when transplanted into mutant embryos, were able to give rise to both floor-plate cells and notochord, indicating that *oep* is required in the floor-plate cells. Recently, positional cloning has identified the zebrafish *oep* as encoding a novel membrane-associated protein with an epiblast growth factor (EGF) motif. Early expression of *oep* is detected in the germ ring, embryonic shield and notochord but not in the neuroectoderm except for the forebrain (Zhang *et al.*, 1998), suggesting that *oep* functions in the early phase of floor-plate induction, probably within the embryonic shield which is equivalent to chicken Hensen's node. Thus, it is expected that *oep* mutant cells remain unspecified toward the floor-plate fate even when exposed to inducing signals. To investigate the cell behavior and cell-cell interaction during the establishment of the floor plate, I took advantage of this defective nature of *oep* mutant cells, and analyzed the distribution and gene expression of donor cells in genetic mosaics, obtained by transplanting embryonic shield or blastoderm cells from wild-type or mutant embryos into hosts of both genotypes. In this study, I first demonstrate a characteristic distribution of mutant shield cells in a wild-type host: they do not colonize in the floor-plate region, suggesting a role for Oep in an early step of cell fate decision within the shield region. I then provide evidence for the presence of a repressive interaction between floor-plate and non-floor-plate neural cells.

Results

Normal inducing ability of oep mutant shield

By transplanting wild-type cells into an *oep* host, Strähle *et al.* (1998) showed that *oep* is required in floor-plate cells. However, the recent observation that *oep* is expressed in the shield and the axial mesoderm (Zhang *et al.*, 1998) raised the possibility that *oep* mutant axial mesoderm also has a defect in inducing the floor-plate. Since the inducing ability of the *oep* tissues has not been tested, I first examined the development of the floor-plate in the secondary axes induced by transplantation

of mutant shield cells. The host embryos received labeled donor cells (about 100 cells) sucked from a part of the shield region at the shield stage, fixed at the 18-somite stage, and examined for gene expression, followed by biotin-peroxidase staining to visualize donor cells (Figs. 1A, B). The floor-plate in normal zebrafish embryos, which is labeled by the antibody zn-5, extends from midbrain to spinal cord (Hatta *et al.*, 1991). Thus, I examined the presence of the floor-plate in the secondary axes at the midbrain to more caudal level. The genotype of host embryos was easily determined by the morphology of the anterior head structures in the primary axes (Schier *et al.*, 1996, 1997). In contrast, mutant and wild-type donor embryos could not be distinguished morphologically due to removal of the cells in the shield. Therefore, the donor embryos, from which a part of the shield or blastoderm cells had been removed, were allowed to develop to 90%-epiboly and were examined for *gsc* expression which is not maintained in *oep* mutants (Fig. 1C; Schier *et al.*, 1997). Under my experimental conditions, all operated wild-type embryos expressed *gsc* at 90%-epiboly (14/14).

To obtain a complete secondary axis including anterior head structures, I transplanted shield cells in the ventral region halfway between the animal pole and blastoderm margin (Koshida *et al.*, 1998). The embryonic shield cells, when transplanted ventrally, differentiated into the notochord and acted on the host cells to induce ectopic neural tube formation (Fig. 1B; Shih and Fraser, 1996; Koshida *et al.*, 1998). In this study, I mainly used *shh* expression as a marker for floor-plate differentiation. Essentially the same results were obtained with other markers such as *F-spondin* (Higashijima *et al.*, 1997) and *axial* (*HNF3β* orthologue; Strähle *et al.*, 1993). Those floor-plate markers has been reported to be induced in response to the activation of Shh signaling (Ungar and Moon, 1996; Chang et al., 1997; Sasaki et al., 1997). In wild-type embryos, *shh* is expressed in the axial mesoderm and then begins to be seen in the floor plate as development proceeds. Later, the expression in the notochord gradually fades away from the rostral part (Krauss *et al.*, 1993). Under my experimental conditions, *shh* transcripts were almost undetectable in the neural tube of the *oep* mutant strain (tz257); I detected a few positive floor-plate cells in one embryo out of the 30 mutants examined.

In control experiments in which both donor and host embryos were wild type, *shh*

expression was detected in the ventral midline of the secondary neural tube (22/22, Fig. 1D). The *shh* expressing domains of the secondary ventral midlines were broader than that of the primary. This tendency was also observed in the samples hybridized with *F-spondin* or *axial* probe (Figs. 1G, J). When the *oep* shield was transplanted into the wild-type host, the secondary axis was induced at a high frequency and the expression of *shh* was detected in the induced neural tube next to the *oep*-derived notochord (19/19, Fig. 1E). The same results were obtained using *F-spondin* (17/18, Fig. 1H) probe. In contrast, when the wild-type shield was transplanted into mutant hosts, *oep* host cells located at the ventral midline of the neural tube neither expressed *shh* (25/25, Fig. 1F), *F-spondin* (12/12, Fig. 1I) nor *axial* (10/11, Fig. 1K). These results clearly show that mutant shields have normal inducing ability and that *oep* is required exclusively for the floor-plate precursors.

oep mutant cells did not colonize the floor-plate region in a wild-type host

I wondered whether wild-type and mutant cells show different behavior during the establishment of the floor-plate region, and examined the distribution of the donor cells in the secondary axes of genetic chimeras. Under my experimental conditions, irrespective of genotype, the notochord in the secondary axis was composed entirely of donor cells (Figs. 1D-K, Figs. 2A-H). When wild-type embryos were used as a donor, grafted shield cells frequently contributed to part of the floor-plate region of the secondary neural tube and expressed floor-plate markers (Figs. 2A, C, D, F-H). Based on the distribution pattern of donor cells in the ventral midline of the secondary neural tube, transplants were divided into three classes; transplants in which the ventral midline of the neural tube is made up of only host cells (Group I), of both host and donor cells (Group II), and of only donor cells (Group III). The proportion of each class in transplantation experiments between *oep* and wild-type embryos is presented in the Table 1. Although the values varied among the experiments, transplants of all three classes were reproducibly obtained when wild-type shield cells were transplanted into mutant hosts (Table 1). A similar result was obtained in a control experiment in which both donor and host were wild-type (data not shown). In sharp contrast, mutant shield cells transplanted into wild-type hosts never contributed to the ventral midline of the secondary neural

tube (Table 1). I occasionally observed that mutant donor cells were distributed in other ventral regions of the neural tube, presumably due to a contamination of neural cell precursors in the grafts. Even in such a case, they were never incorporated into the ventral midline which was occupied by wild-type cells expressing floor-plate markers (Fig. 2B, E).

Inhibition of floor-plate differentiation by adjacent oep mutant cells

In cases in which a group of wild-type donor cells were incorporated in the ventral midline of the mutant neural tube and aligned along the AP axis (classified as Group II in Table 1), the wild-type cells expressed *shh* in response to inducing signals from the wild-type grafts (Fig. 2C). However, careful examination of serial sections revealed that the wild-type cells which were in contact with mutant cells, i.e., at both ends of the donor cells along the AP axis, tended to be less positive or negative for *shh* transcripts (14/16). Suppression of *shh* expression was seen in an area one- or two-cells wide along the AP axis (Figs. 3A-C, G). Thus, the mutant cells exhibited an inhibitory effect on floor-plate differentiation in neighboring wild-type cells. A similar result was obtained from examinations at an earlier stage (8-somite stage) with the expression of *axial* (Figs. 3D-G). Zebrafish *axial* is activated earlier and is placed upstream of *shh* (Chang *et al.*, 1997) and therefore, suppression may occur in the early phase of differentiation. I obtained essentially the same results in the midbrain/hindbrain (Figs. 3A-F) and spinal cord region (data not shown).

To extend this observation to the primary axis, I created genetic mosaics by injecting labeled wild-type cells into *oep* mutants or vice versa at the sphere (blastula) stage (Fig. 4A). As expected, transplanted mutant cells did not contribute to the floor-plate region in wild-type hosts. I, therefore, examined only mutant hosts in which wild-type donor cells contributed to the ventral midline of the neural tube. In control experiments, both wild-type donor and host cells expressed *shh* in the neural tube (9/9, Figs. 4B, C). In the mutant hosts, the wild-type cells incorporated into the ventral midline as single cells never expressed *shh* (7/7), but did so when incorporated as a group. As observed in the secondary axes, serial sections revealed that *shh* expression was suppressed in one or two wild-type cells adjacent to the mutant cells along the AP axis (2/3; Figs. 4D-G). These observations were

consistent with those in the mutant secondary axes induced by the wild-type shield.

To interpret these results, I examined the character of midline *oep* mutant cells positioned anteroposteriorly to wild-type floor-plate cells. It is possible that, although located at the ventral midline, they are neural precursors which would otherwise be located dorsally on either side of the floor-plate cell in wild-type embryos. To test this idea, I examined the expression pattern of *nk2.2* in wild-type and mutant embryos. Zebrafish *nk2.2*, a member of the NK-2 family of homeobox genes, is normally expressed in the ventral part of the CNS, at high levels in the forebrain and midbrain, and at low levels in the hindbrain and spinal cord (Barth and Wilson, 1995). In *oep* mutants, the expression in the forebrain and midbrain is lost (Schier *et al.*, 1997), while that in the hindbrain and spinal cord persists. Within the hindbrain, *nk2.2* is expressed in several cells on either side of the floor-plate which is negative for the transcripts (Fig. 5A; Bath and Wilson, 1995). In *oep* mutants, however, the expression domain narrows and the cells located at the ventral midline are also positive for the transcripts (Fig. 5B), suggesting that these cells in the *oep* neural tube are committed to a neural fate, similar to those located on either side of the floor-plate. This is further supported by the observation that motor neurons were present judging from the expression of *islet-1* (Inoue et al., 1994), but the position became close to the ventral midline (Figs 5C, D).

Discussion

oep is required exclusively in floor-plate precursors

I show that *oep* mutant shield or axial mesodermal cells have normal inducing ability, confirming that *oep* acts autonomously in the floor-plate (Strähle *et al.*, 1998). In line with this conclusion, recent molecular cloning of the *oep* gene revealed that Oep protein has a functional signal sequence but is membrane-associated, suggesting a cell-autonomous function (Zhang *et al.*, 1998).

Several lines of evidence support the idea that the inductive sequence of a floor-plate is initiated early within the embryonic shield. Both the notochord and the floor-plate originate from

the dorsal 'organizer' region, Hensen's node in chick and the embryonic shield in zebrafish (Catala *et al.*, 1996 for chick; Halpern *et al.*, 1993 for zebrafish). Consistently, cell lineage analyses suggest that cells of the shield region are already specified to develop particular tissue types (Melby *et al.*, 1996), and that floor-plate and notochord precursors occupy overlapping areas in this region (Shih and Fraser, 1995). Furthermore, *oep*, which acts autonomously in floor-plate differentiation, is expressed in the shield but not in the neuroectoderm with the exception of the forebrain (Zhang *et al.*, 1998). Therefore, it is reasonable to say that *oep* is required for early induction of floor-plate precursors, which takes place within the shield region.

Characteristic behavior of oep shield cells in a wild-type environment

I demonstrated that *oep* shield cells, when transplanted into wild-type host, did not colonize the floor-plate region of the secondary axis while they mainly differentiated into the notochord. The same tendency was observed in the primary axis of the wild-type hosts which had received mutant blastomeres at the blastula stage. This behavior of *oep* mutant cells contrasts with that of *no tail* (*ntl*; *Brachyury* orthologue) mutant cells. Cell transplantation in zebrafish demonstrated that *ntl* mutant cells only populate the host floor-plate and not the notochord (Halpern *et al.*, 1993). Similarly, in mouse chimera experiments, *Brachyury* mutant cells in a wild-type environment were preferentially incorporated into the ventral neural tube, including the floor plate (Wilson *et al.*, 1995). Based on these findings, Halpern *et al.* (1997) have proposed that, in the early organizer region, *ntl* functions as a switch in the choice of cell fate between the notochord and floor plate, mediated by the Ntl protein acting to antagonize the floor plate as well as to promote notochord development. My study suggests that Oep could be involved in this process as a necessary factor for floor-plate development. Presumably, in the organizer region, *ntl*/*Brachyury* mutant cells that are blocked in notochord differentiation tend to choose a floor-plate fate and colonize the ventral midline of the neural tube, while *oep* mutant cells blocked in floor-plate differentiation adopt a notochord fate. In the secondary axes, because of the normal inducing ability of *oep* mutant shield, substantial amounts of the floor-plate precursors were induced *de novo* from the wild-type host

epiblast. Thus, wild-type floor-plate precursors and non-precursor *oep* mutant cells would coexist in the same region of genetic mosaics. As development proceeds, wild-type floor-plate precursors are incorporated into the ventral midline of the neural tube while mutant cells are distributed in the notochord and other parts of the neural tube; as a result, the floor-plate was composed of only wild-type host cells. At present, it is not clear at what developmental stage the floor-plate precursors start to colonize the ventral midline. However, complete exclusion of mutant cells from the floor-plate region in the mutant hosts (Table 1) suggests that the precursors are incorporated into the ventral midline as soon as they are specified or leave the organizer region.

When *oep* hosts received wild-type shield cells, three types of distribution pattern were consistently observed. This can be explained as follows. Unlike the reciprocal transplant (*oep* -> wild-type) described above, floor-plate precursors are not additionally provided by the mutant host, and therefore, the number of floor-plate precursors totally depends on that derived from the grafts. Under my experimental conditions, the amount of floor-plate and notochord precursors in a graft (part of the shield) could vary in each transplantation, due to their closely overlapping fate within the shield region. Consequently, depending on the number of precursors available, three distribution patterns are consistently obtained in *oep* hosts transplanted with wild-type shield cells.

Repressive interaction between floor-plate and non-floor-plate cells

The most important finding in this study is that wild-type cells located adjacent to mutant cells failed to differentiate into the floor plate even when they had been exposed to inducing signals and incorporated into the ventral midline. This inhibition of floor-plate differentiation by an adjacent mutant cell may reflect a repressive interaction between floor-plate cells and non-floor-plate neural cells located on either side of the floor plate. If a sufficient amount of wild-type floor-plate precursors is not available, *oep* mutant cells may colonize the ventral midline, not as a floor-plate, but as a neural precursor. The expression pattern of *nk2.2* in *oep* mutant neural tube supports this postulate. *oep* mutant cells at the ventral midline expressed *nk2.2* which is normally expressed in the ventral neural cells adjacent to the floor plate. In fact, it is believed that, in *oep* mutants, only

floor plate is missing and other cell types in the neural tube persist. For example, *islet-1*-positive primary motor neurons (Fig. 5D; Strähle *et al.*, 1998) and zn-1-positive secondary motor neurons (Strähle *et al.*, 1998) differentiate in the ventral region of the mutant neural tube but their location is ventrally shifted due to a lack of the floor plate.

My results, however, contrast with those obtained with *cyclops* (*cyc*) mutants which revealed the presence of homeogenetic induction between floor-plate cells. When wild-type cells transplanted into *cyc* mutants subsequently differentiated as floor plate, adjacent mutant cells also did so (Hatta *et al.*, 1991). Homeogenetic induction between floor-plate cells was also observed in chick embryos by *in vitro* culture of the dissected neural tube with a notochord or floor plate (Placzek *et al.*, 1993), and is thought to contribute to the establishment of the floor-plate region.

What role does the inhibitory interaction have? During normal development, ventral neural cells must antagonize homeogenetic signals from the floor plate to differentiate as a neuron. This ability may play an important role in restricting the floor plate to a small region in the ventral midline. Thus, the vertebrate floor-plate region could be defined by the balance between homeogenetic and repressive signals. Again, it is not entirely clear when this interaction takes place during the course of floor-plate development. My data only suggest that it occurs after incorporation of floor-plate precursors into the ventral midline.

In conclusions, by analyzing the genetic mosaics between wild-type and *oep* mutants, I demonstrated that *oep* shield cells preferentially adopt a notochord fate in a wild-type environment. I then provided evidence for the repressive interaction between floor plate and the other parts of the neural tube. To date, this interaction has been observed only in this study, and should be further tested in other systems such as *in vitro* culture or different mutants showing similar floor-plate defects.

Chapter 2: Functional analysis of zebrafish *dkk-1* expressed in the prechordal plate

Introduction

Two signal model, in which the axial mesoderm plays major roles (Nieuwkoop, 1952; Toivonen and Saxen, 1968), have long been accepted to explain patterning of neuroectoderm along the AP axis, and enormous efforts have been devoted to find the signaling molecules emanated from the axial mesoderm. However, this traditional view has been questioned by several recent studies in zebrafish. Ablation of the embryonic shield leads to absence of axial mesoderm including the prechordal plate, but to normal AP neural patterning (Shih and Fraser, 1996; Driever et al., 1997). In addition, Koshida et al. (1998) showed that the ventralized embryo which lack axial mesoderm completely (Mizuno et al., 1999), still retains initial AP pattern in its ectoderm. A zebrafish *oep* mutant, which lacks the prechordal plate, has an anterior neural structure and normal AP pattern in the neural tube (Schier et al., 1997; Strähle et al., 1998). Furthermore, in *squint* (*sqt*) and *cyc* double mutants (Feldman et al., 1998) and Antivin overexpressed embryos (Thisse and Thisse, 1998), although no prechordal plate and notochord form, the head is induced. These data illustrate the necessity to reconsider the function of the axial mesoderm in AP patterning of neuroectoderm.

From the studies in *Xenopus*, Glinka et al. (1997) proposed two-inhibitor model in which inhibition of both Wnt and Bmp (bone morphogenetic protein) signaling is necessary to induce head region. Following to this model, they cloned *Xenopus dickkopf-1* (*Xdkk-1*) based on its complete second head inducing ability in embryos in which Bmp signaling is inhibited by the coinjection of dominant-negative form of Bmp receptor (tBR) RNA (Glinka et al., 1998). *dkk-1* forms a new gene family which inhibits the Wnt pathway in *Xenopus*, chick, mouse and human. Overexpression of Xdkk-1 led the anteriorized neuroectoderm, and blocking of Xdkk-1 using antibody produced the embryos with reduced head region (Kazanskaya et al., 2000), indicating *dkk-1* involved in AP

patterning of neuroectoderm. However, because Xdkk-1 is expressed in the Spemann organizer, prechordal plate and anterior endoderm which is considered as a equivalent tissue to the AVE in mouse, it is not clear from which tissue *dkk-1* affects to pattern along AP axis.

I thus cloned *dkk-1* in zebrafish (*zfdkk-1*) and examined the function of Dkk-1 in the prechordal plate taking advantages that mutants without the prechordal plate are available in zebrafish. Overexpression of Zfdkk-1 in the prechordal plate revealed the expansion of the anterior forebrain in expense of the posterior forebrain and midbrain, and did not affect the position of the MHB. Moreover, overexpression of *zfdkk-1* at the position of the prechordal plate in mutants which lack the prechordal plate mimic the above results. Hence, *zfdkk-1*, secreted from the prechordal plate, may act directly upon the neuroectoderm and affect to AP patterning in the fore- and midbrain region.

Results

Isolation of zfdkk-1 cDNA

Through screening a zebrafish shield stage cDNA library with *Xenopus dkk-1* cDNA , (Glinka et al., 1998) two clones for the *Xdkk-1* homologue were obtained. The longer clone contains an open reading frame encoding a putative protein of 241 amino acids with a signal sequence in its N-terminal and two cysteine-rich domains (Fig. 6A). One of these cysteine rich domains (Cys 1) has the consensus amino-acid sequence referred to as $CX_vCX_2CX_6CX_5CCX_4CX_2GXC$ (Glinka et al., 1998). The other (Cys 2) has also the consensus sequence ($GX_2GX_2CX_4DCX_2GXCCAX_vCX$-$PX_4GX_2CX_vRCXCX_2GLXC$) with the one exception that the third glycine in the sequence is a threonine.

To check whether *zfdkk-1* is a secreted protein, FLAG-tagged *zfdkk-1* was transfected to COS7 cells and western blot analysis of the culture supernatant was performed (Fig. 6B). The major band in the cell lysate migrated as a protein of $26X10^3$ M_r and the major band in the culture medium

migrated as a protein of $43X10^3$ M_r, suggesting that Zfdkk-1 is secreted and post-translationally modified before secretion.

Temporal and spatial expression of zfdkk-1

Northern blot analysis revealed a single band of the *zfdkk-1* transcript (Fig. 6C). *zfdkk-1* message can not be detected in the cleavage stage and in the ovary, suggesting that there are no *zfdkk-1* maternal transcripts. From the sphere stage, slightly after the mid-blastula transition (MBT), *zfdkk-1* starts to be expressed and the expression is maintained at the same level during gastrulation. After its peak at the early somite stage, the *zfdkk-1* signal gradually decreases. *zfdkk-1* can be found still in hatching stage embryos, but no longer in adult fish.

To access the function of *zfdkk-1* for anterior head patterning, localizations of *zfdkk-1* transcripts were examined in the potential head patterning tissue during early development by whole-mount in situ hybridization (Fig. 7). *zfdkk-1* transcripts could be initially detected around the high stage (3.5 hours post fertilization, hpf) in one side of the blastoderm margin (Fig. 7B), that corresponds to the future dorsal side revealed by the double staining with *dharma* (data not shown, Yamanaka et al., 1998). At the sphere stage, *zfdkk-1* is transcribed in the yolk syncytial layer (YSL) and the dorsal margin of blastoderm (Figs. 7C, D), as confirmed by simultaneous staining of *gsc* (data not shown, Stachel et al., 1993; Schulte-Merker et al., 1994). The YSL is the extraembryonic tissue that is now focused as a signaling source (Mizuno et al., 1996, 1999). This early expression pattern of *zfdkk-1* is similar to that of *dharma* and is maintained until 40%-epiboly. At 50%-epiboly, *zfdkk-1* mRNA accumulates in cells around the circumference of the blastoderm margin (Fig. 7E).

At the onset of gastrulation, the *zfdkk-1* signal was detected in involuting mesendoderm but no longer in the YSL (Figs. 7F, G). The *zfdkk-1* expression in marginal cells disappears after the shield stage and the signal in mesendoderm persists during gastrulation in a graded fashion from anterior to posterior (Figs. 7H-J). Only cells at the axial mesoderm margin express *zfdkk-1* during gastrulation (Figs. 7H, J). The signal in axial mesoderm disappears from posterior to anterior as gastrulation proceeds and disappears completely by the 3-somite stage (Fig. 7K). At 90%-epiboly,

new *zfdkk-1* expression domains appear weakly in lateral sides of the embryonic axis caudal to the otic vesicles (Fig. 7J). These expression domains converge towards the caudal and coalesce behind the closing yolk plug (Fig. 7L). Thus, *zfdkk-1* is expressed in the YSL and the prechordal plate, both of which are potential head inducing and patterning tissues (Toivonen and Saxen, 1968; Nieuwkoop, 1985; Houart et al., 1998).

Inhibition of Wnt signaling by Zfdkk-1

Xenopus and mouse *dkk-1* has been shown to inhibit secondary axis induction by *Xwnt-8* RNA injection when they were co-injected into the *Xenopus* embryos (Glinka et al., 1998). To study whether *zfdkk-1* also has the ability to inhibit Wnt signaling, I investigated whether the secondary axis induction caused by co-injecting *zfwnt8b* and zebrafish *frizzled2* (*zffz2*) or *frizzled5* (*zffz5*) RNA (Furutani-Seiki et al., unpublished data) can be suppressed by supplementing *zfdkk-1* RNA. Co-injecting *zfwnt8* and *zffz* RNAs at the dose at which injection of each RNA alone does not induce any effects, induces secondary axis at a high frequency or strong dorsalization (Furutani-Seiki et al., unpublished data, Fig. 8A, Table 2). Secondary axis induction by *zfwnt8* and *zffz* RNAs co-injection was completely inhibited by adding *zfdkk-1* mRNA (Fig. 8B). *zfdkk-1* RNA efficiently inhibited also strongly dorsalized phenotypes induced by co-injection of *zfwnt8* and *zffz* RNAs (Table 2). Taken together, *zfdkk-1* could inhibit Wnt signaling in the potential head patterning tissue, YSL and the prechordal plate.

Phenotypes of embryos with ubiquitous overexpression of Zfdkk-1

I then analyzed the function of *zfdkk-1* by injecting synthetic *zfdkk-1* RNA into 1-2 cell stage embryos at several doses (12.5-500 pg, Table 3). Criteria for grouping *zfdkk-1* RNA injection phenotypes are described in Table 3. Injection of out-of-frame *zfdkk-1* RNA and *GFP* RNA did not affect the normal development (46/51 for out-of-frame *zfdkk-1*, 49/50 for *GFP*). At any dose of *zfdkk-1* RNA injection, the anterior head region including eyes and the telencephalon was apparently expanded (Table 3, Figs. 9). The portion of the tectum region against the telencephalon

or the eye region appeared to be reduced depending on the injected dose (Figs. 9B-D). The otic placodes of *zfdkk-1* injected embryos became smaller in a dose-dependent manner but were never lost (Figs. 9A, C, D). The trunk and tail regions showed graded truncation depending on the amount of injected *zfdkk-1* RNA (class I-IV in Table 3 and Fig. 9A). One third of embryos injected with higher doses (200 or 500 pg) of *zfdkk-1* had no notochord. When 500 pg of *zfdkk-1* was injected, about one fourth of embryos did not develop somites. Involution of mesendoderm proceeded normally in low-dose injected embryos but was slightly perturbed in high-dose injected embryos.

Effects of Zfdkk-1 on the mesoderm patterning

I analyzed the effect of *zfdkk-1* RNA injection in detail by using molecular markers. Embryos injected with a low dose (25 pg) and a high dose (200 pg) of *zfdkk-1* RNA were examined. Essentially similar results were obtained at both doses. Expression domains of the prechordal plate makers such as *gsc* (16/19, Fig. 10B) and *hlx-1* (Fjose et al., 1994; 20/20, Fig. 10D) were expanded. *twist* (Halpern et al., 1995; Fig. 10F) and *ntl* (Schulte-Merker et al., 1992; Fig. 10H) expression at 90%-epiboly showed that the notochord was shortened and broadened in injected embryos. However, the total stained area did not seem to be changed (15/18 for *twist*, 19/20 for *ntl*). Marginal mesoderm was reduced based on *ntl* (20/20, Fig. 10J) and *wnt8* (Kelly et al., 1995; 16/16, Fig. 10L) expression. *myoD* expressed in adaxial cells at 75%-epiboly (Weinberg et al., 1996) was reduced in *zfdkk-1* injected embryos (15/18, Fig. 10N). At the 12-somite stage, *myoD* expression in somites, derivatives of paraxial mesoderm, was also reduced (22/22, Fig. 10P). However, the width between two stripes of adaxial cells (the notochord area) in these embryos remained unaltered compared to the controls (22/22), suggesting that convergence and extension cell movements take place properly. Intermediate mesoderm stained with *pax2* (pronephros primordia; Krauss et al., 1991; 17/17, Fig. 10R) and ventral mesoderm stained with *gata-1* (blood primordia; Detrich et al., 1995; 16/16, Fig. 10T) were decreased.

To determine if these changes in the mesoderm patterning occurred in earlier stages, I examined expression of organizer marker genes at the shield stage. Although there was no ectopic

expression of *gsc* or *chordin* (*chd*) in the ventral side (Schulte-Merker et al., 1997; Miller-Bertoglio et al., 1997), *gsc* and *chd* expression domains were expanded laterally (16/25, Fig. 10V for *gsc*, 20/20, Fig. 10X for *chd*).

Effects of Zfdkk-1 on the AP pattern in the neural plate

Next, I examined the effect of *zfdkk-1* RNA injection on the neural patterning using AP brain markers. The expression domain of *emx1* (Morita et al., 1995), that corresponds to the dorsal telencephalon, strongly expanded in *zfdkk-1* RNA injected embryos (57/58 for low dose, 71/72 for high dose, Figs. 11A-C). The MHB stained by both *her-5* (Muller et al., 1996) and *pax2*, was reduced slightly in low-dose injected embryos (14/14 for *her-5*, Fig. 11B, 22/23 for *pax2*, data not shown) and strongly in high-dose injected embryos (91/92 for *her-5*, Fig. 11C, 47/50 for *pax2*, data not shown). *krox-20* (*krx-20*) (Oxtoby and Jowett, 1993) expression domains, which corresponds to the rhombomeres 3 and 5, were also reduced dose-dependently (Figs. 11B, C). The rhombomere 5 was more affected than rhombomere 3. Therefore, the more anterior structures became more expanded in low-dose RNA injected embryos. It seems, however, that *zfdkk-1* high-dose injection reduces the midbrain region in the anteriorized neural plate (Figs. 9).

The midbrain region of *zfdkk-1* RNA injected embryos was then examined, using several markers that define this region. *wnt-1* defines the dorsal midbrain region, as its anterior limit of expression is just behind the epiphysis that belongs to the diencephalon and its posterior limit corresponds to the MHB (Figs. 11D-F; Molven et al., 1991). *axial* stains ventral neural tube caudally from the posterior diencephalon (Figs. 11G-I; Strähle et al., 1993; Macdonald et al., 1994). *axial* and *her-5* staining thus define the posterior head region (the region including the posterior diencephalon and the midbrain) (Figs. 11G-I). In low-dose *zfdkk-1* RNA injected embryos, the size of the posterior head region was unaltered (14/19 for *wnt-1*, 11/21 for *axial*, *her-5*) or slightly smaller (5/19 for *wnt-1*, 10/21 for *axial*, *her-5*, Figs. 11E, H). In high-dose injected embryos, the posterior head region was apparently reduced (15/17 for *wnt-1*, 16/16 for *axial*, *her-5*, Figs. 11F, I). The ratio of the anterior (the region including the telencephalon and the anterior diencephalon) to

the posterior head region is roughly 2:3 in normal embryos (Figs. 11D, G). This ratio is approximately 1:1 in low-dose injected embryos (19/19 for *wnt-1*, 21/21 for *axial*, *her-5*, Figs. 11E, H), and 3:2 in high-dose injected embryos (17/17 for *wnt-1*, 16/16 for *axial*, *her-5*, Figs. 11F, I). These results suggest that the anterior head region expands at the expense of posterior head region dose-dependently in the anteriorized neural plate in *zfdkk-1* RNA injected embryos.

To determine whether the alteration of the neural patterning by *zfdkk-1* RNA injection occurs during gastrulation when specifications in the neural plate take place, I examined AP neural plate marker gene expressions in late gastrulae. The expression domain of *emx1* in the presumptive telencephalon at the bud stage extended posteriorly in the *zfdkk-1* injected embryos (Figs. 11J, K; 17/17 in low dose, 14/14 in high dose). *anf-1* (Kazanskaya et al., 1997) stains the anterior neuroectoderm, whose posterior boundary slightly overlaps with the anterior part of *her-5* expression in the presumptive midbrain according to the double staining analysis at the end of gastrulation (data not shown). The expression domain of *anf-1* also expanded posteriorly in *zfdkk-1* RNA injected late gastrulae (40/40 in low dose, Fig. 11M, 35/36 in high dose). *otx2*, which marks the future forebrain and the midbrain (Mori et al., 1994; Li et al., 1994), was expanded posteriorly at the expense of the posterior neural marker *hoxa-1* (Alexandre et al., 1996; 21/21 in low dose, Fig. 11O, 17/17 in high dose). The *pax2* expression domain, that corresponds to the future MHB, shifted posteriorly (20/20 for low dose, Fig. 11K, 14/14 for high dose) and its width became narrower in about one half of the embryos injected with low dose and all the embryos injected with high dose, as compared to the controls. To analyze the area of the future posterior head region in *zfdkk-1* RNA injected embryos, I used *her-5*, which is expressed in the midbrain region until early gastrulation (Muller et al., 1996). The expression domain of *her-5* became thinner in low-dose injected embryos (11/20, Fig. 11Q), and 2 out of 20 embryos had no staining. In high-dose injection, about 80% of embryos (13/16) did not have the *her-5* stripe. To confirm this result, I performed double staining using fluorescence for *otx2* and normal blue staining for *anf-1*. In these double stained embryos, the posterior head domain expressing only *otx2* but not *anf-1* can be seen by fluorescence (Fig. 11R). The domain expressing *otx2* alone was significantly reduced (38/45 in low dose, Fig. 11T, 18/33 in

high dose) or disappeared (7/45 in low dose, 15/33 in high dose) in *zfdkk-1* RNA injected embryos. The size of the neural plate in the gastrulae was not changed, as judged by the expression domain of *gata-3* (Neave et al., 1995; data not shown) and *dlx3* (Akimenko et al., 1994; data not shown). These results suggest that *zfdkk-1* RNA injection alters specification in the AP neural patterning by expanding the anterior head region and reducing the posterior head region in the anteriorized neural plate.

Effects of Zfdkk-1 in the prechordal plate on the neuroectoderm

Although overall ubiquitous expression of Zfdkk-1 altered AP patterning of the neural plate, it was not clear, in which tissue the expression of *zfdkk-1* caused this effect. As *zfdkk-1* is most abundantly expressed in the prechordal plate among mesendoderm during gastrulation (Figs. 7H-J), I transplanted mammalian COS7 cultured cells transfected with FLAG-tagged *zfdkk-1* (Dkk-1 COS7) in the dorsal side near the animal pole or around the embryonic shield of the shield stage embryos (Fig. 12A). As has been reported previously (Koshida et al., 1998), COS7 cells transplanted near the animal pole still remained to be integrated into migrating prechordal plate at 90%-epiboly. COS7 cells transplanted next to the embryonic shield moved up to the animal pole together with involuting mesendoderm, again resulting in colocalization with the prechordal plate at the 90%-epiboly stage. Both modes of transplantations gave the same results. COS7 cells transfected with ß-galactosidase (ß-gal COS7) were transplanted as a control.

The embryos grafted with Dkk-1 COS7 had big eyes and expanded telencephalon at 24 hpf compared to the controls (27/29, Fig. 12C). Other structures appeared normal. In situ hybridization analysis of these embryos with *emx1*, *her-5* and *krx-20* revealed that the dorsal telencephalon, stained by *emx1*, was expanded (19/22) but the expression of *her-5* and *krx-20* remained unaltered (22/22, Fig. 12E). Neither *otx2* nor *hoxa-1* expression at the end of gastrulation was affected by the transplanted Dkk-1 COS7 (27/29 for *otx2*, 19/20 for *hoxa-1*, Fig. 12G). Conversely, the expression domain of *anf-1* was expanded posteriorly (23/29, Fig. 12I) and the region only expressing *otx2* but not *anf-1* was reduced (18/20) from the double staining analysis with *anf-1* and *otx2* (Fig. 12K).

Dkk-1 COS7 did not affect the prechordal plate or notochord as seen from the expression of *gsc* (14/17, Fig. 12M) and *ntl* (16/16, Fig. 12O). These results suggest that Zfdkk-1 overexpression in the prechordal plate affect the patterning within the fore- and midbrain region.

To determine whether Zfdkk-1 patterns neuroectoderm directly or indirectly via other factors emanating from the prechordal plate, Dkk-1 COS7 was transplanted into the animal pole of *oep* mutants, which have no prechordal plate. If Zfdkk-1 can affect neuroectoderm directly, the anterior head region of the *oep* mutants is expected to expand. As shown in Fig. 12Q, the anterior head in *oep* homozygous mutants was clearly expanded (7/9), but the eyes were still fused. Transplanted Dkk-1 COS7 did not induce the prechordal plate (data not shown). Analysis with several head markers revealed expansion of the dorsal telencephalon in the transplanted *oep* mutants (6/8, Fig. 12U). These results suggest that *zfdkk-1* exerts its function to pattern the anterior head probably by acting directly upon neuroectoderm.

Discussion

In this study, I cloned zebrafish *dkk-1* and performed the functional analyses by use of RNA injection and cell transplantation techniques. The results show that Zfdkk-1 is able to antagonize Wnt signaling and to maintain the prechordal plate. Furthermore, Zfdkk-1 secreted from the prechordal plate is shown to function in the maintenance of the anterior neuroectoderm.

Early expression of Zfdkk-1 maintains the prechordal plate

Overexpression of Zfdkk-1 in entire embryos resulted in the dorsalization of the mesoderm at the early gastrula and in enlarged prechordal plate, the most dorsal mesoderm, at the late gastrula stage. In *Xenopus*, both *dkk-1* and *frzb* can dorsalize the mesoderm under the inhibition of Bmp signaling. However complete secondary axes with two eyes are induced only by co-injection of *dkk-1* and *tBR* RNA, while cyclopic secondary axes are induced by co-injection of *frzb* and *tBR* RNAs (Glinka et

al., 1998; Kazanskaya et al., 2000). Above data imply that the region of the presumptive prechordal plate is maintained in *dkk-1*-injected embryos but not in *frzb*-injected embryos. Furthermore, blocking Dkk-1 activity by anti-Dkk-1 antibodies induces cyclopic embryos (Glinka et al., 1998) with reduced prechordal plate (Kazanskaya et al., 2000). All these results support the notion that Dkk-1 plays a role in maintenance of the prechordal plate.

How overexpression of Zfdkk-1 affects AP patterning of the entire neuroectoderm?

In contrast to the transplantation of COS cells, in which anteriorization was observed in only fore- and midbrain region, in RNA injection experiments, the anteriorization was observed in entire neuroectoderm (compare Figs. 11N, O and 12F, G). One possible explanation for this is that a reduction of the marginal mesoderm affects the entire neural patterning. The marginal mesoderm has been reported to posteriorize the neuroectoderm (Woo and Fraser, 1997; Koshida et al., 1998). When this tissue is transplanted in the anterior neuroectoderm, it suppresses the expression of *otx2*, fore- and midbrain marker, and, instead, induces the expression of *hoxa-1* which is expressed in the hindbrain and spinal cord (Koshida et al., 1998). The predicted phenotype with a reduction of the marginal mesoderm matches well to that obtained by *zfdkk-1* injection. In fact, *zfdkk-1*-injected embryos show the reduced marginal mesoderm, judging from *ntl* expression at shield stage. Another possibility is that *zfdkk-1*, expressed in the marginal mesoderm at the late blastula stage, directly determines the position of the MHB. Since Wnt8 is expressed in the marginal mesoderm and suggested posteriorizing activity from overexpression studies of *wnt8* and dominant-negative form of *wnt8* (Kelly et al., 1995; Koshida, 1999; Fekany-Lee et al., 2000), Zfdkk-1 might regulate patterning of the whole neuroectoderm by antagonizing Wnt8 in the marginal mesoderm.

Zfdkk-1 expression in the prechordal plate is required to maintain the anterior head region

Zebrafish *oep* mutants which lack the prechordal plate secreting Dkk-1, exhibit a reduction in the size of the eye field and in expression of anterior neural makers such as *emx1* and *anf-1* (data not shown). I found in this study that the transplantation of Dkk-1 secreting COS7 cells underneath the

anterior neuroectoderm of the wild-type or *oep* mutants expanded or recovered the presumptive anterior forebrain region with the posterior border of midbrain unchanged. Hashimoto et al. (2000) also reported a similar result: the anterior head region was recovered by Zfdkk-1 overexpression in the embryos in which development of the prechordal plate was inhibited by injection of *antivin* RNAs. These results indicate that Dkk-1 secreted from the prechordal plate acts directly on the neuroectoderm, and functions in maintenance of the anterior head region. Supporting this idea, in *Xenopus*, the injection of anti-Dkk-1 antibody into the blastocoel at blastula stage results in a reduction of the forebrain region, including the telencephalon and eye field (Kazanskaya et al., 2000). In these embryos, the prechordal plate is reduced but still present. Since *wnt-1* is expressed throughout the midbrain and MHB premordium around the late gastrula stage (Lun and Brand, 1998), Dkk-1 in the prechordal plate may antagonize Wnt signaling to secure the anterior head territories.

Chapter 3: Functional analysis of Fgf signaling in the anterior head region

Introduction

The telencephalon is the anterior-most structure in the CNS. Though its morphologies are quite divergent in different species, organization of telencephalic subdivisions, subpallial (ventral) and pallial (dorsal) territories, are basically conserved among species (reviewed in Wilson and Rubenstein, 2000). The subpallial telencephalon constitutes most of the basal ganglia and the pallial telencephalon contains the progenitors in the cerebral cortex in mammals. Fate-mapping studies revealed that the telencephalon derives from cells at the anterior margin of the neural plate (Rubenstein and Shimamura, 1998; Whitlock and Westerfield, 2000). Experiments with mice and zebrafish have demonstrated that the tissue located in the ANB plays an important role in induction and patterning of the telencephalic region (Shimamura and Rubenstein, 1997; Houart et al., 1998). Fgf8 expressed in the ANB has been implicated in these processes (Shimamura and Rubenstein, 1997; Reifers et al., 1998; Shanmugalingam et al., 2000). The phenotypes of zebrafish *ace* mutants, in which no functional Fgf8 is produced, reveal the function of *fgf8* in the regionalization of the telencephalon; some subpallial markers are down-regulated in the mutants (Reifers et al., 1998; Shanmugalingam et al., 2000). Furthermore, mutant mice in which *fgf8* function is reduced, show the loss of olfactory bulb and reduction of the forebrain (Meyers et al., 1998). However, due to overlapping expression and functional redundancy of Fgf family genes (Maruoka et al., 1998; Xu et al., 1999), a precise role of Fgf signaling in development of the telencephalon remains unclear.

I addresses this question in zebrafish embryos by direct observation of the response to Fgfs. Fgf receptors are members of the receptor tyrosine kinase (RTK) superfamily (Klint and Claesson-Welsh, 1999; Ornitz, 2000). At present, four members are known and each of them has several splicing isoforms (Klint and Claesson-Welsh, 1999). In general, RTKs trigger, by way of Ras, a sequential activation of MAP kinase (or extracellular signal-regulated kinase: ERK) signaling

cascade (for review, see Cobb and Goldsmith, 1995). ERK is activated by dual phosphorylation of threonine and tyrosine residues by MAPK/ERK kinase (MEK) (Crews et al., 1992). A monoclonal antibody raised against a dually phosphorylated form of ERK (dpERK) has been successfully applied to *Drosophila* and *Xenopus*, and reveals a dynamic dpERK staining pattern in early embryos (Gaby et al., 1997a and b; Christen and Slack, 1999). In *Drosophila*, several different RTKs participate in ERK activation, while, in *Xenopus*, the Fgf family seems to be responsible for the full pattern of dpERK in early development since activation can be blocked by the expression of a dominant-negative form of Fgf receptor (Christen and Slack, 1999).

In this study, I find that ERK is activated in the zebrafish ANB. Like *Xenopus*, the activation in the ANB is attributable to a Fgf signal. Interestingly, ERK activation in the ANB is maintained in *ace* mutants, suggesting other Fgfs function in this region. I then examines the function of Fgf signaling in zebrafish forebrain patterning by use of several inhibitors to Fgf signaling cascade such as dominant-negative form of Ras (Ras^{N17}) and Fgf receptor (Fgfr), and a chemical inhibitor of Fgfr, SU5402. In treated embryos, the induction of telencephalic territory normally proceeds but the development of the subpallial telencephalon is suppressed, indicating that Fgf signaling is required for the regionalization within the telencephalon. Finally, I show by antisense technique that both Fgf3 and Fgf8 are required for normal development of the subpallial region.

Results

ERK activation pattern in developing embryos

ERK is one of well-known downstream mediators of Fgf receptor (Gotoh and Nishida, 1996; Chirsten and Slack, 1999). I examined the pattern of ERK activation in whole embryos, focusing on the anterior neural region. During gastrulation, strong activation is detected in the blastoderm margin which gives rise to the mesoderm (Fig. 13A). This activation is finally confined to the tailbud region by the end of gastrulation. The MHB becomes positive at the end of gastrulation, and

the activation reaches a peak level at 3-somite stage (Fig. 13B). Following the activation in the MHB, the anterior part of the forebrain becomes positive at 3-somite stage, and the strongest staining is observed at 5-somite stage (asterisk in Fig. 13C). Histological sections of 5-somite stage embryos reveal that ERK activation in the forebrain is confined to the ANB (Fig. 13D). The activation gradually decrease (Figs. 13E, F), and become undetectable by the stages later than 12-somite. The activated pattern closely resembles that reported in *Xenopus* (Christen and Slack, 1999).

Fgf dependent activation of ERK at segmentation stages

Since ERK activation is triggered by downstream targets of various RTKs (see Introduction), I examined the contribution of Fgf signaling toward ERK activation by use of inhibitors to Fgf signaling cascade. I first tested whether or not ERK activation at segmentation stages is Ras-dependent by injecting synthetic RNAs encoding dominant-negative form of human Ras (Ras^{N17}), in which serine at position 17 had been substituted by asparagine (Deng and Karin, 1994). The synthetic RNAs were injected at 1- to 2-cell stages and stained for dpERK at segmentation stages. In Ras^{N17}-injected embryos, all positive staining disappeared (43/48, Figs. 14A, B). I then examined the effects of XFD (Amaya et al., 1991) and bΔFR4 (Hongo et al., 1999), a dominant-negative form of *Xenopus* Fgfr-1 and Fgfr-4a, respectively. Both types of dominant-negative Fgfrs effectively reduced ERK staining (24/24 for XFD and 30/30 for bΔFR4; Fig. 14C). Finally developing embryos were treated with a chemical inhibitor to Fgfr, SU5402. SU5402 has been reported to specifically inhibit the kinase activity of nearly all types of Fgfr (Mohammadi et al., 1997). I injected 10 mg/ml of SU5402 into the anterior thick region of the brain near the ANB at tailbud stage (see Fig. 14D), and the embryos were fixed at 5-somite, followed by anti-dpERK staining. Again, the positive staining in the ANB was greatly reduced in injected embryos (19/19, Figs. 14E, F).

Fgf-dependent activation of ERK was further examined by transplantation of Fgf-soaked beads into the anterior head region. Ectopic activation of ERK was induced around the transplanted

beads that had been soaked in PBS containing recombinant mouse Fgf8b (15/15, Fig. 14H), while no such activation was detected around BSA-soaked bead (12/13, Fig. 14G). Taken together, I conclude that under our experimental conditions, ERK activation in the ANB was entirely dependent on Fgf signaling. Though ERK activation may not represent all the activity of Fgf signaling, it is reasonable to assume that the positive staining is an indicator for the activation of Fgf signaling.

ERK is activated in the ANB of ace mutants

I then examined ERK activation in *ace* mutants. The *ace* mutation is a G to A transition in the splice site after the second exon of the *fgf8* gene, which leads to incorrect splicing generating a truncated non-functional protein (Reifers et al., 1998). Since, at 5-somite stage, homozygous *ace* mutants can not be distinguished morphologically from wild-type embryos, I examined the expression pattern of *myoD* in the trunk region. It has been reported that the adaxial cells of homozygous *ace* mutants show reduced and fragmented expression of *myoD* (Reifers et al., 1998). Although the intensity of ERK staining varies to some degree and tends to be weaker as compared with wild-type siblings, a substantial amount of positive reactions are reproducibly observed in the ANB (7/10, Figs. 15A, B) of *ace* mutants. Western blot analysis confirmed this result. As shown in Fig. 15C, one major band (50 kDa) was detected by anti-dpERK antibody. The intensity of this band decreased in *ace* mutants by about 40%, and it was nearly undetectable when the embryos were treated with SU5402. These results indicated that Fgf signaling remains activated in the ANB in the absence of Ace/Fgf8.

Zebrafish fgf3 expressed in the wild-type and ace ANB

During the course of the study, I found that the temporal and spatial pattern of ERK activation correlated well with that of *fgf3* expression in the ANB (compare Figs. 13C, D and Figs. 16C, D). Zebrafish *fgf3* starts to be expressed at the end of the gastrulation in the anterior head region, the anterior forebrain and MHB (Fig. 16A), and its expression persists until around 10-somite stage (Fig. 16C). Histological sections reveal that the anterior staining is located in the ANB (Figs. 16B, D), where *fgf8* is also expressed (Shanmugalingam et al., 2000). Importantly, *fgf3* expression is maintained in the ANB of *ace* homozygous embryos at the tailbud stage (10/10, Fig. 16E) and mid-somite stage (10/10, Fig. 16F), suggesting that Fgf3 may compensate for the function of Fgf8 in the *ace* ANB. Indeed, Fgf3 is a potent activator of ERK: *fgf3* RNA injection into 1- to 2-cell stage embryos induced ERK activation in entire embryo (25/25, Fig. 16G), while this activation was abolished by coinjection of Ras^{N17} RNAs (38/38, Fig. 16H).

Inhibition of Ras-dependent pathway suppresses the development of subpallial telencephalon

To explore the roles of Fgf signaling in zebrafish forebrain development, I examined the effects of Ras^{N17} injection. Morphologically, Ras^{N17}-injected embryos showed obvious defects in the MHB and tail region. In most cases, the tail and yolk tubes did not extend well and the segmented structures in the trunk was hardly observed, indicating that the disruption of Fgf signaling cascade affected mesodermal tissues. Furthermore, I observed that the forebrain and midbrain region tended to be enlarged, probably due to reduced posteriorising signals derived from the non-axial mesoderm (Woo and Fraser, 1997; Koshida et al., 1998). In addition to the MHB and tail, in more than half of Ras^{N17}-injected embryos the telencephalic region became turbid at 33 hpf, especially in the ventral part of the telencephalon (Figs. 17A, B). DNA fragmentation analysis revealed that apoptotic cells were induced by overexpression of Ras^{N17} (8/11, Figs. 17C, D). Apoptotic cells were frequently observed in the ventral part of telencephalon but less in the dorsal. However, at 26 hpf, there was little apoptotic cell detected in the entire telencephalon of Ras^{N17}-injected embryos (18/18, Figs. 17E, F).

To determine whether the telencephalic patterning was altered before the appearance of apoptosis, I stained injected embryos with forebrain markers at different developmental stages between bud to 26 hpf. In situ hybridization analyses with one-day old embryos revealed that, in Ras^{N17}-injected embryos, development of the subpallial telencephalon was severely affected. In zebrafish, the *distal-less* related gene, *dlx2*, is normally expressed in the subpallial telencephalon and diencephalon (Akimenko et al., 1994). Overexpression of Ras^{N17} reduced or abolished *dlx2*

expression in the telencephalon (42/60, Figs. 17G, H), while the expression in the diencephalon was unaffected. Overexpression of Ras^{N17} also reduced the expression of zebrafish *nk2.1b* (Rohr et al., in press), which is a basal telencephalic marker related to mouse *Nkx2.1* (Shimamura et al., 1995; Rubenstein and Shimamura, 1998) (61/64, Figs. 17I, J). Contrary to the subpallial markers, the expression domains of*emx1*, *eomesodermin* (*eom*) and *T-brain-1* (*tbr1*) (Mione et al., 2001), which are normally confined to the pallial region of the telencephalon at 26 hpf, nearly covered the entire region of the telencephalon in Ras^{N17}-injected embryos (32/40 for *emx1*, Figs. 17K, L; 25/25 for *eom*, Figs. 17M, N; 24/24 for *tbr1*, Figs. 17O, P).

The loss of the subpallial telencephalon was detected as early as segmentation stages. In normal embryos, *nk2.1b* expression in the telencephalon starts to be detected around 14-somite stage (Rohr et al., in press). However, *nk2.1b* expression was not detected throughout development in Ras^{N17}-injected embryos (20/20, Figs. 17Q, R). Consistently, *dlx2* expression in the telencephalon, which starts to be activated at around the 15-somite stage (Akimenko et al., 1994), was not observed in Ras^{N17}-injected embryos at any stages (30/36, Figs. 17S, T). In normal embryos, *emx1* is first expressed in the telencephalic region, and, by 10-somite stage, the expression is down-regulated in the anterior-most of the forebrain, which may be fated to the subpallial telencephalon (Morita et al., 1995; Shanmugalingam et al., 2000). This down-regulation, however, was never observed in Ras^{N17}-injected embryos (29/29, Fig. 17V). Thus, the regionalization within the telencephalon was stopped at its early phase (at least as early as 10-somite stage of development) when Ras/MAPK cascade was blocked.

In addition to the region-specific markers, Ras^{N17} affected markers for neuronal differentiation in the telencephalon. *islet-1* expression around the anterior commissure (Inoue et al., 1994; Fig. 17W) was not observed in Ras^{N17}-injected embryos at 26 hpf (19/20, Fig. 17X). *zash1a* expression in the telencephalon was also undetectable in Ras^{N17} injection (20/24, Figs. 17Y, Z). *zash1a*, one of the zebrafish genes related to *Drosophila achaete-scute* (reviewed in Campuzano and Modolell, 1992), starts to be activated in the part of the subpallial telencephalon at 12-somite stage (Allende and Weinberg, 1994). These data demonstrated that Ras^{N17} suppressed the

differentiation of putative subpallial neurons.

In contrast to the regionalization within the telencephalon, early overall patterning of the forebrain appeared normal in Ras^{N17}-injected embryos. As described above, *emx1*, an early telencephalic marker, was normally activated at the tailbud stage in the prospective telencephalic region of the Ras^{N17}-injected embryos (21/22, Figs. 18A, B). The expression of another early telencephalic marker, *bf-1*, which is expressed in the telencephalon and a part of eyes (Toresson et al., 1998), was not altered by Ras^{N17} injection when examined at the 5-somite stage (20/20, Figs. 18C, D) and 24 hpf (41/41, Figs. 18E, F). Furthermore, down-regulation of *otx2* at mid-somite stage in the region fated to the telencephalon and ventral diencephalon (Mori et al., 1994) normally occurred in injected embryos (33/34, Figs. 18G, H). Thus, the establishment of telencephalic and diencephalic territories normally takes place even when the Ras/MAPK cascade is suppressed.

I also confirmed that Ras^{N17} did not affect the development of other parts of CNS: for example, the expression of *shh* in the ventral spinal cord and ventral diencephalon was normal in Ras^{N17}-injected embryos (18/18, Figs. 18I, J).

bΔFR4 and SU5402 produced the same phenotypes as those with Ras^{N17}

When specific inhibitors to Fgfr-mediated signal were employed, essentially the same results were obtained. In *bΔFR4*-injected embryos, expression of *dlx2* (26/30, Figs. 19A, B), *nk2.1b* (35/38, Figs. 19C, D) and *islet-1* (20/30, Figs. 19E, F) in the subpallial telencephalon at 26 hpf was suppressed while pallial markers, *emx1* (40/45, Figs. 19G, H), *eom* (23/29, Figs. 19I, J) and *tbr1* (23/25, Figs. 19K, L) expression covered the entire telencephalon. These effects were already observed at mid-somite stage. In the *bΔFR4*-injected embryos, *nk2.1b* expression was suppressed (15/18, Figs. 19M, N) at the 14-somite stage and *emx1* was expressed throughout the telencephalon at the 15-somite stage (43/44, Figs. 19O, P). In contrast, the territory of the telencephalon was established normally, judging from the expression pattern of *emx1* at tailbud stage (22/25, Figs. 19Q, R), *bf-1* at 5-somite stages (21/21, Figs. 19S, T) and *otx2* at 15-somite stage (23/23, Figs. 19U, V).

Although the size of telencephalon tended to be smaller as compared with overexpression of

Ras^{N17} and bΔFR4, the injection of SU5402 (10 mg/ml) into the anterior head region at the tailbud stage (see Fig. 14D) gave rise to similar phenotypes in gene expressions of *dlx2* (20/26, Figs. 20A, B), *emx1* (9/13, Figs. 20C, D) and *islet-1* (11/18, Figs. 20E, F).

bΔFR4 and SU5402 also induced apoptosis in the ventral part of telencephalon, but the effect was weaker as compared with that in Ras^{N17}-injected embryos. Furthermore, by unknown reasons, the effect of XFD on telencephalic markers were much weaker as compared with bΔFR4 and SU5402; e.g. only 5 out of 18 embryos injected with 700 ng/μl of XFD RNAs showed reduced expression of *dlx2*.

Overall, the above results demonstrate that Fgf signaling through Ras/MAPK cascade is required for the development of the subpallial telencephalon.

The subpallial telencephalon requires Fgf signaling at early segmentation stages

Anti-dpERK staining revealed that ERK activation reached a level peak at 5-somite stage and, thereafter, gradually decreased. To address when Fgf signaling might be required for development of the subpallial telencephalon, I treated embryos with SU5402 at tailbud, 5-somite, 10-somite and 15-somite stages, and its effect on *dlx2* expression was examined. In this series of experiments, I soaked embryos in 0.1 mg/ml or 0.2 mg/ml SU5402 in 1/3 Ringer's solution for 10 minutes. This worked well and the resulting phenotype in the telencephalon was identical to that obtained with injection of SU5402.

As summarized in Table 4, early treatment (bud to 5-somite) with SU5402 led to loss or severe reduction of *dlx2* in the subpallial telencephalon (Fig. 20G). In contrast, treatment from 10- and 15-somite stage gave rise to normal *dlx2* expression in this region (Fig. 20H). Thus, Fgf signaling up to 5-somite stage is crucial for the establishment of the subpallial telencephalon but, thereafter, *dlx2* expression can be maintained without Fgf signaling.

Zebrafish Fgf3 functions with Fgf8 in the development of the subpallial telencephalon

As described above, *fgf8* and *fgf3* are co-expressed in zebrafish ANB and ERK activation is

maintained in *ace* mutants. This led me to analyze the role of Fgf3 in the development of the subpallial telencephalon. To do this, I blocked the function of Fgf3 by using antisense morpholino-modified oligonucleotides (morpholino) that were targeted to the zebrafish *fgf3* gene (fgf3-MO). Morpholinos have been reported to work well as effective and specific translational inhibitors in zebrafish (Nasevicius and Ekker, 2000). Indeed, injection of *fgf8*-targeted morpholino (fgf8-MO) at a concentration of 20 μg/μl resulted in a phenocopy of *ace* mutants, in which *nk2.1b* expression in the subpallial telencephalon was reduced (29/29, Fig. 21B), although the phenotype tended to be milder (compare Figs. 21B and F). Injection of 10 μg/μl fgf3-MO also reduced the *nk2.1b* expression (28/29, Fig. 21C). However, co-injection of fgf8-MO and fgf3-MO resulted in more severe reduction in *nk2.1b* expression (29/29, Fig. 21D). These results indicate a co-operative action of Fgf3 and Fgf8 on *nk2.1b* expression.

In the MHB, the effects of fgf8-MO and fgf3-MO were different to each other. Injection of fgf8-MO reduced the expression of *en2* (11/11, Fig. 21B') (Ekker et al., 1992) phenocopying the *ace* mutant, while that of fgf3-MO did not affect the expression (23/23, Fig. 21C').

The specificity of fgf3-MO was tested by co-injection of *fgf3* RNAs. When *fgf3* mRNAs were injected at 5 ng/μl, the phenotype induced by fgf3-MO was rescued in a half of the injected embryos (9/18, Fig. 21E). I was unable to obtained 100% rescue because the increased amount of *fgf3* RNAs suppressed the head development in injected embryos even in the presence of fgf3-MO, probably due to strong posteriorising effect of Fgf3 at the gastrulation stage (Koshida et al., submitted). Finally, I injected fgf3-MO (10 μg/μl) in embryos obtained from *ace* heterozygous crosses. 17 out of 58 injected embryos showed no or faint *nk2.1b* expression (Fig. 21H), while such enhanced phenotype was not observed by injection of fgf8-MO (54/54, Fig. 21G).

Discussion

In this study, I report for the first time the spatial pattern of ERK activation in fish development.

Strong ERK activation is detected in the mesoderm, ANB, MHB and tailbud in developing zebrafish embryos. Like *Xenopus* embryos (Christen and Slack, 1999), ERK activation at zebrafish segmentation stages depends on Fgf signaling. I then examine the role of Fgf signaling in forebrain development by use of inhibitors to Fgf signaling. Shanmugalingam et al (2000) have shown that, in *ace* embryos, differentiation of the basal telencephalon and some putative telencephalic neurons were disrupted. In my study, the phenotype obtained by suppression of Fgf signaling encompasses that reported in *ace* mutants. In addition, I observe overall loss of subpallial fate and increased apoptosis in the ventral telencephalon, which are not seen in *ace* embryos. These data demonstrate that Fgf signaling in the ANB is required for the development of the subpallial telencephalon.

Fgf8 is not a sole Fgf involved in ERK activation in the ANB

As in other vertebrates, zebrafish *fgf8* is expressed during gastrulation in the mesoderm, presumptive MHB and telencephalon. (Fürthauer et al., 1997; Reifers et al., 1998). Expression in the CNS is prominent in the MHB and in the antero-ventral telencephalon at segmentation stages (Reifers et al., 1998; Shanmugalingam et al., 2000). ERK activation appears to follow the expression pattern of *fgf8* up to mid-somite stage, suggesting that *fgf8* is responsible for ERK activation. However, the analysis with *ace* mutants, in which no functional Fgf8 is produced (Reifers et al., 1998), suggests that Fgf8 is not a sole Fgf responsible for ERK activation. Although the level of activation tends to be weaker, substantial amount of ERK activation persists in the ANB of *ace* homozygous mutant. Expression analysis and overexpression experiments suggest that Fgf3 is one of the candidates involved in ERK activation in the ANB.

After mid-somite stage, the level of ERK activation gradually decreases in the MHB and then in the ANB, whereas *fgf8* expression remains high in these regions. This suggests that Fgfs, albeit expressed, do not necessarily activate their signaling pathway. Alternatively, ERK activation may not represent all Fgf activity, or antibody labeling may not detect low levels of ERK activation. In fact, Fgfs are known to utilize various signaling cascades other than Ras/MAPK such as phosphatidylinositol 3' kinase (reviewed in Klint and Claesson-Welsh, 1999).

Roles of Fgf signaling in normal development of the subpallial telencephalon

Analysis with telencephalic markers reveals loss of the subpallial fate after treatment with inhibitors to Fgf receptors. In addition to region specific markers, disruption of Fgf signaling reduces or abolishes the expression of differentiation markers specific to putative subpallial neurons. These results indicate that Fgf signaling in the ANB is required for differentiation of subpallial neurons as well as establishment of the subpallial region.

There are at least three possible explanations for the phenotype in affected embryos: (1), the ventral telencephalon fails to acquire subpallial fate and develops into the pallium; (2), the subpallial region is established but disappears due to cell death; and (3), cells in the subpallium fail to proliferate and remains in a small number, while development of the pallial telencephalon proceeds normally. Since cell death in the telencephalon is detected only after loss or reduction of the subpallial markers, the second possibility seems less likely. The analysis of cell proliferation and movements in the developing subpallial telencephalon has not been done in fish. Thus, I can not rule out either the first or third explanations. However, the following observation favors the first one. In affected embryos, subpallial markers such as *dlx2* and *nk2.1b* are never detected at any stages examined, suggesting that the subpallial fate is not induced from the beginning.

Brief treatment of developing embryos with SU5402 reveals that Fgf signaling is not required for subpallial development after 10-somite stage. The critical period coincides with the stage when the strongest activation of ERK is observed. However, it has been reported that the same treatment at 18-somite stage still causes some defects in axon guidance between anterior commissure and post-optic commissure (Shanmugalingam et al., 2000). Thus, it is likely that a critical period for requirement of Fgf signaling varies, depending on the region and developmental processes of the telencephalon.

Fgf signaling is not required for the induction of the telencephalic territory in zebrafish

Studies in mice provided evidence that the anterior neural ridge (ANR), which is located in the

anterior boundary between the neural and non-neural ectoderm, plays an important role in induction of the telencephalon. Shimamura and Rubenstein (1997) demonstrated by *in vitro* culture method that the ANR in mice is necessary and sufficient for the induction of telencephalic *bf-1* expression. In zebrafish, the most anterior neural cells in the ANB, called row-1 cells, were found to possess the similar inducing ability to the mouse ANR (Houart et al., 1998). The ablation of row-1 cells resulted in the loss of telencephalic markers and apoptosis in the anterior head region (Houart et al., 1998). Since *in vitro* experiments in mice demonstrated that Fgf8-soaked beads mimic nearly all activity of the ANR in mammals (Shimamura and Rubenstein, 1997), Fgf signaling has been proposed to account for the inducing ability of the ANR.

However, I observe in this study that the establishment of the telencephalic and diencephalic territories normally proceeded in the Ras^{N17}-injected embryos, as indicated by normal expression patterns of *bf1*, *emx1* and *otx2* at early segmentation stages. This suggests more restricted functions of Fgf signaling in telencephalic development. In deed, no expression of any *fgf* or activation of ERK is detected in the ANB at the gastrula stage when the row-1 cells already acquires full inducing ability. These findings strongly suggest that, in zebrafish, Fgf signaling is not required for induction of the telencephalon.

Overlapping and distinct functions of Fgfs expressed in the CNS

My antisense experiments suggest that Fgf3 co-operates with Fgf8 in the ANB. In this study, I am able to generate a phenocopy of *ace* mutant by injecting fgf8-MO. While the injection of fgf8-MO or fgf3-MO alone results in slight reduction of *nk2.1b* expression, severe reduction of *nk2.1b*, is observed following co-injection of fgf8-MO and fgf3-MO. These results demonstrate that both Fgf8 and Fgf3 are required for normal development of the subpallial telencephalon. This may account for relatively mild defects in the subpallial telencephalon of *ace* mutants.

In contrast, zebrafish Fgf8 has a major role in the MHB as indicated by the phenotype of *ace* mutant, even though *fgf3* expression is detected in the MHB (Fig. 16E). In support for this, the expression of *en2* persists in fgf3-MO-injected embryos while the expression is reduced in fgf8-

MO-injected embryos. Thus, Fgf8 and Fgf3 possess overlapping and distinct functions in the ANB and MHB, respectively. Considering that there are certainly further Fgfs in zebrafish that have yet to be identified, further molecular and genetic analyses will be required to elucidate full functions of Fgf signaling in the developing CNS.

General discussion

In the thesis, I studied mechanisms for the DV and AP neural patterning by use of zebrafish as a model system. Combining mutants and experimental manipulations I obtained novel findings as summarized below.

1) Development of the floor-plate cells initiates in the shield region where mesodermal and ectodermal cells are not segregated yet. Floor-plate precursors are first determined in this region and selectively incorporated into the ventral neural tube. Furthermore, non-floor-plate cells in the neural tube inhibit differentiation of the floor-plate cells.
2) Zfdkk-1 is a secreted protein expressed in the dorsal YSL at the sphere stage, in the marginal mesoderm at the late blastula and in the prechordal plate at the gastrula. Zfdkk-1 is able to antagonize Wnt signaling *in vivo*. Functional analyses revealed two distinct activities of Zfdkk-1 in neural patterning. One is required for maintenance of the prechordal plate, and the other is for establishment of the anterior head region.
3) Fgf/MAPK signaling is activated in the anterior ANB. Both Fgf3 and Fgf8 are responsible for this activation, and are required for normal development of the ventral telencephalon (subpallial region).

These findings demonstrate that both AP and DV patterning consist of multi-step processes, and that the axial mesoderm involves in some of those steps at relatively later stages. Oep act as an essential extracellular cofactor for Nodal signaling during vertebrate development (Gritsman et al., 1999). Furthermore, loss of the ventral midline is observed in another mutant defective in *cyc*, a gene encoding *nodal*-related protein, which is expressed in the embryonic shield and axial mesoderm (Sampath et al., 1998). These recent data demonstrate that in addition to Shh signaling which is important in development of the ventral midline identity (Marti *et al.*, 1995; Roelink *et al.*, 1995; Chiang et al., 1996), Nodal signaling plays a crucial role in formation of the ventral midline. Furthermore, Bmp, Fgf and Wnt signalings are known to be involved in the neural patterning (Dale

et al., 1997; Glinka et al., 1997, 1998; Shanmugalingam et al., 2000). Here, I will discuss the interactions among these signaling pathways and the tissues involved in regional specification of neural tissues.

The developmental process of the ventral midline in the midbrain, hindbrain and spinal cord

Fate-mapping studies (Catala et al., 1996; Shih and Fraser, 1996) and my study shown here demonstrate that developmental process of the floor-plate consists of at least three steps: (1) precursor cells of the floor plate are induced in the shield region, (2) they colonize the ventral neural tube, and (3) differentiate into mature floor-plate cells. In chapter 1, I demonstrate that *oep* gene product functions in the first step, suggesting that Nodal signaling in the shield region is required in the early step of the floor-plate formation. Shh plays a major role in induction of the floor plate (Marti *et al.*, 1995; Roelink *et al.*, 1995). However, at least in the initial phase of floor-plate development, *shh* is not likely to be an inducer because specification of the floor-plate precursors starts at the shield stage, two hours before *shh* expression can be detected (Krauss et al., 1993). Considering that floor-plate cells are not induced in *shh* mutant mice in spite of the presence of a differentiated notochord during early stages (Chiang et al., 1996), I propose that Shh from the axial mesoderm functions as a differentiation factor that promotes the floor-plate precursors into mature floor-plate cells. Consistent with this, a recent study reported that activation of Nodal signaling in the neuroectoderm by a constitutively active form of *smad2* induces *shh* expression in the ventral neural tube (Müller et al., 2000), and the two-step model for development of the ventral midline has been proposed. The first step requires Nodal signaling to establish *shh* expression in floor-plate precursors. During the second step, local Shh signals activates the downstream target genes in the precursors, leading to final differentiation. My study with *oep* mutants supports this model, and shows that the first step takes place in the shield region.

The development of the ventral midline in the head region

The floor plate extends from the spinal cord anteriorly to mid-diencephalon (Placzek et al., 1993) or

to forebrain-midbrain boundary (Hatta et al., 1991). Both floor-plate and ventral midline cells in more anterior neuroectoderm such as diencephalon, possess the ability to pattern the surrounding neural tissue (Hatta et al., 1994). However, the mechanisms of their development are somehow different to each other. As in the spinal cord, development of the anterior ventral midline depends on signals from the prechordal plate, and without this tissue, cyclopic embryos develop (Adelmann, 1936; Shih and Fraser, 1996; Driever et al., 1997). In fact, both Nodal and Shh signalings were shown to be necessary for development of the anterior ventral midline as following. Anti-Shh antibody blocked the induction of ventral midline cells by the prechordal plate (Dale et al., 1997). Furthermore, the expression of *nk2.1a* (a marker for the ventral midline in the diencephalon (Rohr and Concha, 2000)) is absent in *cyc* mutants in which the prechordal plate is present under this region (Thisse et al., 1994), indicating the requirement of Nodal signaling in development of the anterior ventral midline. Since a loss of *nk2.1a* expression in *cyc* mutants can not be restored by overexpression of Shh alone (Rohr et al., in press), Shh signaling is not sufficient to induce the ventral midline in the diencephalon. However, in addition to Shh and Nodal, a Bmp signal from the prechordal plate is required for specification of the anterior ventral midline. Dale et al. (1997) have shown that the prechordal plate treated with anti-Bmp7 antibody failed to induce anterior type of the ventral midline but, instead, induced the floor plate. Thus, combination of different secreted factors could create regional differences within the ventral midline.

The telencephalon is derived from cells in the ANB (Woo and Fraser, 1995; Whitlock and Westerfield, 2000). During development, the anterior part of the ANB gives rise to the ventral telencephalon, whereas the posterior one contributes to the dorsal telencephalon (Whitlock and Westerfield, 2000). The expression of *nk2.1b*, a marker for the ventral midline in the telencephalon as well as the diencephalon, is reduced in *sonic-you* (*syu*) mutants in which *shh* gene is mutated (Schauerte et al., 1998), and lost in *oep* mutants (Rohr et al., in press). In *oep* mutants, the prechordal plate is missing (Brand *et al.*, 1996; Hammerschmidt *et al.*, 1996; Schier *et al.*, 1996, 1997; Strähle et al., 1998). In contrast to more posterior midline, overexpression of Shh in *oep* mutants is sufficient to restore *nk2.1b* expression in the telencephalon, indicating that development

of the ventral midline in the telencephalon mainly depends on Shh but not on Nodal signaling (Rohr et al., in press). This region, however, requires another signaling molecule, Fgf. The analysis of *ace* (*fgf8*) mutants (Shanmugalingam et al., 2000) and my study show that Fgf3 and Fgf8, expressed in the ANB, cooperate in development of the ventral telencephalon. Since *fgf3* expression remains in *oep* mutants, though slightly reduced (data not shown), the above fact that Shh alone is able to rescue *nk2.1b* expression in the telencephalon of *oep* mutants (Rohr et al., in press) could be interpreted by cooperation of Shh and Fgf signalings. Interestingly, recent study in Medaka revealed that Fgf signaling is required for Shh to regulate its target genes in the MHB and proximal eye region (Carl and Wittbrodt, 1999), indicating the presence of coordination of Fgf and Shh signaling pathways in the anterior ventral region.

AP patterning in the neuroectoderm

Cells in the animal pole, when isolated at the shield stage and cultured, express the forebrain marker, indicating that the anterior neuroectoderm at the shield stage is already specified for anterior-type neural tissue (Grinblat et al., 1998). At the same time, the most precocious posterior marker, *hoxa-1*, starts to be activated in the posterior neuroectoderm near the margin by the shield stage (Koshida et al., 1998). This is the first AP specification in the neuroectoderm. Experiments with chick and zebrafish revealed that this early AP specification is achieved by posteriorizing signals secreted by non-axial mesoderm which locates in the margin at the early gastrula stage, is known to posteriorize the neuroectoderm (Bang et al., 1997; Woo and Fraser, 1997; Koshida et al., 1998). When the embryos reach the mid-gastrula stage, two local organizing centers, the MHB and row-1 cells in the ANB are established in the neuroectoderm (Miyagawa et al., 1996; Houart et al., 1998). At later stage of development, the MHB and row-1 cells are crucial in AP patterning of midbrain and anterior hindbrain (reviewed in Lumsden and Krumlauf, 1996), and the forebrain (Houart et al., 1998), respectively.

The position of the MHB is determined by antagonistic interaction between two transcription factors, Otx2 expressed in the midbrain and forebrain, and Gbx2 in the hindbrain

(reviewed in Simeone, 2000). Since the marginal mesoderm defines the posterior boundary of *otx2* expression (Koshida et al., 1998), the position of MHB could depend on the signals derived from the marginal mesoderm. On the other hand, the mechanism for establishment of the row-1 cells is still unknown. However, the axial mesoderm may not be involved in this process, because the activity of row-1 cells can be detected before the axial mesoderm underlies this region (Houart et al., 1998). Furthermore, *emx1* expression in the ANB, of which expression depends on the row-1 cells (Houart et al., 1998), is detected in *oep* mutants in which the underlying prechordal plate is missing (data not shown).

Judging from phenotypes of midline mutants and manipulated embryos, the axial mesoderm after the onset of gastrulation seems less important in AP neural patterning than expected before (Shih and Fraser, 1996; Driever et al., 1997; Schier et al., 1997; Feldman et al., 1998; Koshida et al., 1998; Strähle et al., 1998; Thisse and Thisse, 1998). In contrast, it has been shown that removal of the presumptive organizer region at the late blastula stage results in a loss of forebrain marker (Grinblat et al., 1998), suggesting that induction of the head region requires signals from the early organizer at the blastula stage. It has been repeatedly shown that inhibition of both Bmp and Wnt signaling is necessary to induce the head region (Glinka et al., 1997). In fact, the early organizer expresses Bmp antagonists such as *chordin* and *cerverus*, and Wnt antagonists such as *dkk-1* and *frzb* (Piccolo et al., 1996, 1999; Leyns et al., 1997; Wang et al., 1997a, b; Schulte-Merker et al., 1998). Probably, non-axial posteriorizing signals (maybe Wnt, see discussion in Chapter 2) and head inducers (*dkk-1* and *frzb*) from the early organizer may cooperate in early head development. As shown in Chapter 2, at later stages, the underlying prechordal plate plays an important role in ensuring the anterior head region, and in promoting the anterior specificity in the ventral midline of the diencephalon.

In conclusion, the regional specification of the CNS is established through a multi-step process in which various signaling molecules from different tissues are involved. My study revealed novel functions of Nodal, Dkk-1 (anti-Wnt) and Fgf signals in neural development. However,

precise mechanisms of their action and interaction remain to be elucidated. Further analyses using genetics and molecular biology will be required.

Materials and Methods

Fish embryos

Zebrafish (*Danio rerio*) embryos were obtained from natural crosses of wild-type fish of the Oregon AB background or *oep* heterozygotes (tz257) and *ace* heterozygotes (ti282a) from Tübingen stock. Collected embryos were maintained at 28.5 °C and sorted into 1/3 Ringer (39 mM NaCl, 0.97 mM KCl, 1.8 mM $CaCl_2$, 1.7 mM HEPES at pH 7.2) and staged according to hours postfertilization at 28.5 °C and morphological criteria (Kimmel *et al.*, 1995).

Transplantation of shield tissue or blastomeres

Embryo-labeling with biotin-dextran, cell transplantation and visualization of labeled cells were performed as described by Miyagawa *et al.* (1996). When embryos reached the appropriate stage, about 100 cells were transplanted with a glass micropipette, as shown in Figs. 1A and 4A.

Whole-mount in situ hybridization

Digoxigenin-labeled and fluorescence-labeled probes were synthesized by *in vitro* transcription using T3, T7 and SP6 polymerases. Whole-mount in situ hybridization in the first chapter was carried out as described by Takeda *et al.* (1994) with some modifications (Koshida *et al.*, 1998). Whole-mount in situ hybridization in the rest was carried out by the protocol described in Schulte-Merker et al. (1992).

Histology

For histological analysis, the specimens in the first and third chapter were embedded in Technovit 8100 (HERAEUS KULZER, Wehrheim) and serially sectioned at 7 μm. The samples in the second chapter were embedded in Leica historesin embedding kit (Leica) and sectioned at 10 μm.

Isolation and characterization of dkk-1 cDNA clone

The zebrafish shield stage cDNA library provided by M. Clark and H. Lehrach was screened at low stringency with *Xenopus dkk-1* cDNA as probe, kindly provided by C. Niehrs. Two clones (MPMGp567L0854Q2 and MPMGp567E15148) out of 25 positive clones were found to be a *Xdkk-1* homologue. Sequencing of the two clones was performed using synthetic oligonucleotide primers in both directions using an automatic fluorescent sequencer LONG READIR 4200 (LI-COR). The nucleotide sequence of the Zfdkk-1 protein reported in this article is deposited in the GenBank nucleotide sequence database under the accession number AF116852.

Preparation of total RNA and Northern hybridization analysis

Total RNAs were prepared by the AGPC (Acid Guanidinium Phenol Chloroform) method (Chomczynski and Sacchi, 1987). 10 μg of denatured total RNA was loaded per lane. Transfer of RNA to the filter and hybridization were performed as described in Molecular Cloning (Sambrook et al., 1989) with some modifications.

Western blot analysis

Western blot analysis in the second chapter was performed by the standard method. Proteins were separated by 12% polyacrylamide gels and transferred to immunobilon™ membranes (Millipore) by electroblotting. Monoclonal antibody against FLAG was used to detect FLAG-tagged proteins. Western blot analysis in the third chapter was performed following of the standard method for ECL western Blotting Detection Reagent (Amersham pharmacia Biotech). Protein were separated by 12.5% polyacrylamide gels and transferred to Hybond™ ECL™ membranes (Amersham pharmacia Biotech) by electroblotting. Monoclonal antibody against dpERK was used at the same concentration as used in immunostaining. The homogenates were prepared from whole embryos at the 6- to 7-somite stage when *ace* homozygotes could be distinguished by morphology.

Immunohistochemistry

Immunostaining with anti-FLAG antibody (Kodak) was performed as previously described (Koshida et al., 1998) with some modifications. For whole-mount immunostaining with anti-dpERK, embryos were fixed with 3.7% formaldehyde/0.2% glutaraldehyde/PBS for 1 hour at the room temperature. After washing with PBS, they were dehydrated with methanol and transferred to PBS. Then, they were washed with MABT (MAB/0.1% TritonX-100) three times for 10 minutes and MABDT (MAB/0.1% TritonX-100/1% DMSO) twice for 30 minutes. After blocking with 2% FCS/MABDT, the embryos were incubated in the blocking solution containing 1:10000 anti-di-phosphorylated ERK1&2 (MAPK-YT) antibody (SIGMA) for overnight at 4°C. They were then washed with MABDT three times for 5 minutes, four times for 30 minutes, and incubated in blocking solution again for 30 minute, followed by incubation with the second antibody (1:500 anti-mouse IgG biotin conjugated antibody) for 2 hours at the room temperature. After the washing with MABDT as described above, the signals were detected with ABC staining kit according to the manufacturer's instructions (Vector Laboratory Inc). To examine ERK activation in *ace* homozygous mutants at 5-somite stage, embryos obtained from two heterozygous *ace* carriers were cut into two pieces at the level of the hindbrain, and they were fixed immediately. The anterior and posterior halves were then processed for dpERK or *myoD* staining, respectively.

mRNA and morpholino injection

Full-length *zfdkk-1*, full-length GFP, or out-frame *zfdkk-1* cDNA were cloned into the CS2+plasmid (Rupp et al., 1994) and capped sense RNAs were synthesized using the mMessage mMachine™ in vitro transcription kit (Ambion). mRNAs synthesized were subjected to microinjection into 1-2 cell stage embryos and injected embryos were grown in 0.3 xDanieau's solution (Westerfield, 1994) in the second chapter. In the third chapter, capped sense RNAs were synthesized using the same kit from the plasmid containing full-length Ras^{N17} (Deng and Karin, 1994), *bΔFR4* (Hongo et al., 1999), *fgf3*, *GFP* and *lacZ*. *GFP* and *lacZ* RNA were used as a control. The mRNAs were diluted to 0.8-1.0 μg/μl with distilled water and 200-500 ng/μl (Ras^{N17}), 400 ng/μl (*bΔFR4*) or/and 5 or 100 ng/μl

(*fgf3*) mRNAs were injected into 1- to 2-cell stage embryos. Morpholino oligonucleotides were solubilised in water at the concentration of 50 μg/μl. The resulting stock solution was diluted to working concentrations in water before injection into 1- to 2-cell stage embryos. Injected embryos were cultured in 1/3 Ringer's solution until use. The sequences of morpholino oligonucleotides used in the present study were as follows: standard control, 5'-CCTCTTACCTCAGTTACAATTTATA-3'; fgf8-MO, 5'-TCAACCGTGAAGGTATGAGTCTC-3'; fgf3-MO, 5'-TATAACCATTGTGGCA-TGGCGGGAT-3'.

COS7 cells transplantation

For transfection and transplantation of COS7 cells, I followed the protocol described in Koshida et al. (1998). 2 μg DNAs mixed with 10 μl lipofectamine (Qiagen) were transfected in a 12-well culture dish. DNAs including *Xenopus noggin*, *chordin* and *lacZ* cDNA cloned in pCDM8 (Invitrogen) or *zfdkk-1* cloned in FLAG-tagged pCMV-5 vectors (Sigma) were subjected for transfection.

Beads transplantation and SU5402 treatment

Mouse recombinant Fgf8b protein (R&D Systems) or BSA was used at the concentration of 0.25 μg/μl. Preparation of the beads soaked in Fgf8b or BSA were performed as described in Makita et al. (1998). Dechorionated embryos at tailbud stage were placed in 3% methylcellulose in 1/3 Ringer's solution and transplanted into the forebrain using a tungsten needle. After transplantation, embryos were cultured at 28.5°C in 1/3 Ringer's solution until use. For injection of SU5402, 10 mg/ml SU5402 (CALBIOCHEM) in DMSO was used. Dechorionated embryos were placed in 1.5% methylcellulose in 1/3 Ringer's solution and injected into thick head region at tailbud stage. DMSO was injected as a control. Alternatively, dechorionated embryos at proper stages were soaked for 10 minutes in SU5402/1/3 Ringer solution at a concentration of 0.1 mg/ml, and washed several times with 1/3 Ringer's solution. Treated embryos were cultured at 28.5°C in 1/3 Ringer's solution until use. I found that the activity of SU5402 varied much, depending on the lot number. Thus, the

incubation was sometimes carried out at a concentration of 0.2 mg/ml.

Detection of apoptosis

Apoptosis in zebrafish whole-mounts was detected according to a protocol given by the manufacturer with some modifications (Dead End™ Colorimetric Apoptosis Detection System; Promega). After fixation overnight in 4% paraformaldehyde in PBS, embryos were transferred in methanol and then rehydrated in PBST (PBS/0.1% Tween 20). Subsequently, embryos were digested in 5 μg/ml Proteinase K in PBS for 5 minutes and postfixed for 20 minutes in 4% paraformaldehyde in PBS. Then the embryos were immersed in acetone for 7 minutes at –20°C and incubated in the equilibration buffer (provided in the kit) for 10 minutes at the room temperature. After incubation 3 hours at 37°C in working strength terminal deoxynucleotidyl transferase (TdT) enzyme, the DNA endlabeling reaction using biotinylated dUTP was stopped by washing in 2XSSC and PBST. Biotin was detected by horseradish-peroxidase-labeled streptavidin with diaminobenzidine (DAB).

Acknowledgement

I would like to thank Drs M. Furutani-Seiki and W. Driever for providing the opportunity to study in their lab for one year and members in Dr W. Driever's lab for their helpful supports. I am also grateful to Drs S. Wilson and C. Houart for useful discussions, Dr M. Furutani-Seiki for providing unpublished cDNAs for zebrafish *frizzled2* and *5*, and Dr K. Rohr for providing an unpublished probe for zebrafish *nk2.1b*. I thank Dr C. Niehrs for the *Xenopus dkk-1* cDNA, Dr Y. Sasai for *Xenopus noggin* and *chordin* cDNAs, Dr R. Moon for *zfwnt8* cDNA, Dr E. Amaya for *XFD* cDNA, Dr H. Okamoto for *bΔFR4* cDNA, Drs T. Deng and M. Karin for Ras^{N17} cDNA, Dr. M. Furutani-Seiki for providing *oep* mutants, Dr M. Kobayashi for providing *ace* mutants, and Drs S. Krauss, U. Strähle, S. Higashijima, I. Dawid, S. Shulte-Marker, E. Weinberg, A. Zaraisky, M. Mishina, H. Mori, H. Okamoto, M. Hibi, M. Mione for providing probes.

Reference

Adelmann, H. B. (1936). The problem of cyclopia. *Quarterly Review of Biology* **11**, 284-304.

Akimenko, M. A., Ekker, M., Wegner, J., Lin, W. and Westerfield, M. (1994). Combinatorial expression of three zebrafish genes related to distal- less: part of a homeobox gene code for the head. *J Neurosci* **14**, 3475-86.

Alexandre, D., Clarke, J. D., Oxtoby, E., Yan, Y. L., Jowett, T. and Holder, N. (1996). Ectopic expression of Hoxa-1 in the zebrafish alters the fate of the mandibular arch neural crest and phenocopies a retinoic acid-induced phenotype. *Development* **122**, 735-46.

Allende, M. L. and Weinberg, E. S. (1994). The expression pattern of two zebrafish achaete-scute homolog (ash) genes is altered in the embryonic brain of the cyclops mutant. *Dev Biol* **166**, 509-30.

Amaya, E., Musci, T. J. and Kirschner, M. W. (1991). Expression of a dominant negative mutant of the FGF receptor disrupts mesoderm formation in Xenopus embryos. *Cell* **66**, 257-70.

Ang, S. L. and Rossant, J. (1994). HNF-3 beta is essential for node and notochord formation in mouse development. *Cell* **78**, 561-74.

Bang, A. G., Papalopulu, N., Kintner, C. and Goulding, M. D. (1997). Expression of Pax-3 is initiated in the early neural plate by posteriorizing signals produced by the organizer and by posterior non- axial mesoderm. *Development* **124**, 2075-85.

Barth, K. A. and Wilson, S. W. (1995). Expression of zebrafish nk2.2 is influenced by sonic hedgehog/vertebrate hedgehog-1 and demarcates a zone of neuronal differentiation in the embryonic forebrain. *Development* **121**, 1755-68.

Brand, M., Heisenberg, C. P., Warga, R. M., Pelegri, F., Karlstrom, R. O., Beuchle, D., Picker, A., Jiang, Y. J., Furutani, S. M., van, E. F. et al. (1996). Mutations affecting development of the midline and general body shape during zebrafish embryogenesis. *Development* **123**, 129-42.

Campuzano, S. and Modolell, J. (1992). Patterning of the Drosophila nervous system: the achaete-scute gene complex. *Trends Genet* **8**, 202-8.

Carl, M. and Wittbrodt, J. (1999). Graded interference with FGF signaling reveals its dorsoventral asymmetry at the mid-hindbrain boundary. *Development* **126**, 5659-67.

Catala, M., Teillet, M. A., De, R. E. and Le, D. M. (1996). A spinal cord fate map in the avian embryo: while regressing, Hensen's node lays down the notochord and floor plate thus joining the spinal cord lateral walls. *Development* **122**, 2599-610.

Chang, B. E., Blader, P., Fischer, N., Ingham, P. W. and Strahle, U. (1997). Axial (HNF3beta) and retinoic acid receptors are regulators of the zebrafish sonic hedgehog promoter. *Embo J* **16**, 3955-64.

Chiang, C., Litingtung, Y., Lee, E., Young, K. E., Corden, J. L., Westphal, H. and Beachy, P. A. (1996). Cyclopia and defective axial patterning in mice lacking Sonic hedgehog gene function. *Nature* **383**, 407-13.

Chomczynski, P. and Sacchi, N. (1987). Single-step method of RNA isolation by acid guanidinium thiocyanate- phenol-chloroform extraction. *Anal Biochem* **162**, 156-9.

Christen, B. and Slack, J. M. (1999). Spatial response to fibroblast growth factor signalling in Xenopus embryos. *Development* **126**, 119-25.

Cobb, M. H. and Goldsmith, E. J. (1995). How MAP kinases are regulated. *J Biol Chem* **270**, 14843-6.

Crews, C. M., Alessandrini, A. and Erikson, R. L. (1992). The primary structure of MEK, a protein kinase that phosphorylates the ERK gene product. *Science* **258**, 478-80.

Dale, J. K., Vesque, C., Lints, T. J., Sampath, T. K., Furley, A., Dodd, J. and Placzek, M. (1997). Cooperation of BMP7 and SHH in the induction of forebrain ventral midline cells by prechordal mesoderm. *Cell* **90**, 257-69.

Deng, T. and Karin, M. (1994). c-Fos transcriptional activity stimulated by H-Ras-activated protein kinase distinct from JNK and ERK. *Nature* **371**, 171-5.

Detrich, H. r., Kieran, M. W., Chan, F. Y., Barone, L. M., Yee, K., Rundstadler, J. A., Pratt, S., Ransom, D. and Zon, L. I. (1995). Intraembryonic hematopoietic cell migration during

vertebrate development. *Proc Natl Acad Sci U S A* **92**, 10713-7.

Driever, W., Solnica, K. L., Abdelilah, S., Meyer, D. and Stemple, D. (1997). Genetic analysis of pattern formation in the zebrafish neural plate. *Cold Spring Harb Symp Quant Biol* **62**, 523-34.

Echelard, Y., Epstein, D. J., St, J. B., Shen, L., Mohler, J., McMahon, J. A. and McMahon, A. P. (1993). Sonic hedgehog, a member of a family of putative signaling molecules, is implicated in the regulation of CNS polarity. *Cell* **75**, 1417-30.

Ekker, M., Wegner, J., Akimenko, M. A. and Westerfield, M. (1992). Coordinate embryonic expression of three zebrafish engrailed genes. *Development* **116**, 1001-10.

Fekany-Lee, K., Gonzalez, E., Miller-Bertoglio, V. and Solnica-Krezel, L. (2000). The homeobox gene bozozok promotes anterior neuroectoderm formation in zebrafish through negative regulation of BMP2/4 and wnt pathways. *Development* **127**, 2333-45.

Feldman, B., Gates, M. A., Egan, E. S., Dougan, S. T., Rennebeck, G., Sirotkin, H. I., Schier, A. F. and Talbot, W. S. (1998). Zebrafish organizer development and germ-layer formation require nodal- related signals. *Nature* **395**, 181-5.

Fjose, A., Izpisua, B. J., Fromental, R. C. and Duboule, D. (1994). Expression of the zebrafish gene hlx-1 in the prechordal plate and during CNS development. *Development* **120**, 71-81.

Furthauer, M., Thisse, C. and Thisse, B. (1997). A role for FGF-8 in the dorsoventral patterning of the zebrafish gastrula. *Development* **124**, 4253-64.

Gabay, L., Seger, R. and Shilo, B. Z. (1997a). In situ activation pattern of Drosophila EGF receptor pathway during development. *Science* **277**, 1103-6.

Gabay, L., Seger, R. and Shilo, B. Z. (1997b). MAP kinase in situ activation atlas during Drosophila embryogenesis. *Development* **124**, 3535-41.

Glinka, A., Wu, W., Onichtchouk, D., Blumenstock, C. and Niehrs, C. (1997). Head induction by simultaneous repression of Bmp and Wnt signalling in Xenopus. *Nature* **389**, 517-9.

Glinka, A., Wu, W., Delius, H., Monaghan, A. P., Blumenstock, C. and Niehrs, C. (1998). Dickkopf-1 is a member of a new family of secreted proteins and functions in head induction. *Nature* **391**, 357-62.

Gotoh, Y. and Nishida, E. (1996). Signals for mesoderm induction. Roles of fibroblast growth factor (FGF)/mitogen-activated protein kinase (MAPK) pathway. *Biochim Biophys Acta* **1288**, F1-7.

Grinblat, Y., Gamse, J., Patel, M. and Sive, H. (1998). Determination of the zebrafish forebrain: induction and patterning. *Development* **125**, 4403-16.

Gritsman, K., Zhang, J., Cheng, S., Heckscher, E., Talbot, W. S. and Schier, A. F. (1999). The EGF-CFC protein one-eyed pinhead is essential for nodal signaling. *Cell* **97**, 121-32.

Halpern, M. E., Ho, R. K., Walker, C. and Kimmel, C. B. (1993). Induction of muscle pioneers and floor plate is distinguished by the zebrafish no tail mutation. *Cell* **75**, 99-111.

Halpern, M. E., Thisse, C., Ho, R. K., Thisse, B., Riggleman, B., Trevarrow, B., Weinberg, E. S., Postlethwait, J. H. and Kimmel, C. B. (1995). Cell-autonomous shift from axial to paraxial mesodermal development in zebrafish floating head mutants. *Development* **121**, 4257-64.

Halpern, M. E., Hatta, K., Amacher, S. L., Talbot, W. S., Yan, Y. L., Thisse, B., Thisse, C., Postlethwait, J. H. and Kimmel, C. B. (1997). Genetic interactions in zebrafish midline development. *Dev Biol* **187**, 154-70.

Hammerschmidt, M., Pelegri, F., Mullins, M. C., Kane, D. A., Brand, M., van, E. F., Furutani, S. M., Granato, M., Haffter, P., Heisenberg, C. P. et al. (1996). Mutations affecting morphogenesis during gastrulation and tail formation in the zebrafish, Danio rerio. *Development* **123**, 143-51.

Hashimoto, H., Itoh, M., Yamanaka, Y., Yamashita, S., Shimizu, T., Solnica-Krezel, L., Hibi, M. and Hirano, T. (2000). Zebrafish Dkk1 functions in forebrain specification and axial mesendoderm formation. *Dev Biol* **217**, 138-52.

Hatta, K., Kimmel, C. B., Ho, R. K. and Walker, C. (1991). The cyclops mutation blocks specification of the floor plate of the zebrafish central nervous system. *Nature* **350**, 339-41.

Hatta, K., Puschel, A. W. and Kimmel, C. B. (1994). Midline signaling in the primordium of the zebrafish anterior central nervous system. *Proc Natl Acad Sci U S A* **91**, 2061-5.

Hemmati-Brivanlou, A. and Melton, D. (1997). Vertebrate embryonic cells will become nerve cells unless told otherwise. *Cell* **88**, 13-7.

Higashijima, S., Nose, A., Eguchi, G., Hotta, Y. and Okamoto, H. (1997). Mindin/F-spondin family: novel ECM proteins expressed in the zebrafish embryonic axis. *Dev Biol* **192**, 211-27.

Hirano, S., Fuse, S. and Sohal, G. S. (1991). The effect of the floor plate on pattern and polarity in the developing central nervous system. *Science* **251**, 310-3.

Hongo, I., Kengaku, M. and Okamoto, H. (1999). FGF signaling and the anterior neural induction in Xenopus. *Dev Biol* **216**, 561-81.

Houart, C., Westerfield, M. and Wilson, S. W. (1998). A small population of anterior cells patterns the forebrain during zebrafish gastrulation. *Nature* **391**, 788-92.

Inoue, A., Takahashi, M., Hatta, K., Hotta, Y. and Okamoto, H. (1994). Developmental regulation of islet-1 mRNA expression during neuronal differentiation in embryonic zebrafish. *Dev Dyn* **199**, 1-11.

Joyner, A. L. (1996). Engrailed, Wnt and Pax genes regulate midbrain--hindbrain development. *Trends Genet* **12**, 15-20.

Kazanskaya, O., Glinka, A. and Niehrs, C. (2000). The role of xenopus dickkopf1 in prechordal plate specification and neural patterning. *Development* **127**, 4981-92.

Kazanskaya, O. V., Severtzova, E. A., Barth, K. A., Ermakova, G. V., Lukyanov, S. A., Benyumov, A. O., Pannese, M., Boncinelli, E., Wilson, S. W. and Zaraisky, A. G. (1997). Anf: a novel class of vertebrate homeobox genes expressed at the anterior end of the main embryonic axis. *Gene* **200**, 25-34.

Kelly, G. M., Greenstein, P., Erezyilmaz, D. F. and Moon, R. T. (1995). Zebrafish wnt8 and wnt8b share a common activity but are involved in distinct developmental pathways. *Development* **121**, 1787-99.

Kimmel, C. B., Ballard, W. W., Kimmel, S. R., Ullmann, B. and Schilling, T. F. (1995). Stages of embryonic development of the zebrafish. *Dev Dyn* **203**, 253-310.

Klint, P. and Claesson-Welsh, L. (1999). Signal transduction by fibroblast growth factor receptors. *Front Biosci* **4**, D165-77.

Koshida, S., Shinya, M., Mizuno, T., Kuroiwa, A. and Takeda, H. (1998). Initial anteroposterior pattern of the zebrafish central nervous system is determined by differential competence of the epiblast. *Development* **125**, 1957-66.

Koshida, S. (1999). ゼブラフィッシュ中枢神経系発生における前後軸に沿った部域特異性の成立機構. Doctoral Thesis, Nagoya University.

Krauss, S., Johansen, T., Korzh, V. and Fjose, A. (1991). Expression of the zebrafish paired box gene pax[zf-b] during early neurogenesis. *Development* **113**, 1193-206.

Krauss, S., Concordet, J. P. and Ingham, P. W. (1993). A functionally conserved homolog of the Drosophila segment polarity gene hh is expressed in tissues with polarizing activity in zebrafish embryos. *Cell* **75**, 1431-44.

Leyns, L., Bouwmeester, T., Kim, S. H., Piccolo, S. and De, R. E. (1997). Frzb-1 is a secreted antagonist of Wnt signaling expressed in the Spemann organizer. *Cell* **88**, 747-56.

Li, Y., Allende, M. L., Finkelstein, R. and Weinberg, E. S. (1994). Expression of two zebrafish orthodenticle-related genes in the embryonic brain. *Mech Dev* **48**, 229-44.

Lumsden, A. and Krumlauf, R. (1996). Patterning the vertebrate neuraxis. *Science* **274**, 1109-15.

Lun, K. and Brand, M. (1998). A series of no isthmus (noi) alleles of the zebrafish pax2.1 gene reveals multiple signaling events in development of the midbrain- hindbrain boundary. *Development* **125**, 3049-62.

Macdonald, R., Xu, Q., Barth, K. A., Mikkola, I., Holder, N., Fjose, A., Krauss, S. and Wilson, S. W. (1994). Regulatory gene expression boundaries demarcate sites of neuronal differentiation in the embryonic zebrafish forebrain. *Neuron* **13**, 1039-53.

Makita, R., Mizuno, T., Koshida, S., Kuroiwa, A. and Takeda, H. (1998). Zebrafish wnt11: pattern and regulation of the expression by the yolk cell and No tail activity. *Mech Dev* **71**, 165-76.

Marti, E., Bumcrot, D. A., Takada, R. and McMahon, A. P. (1995). Requirement of 19K form of Sonic hedgehog for induction of distinct ventral cell types in CNS explants. *Nature* **375**, 322-5.

Maruoka, Y., Ohbayashi, N., Hoshikawa, M., Itoh, N., Hogan, B. L. M. and Furuta, Y. (1998). Comparison of the expression of three highly related genes, Fgf8, Fgf17 and Fgf18, in the mouse embryo. *Mech Dev* **74**, 175-7.

Melby, A. E., Warga, R. M. and Kimmel, C. B. (1996). Specification of cell fates at the dorsal margin of the zebrafish gastrula. *Development* **122**, 2225-37.

Meyers, E. N., Lewandoski, M. and Martin, G. R. (1998). An Fgf8 mutant allelic series generated by Cre- and Flp-mediated recombination. *Nat Genet* **18**, 136-41.

Miller, B. V., Fisher, S., Sanchez, A., Mullins, M. C. and Halpern, M. E. (1997). Differential regulation of chordin expression domains in mutant zebrafish. *Dev Biol* **192**, 537-50.

Mione, M., Shanmugalingam, S., Kimelman, D. and Griffin, K. (2001). Overlapping expression of zebrafish T-brain-1 and eomesodermin during forebrain development. *Mech Dev* **100**, 93-97.

Miyagawa, T., Amanuma, H., Kuroiwa, A. and Takeda, H. (1996). Specification of posterior midbrain region in zebrafish neuroepithelium. *Genes Cells* **1**, 369-77.

Mizuno, T., Yamaha, E., Wakahara, M., Kuroiwa, A. and Takeda, H. (1996). Mesoderm induction in zebrafish. *Nature* **383**, 131-132.

Mizuno, T., Yamaha, E., Kuroiwa, A. and Takeda, H. (1999). Removal of vegetal yolk causes dorsal deficencies and impairs dorsal- inducing ability of the yolk cell in zebrafish. *Mech Dev* **81**, 51-63.

Mohammadi, M., McMahon, G., Sun, L., Tang, C., Hirth, P., Yeh, B. K., Hubbard, S. R. and Schlessinger, J. (1997). Structures of the tyrosine kinase domain of fibroblast growth factor receptor in complex with inhibitors. *Science* **276**, 955-60.

Molven, A., Njolstad, P. R. and Fjose, A. (1991). Genomic structure and restricted neural expression of the zebrafish wnt- 1 (int-1) gene. *Embo J* **10**, 799-807.

Mori, H., Miyazaki, Y., Morita, T., Nitta, H. and Mishina, M. (1994). Different spatio-temporal expressions of three otx homeoprotein transcripts during zebrafish embryogenesis. *Brain Res Mol Brain Res* **27**, 221-31.

Morita, T., Nitta, H., Kiyama, Y., Mori, H. and Mishina, M. (1995). Differential expression of two zebrafish emx homeoprotein mRNAs in the developing brain. *Neurosci Lett* **198**, 131-4.

Muller, M., Weizsacker, E. v. and Campos-Ortega, J. A. (1996). Transcription of a zebrafish gene of the hairy-Enhancer of split family delineates the midbrain anlage in the neural plate. *Devlopmental Genes Evolution* **206**, 153-160.

Müller, F., Albert, S., Blader, P., Fischer, N., Hallonet, M. and Strahle, U. (2000). Direct action of the nodal-related signal cyclops in induction of sonic hedgehog in the ventral midline of the CNS. *Development* **127**, 3889-97.

Nasevicius, A. and Ekker, S. C. (2000). Effective targeted gene 'knockdown' in zebrafish. *Nat Genet* **26**, 216-20.

Neave, B., Rodaway, A., Wilson, S. W., Patient, R. and Holder, N. (1995). Expression of zebrafish GATA 3 (gta3) during gastrulation and neurulation suggests a role in the specification of cell fate. *Mech Dev* **51**, 169-82.

Nieuwkoop, P. D. (1952). Activation and organization of the central nervous system in amphibians. *J Exp Zool* **120**, 1-108.

Nieuwkoop, P. D. (1985). Inductive interactions in early amphibian development and their general nature. *J Embryol Exp Morphol* **89**, 333-47.

Ornitz, D. M. (2000). FGFs, heparan sulfate and FGFRs: complex interactions essential for development. *Bioessays* **22**, 108-12.

Oxtoby, E. and Jowett, T. (1993). Cloning of the zebrafish krox-20 gene (krx-20) and its expression during hindbrain development. *Nucleic Acids Res* **21**, 1087-95.

Piccolo, S., Sasai, Y., Lu, B. and De, R. E. (1996). Dorsoventral patterning in Xenopus: inhibition of ventral signals by direct binding of chordin to BMP-4. *Cell* **86**, 589-98.

Piccolo, S., Agius, E., Leyns, L., Bhattacharyya, S., Grunz, H., Bouwmeester, T. and De Robertis, E. M. (1999). The head inducer Cerberus is a multifunctional antagonist of Nodal, BMP and Wnt signals. *Nature* **397**, 707-10.

Placzek, M., Yamada, T., Tessier-Lavigne, M., Jessell, T. and Dodd, J. (1991). Control of

dorsoventral pattern in vertebrate neural development: induction and polarizing properties of the floor plate. *Development* **Suppl**, 105-22.

Placzek, M., Jessell, T. M. and Dodd, J. (1993). Induction of floor plate differentiation by contact-dependent, homeogenetic signals. *Development* **117**, 205-18.

Placzek, M. and Furley, A. (1996). Patterning cascades in the neural tube. Neural development. *Curr Biol* **6**, 526-9.

Reifers, F., Bohli, H., Walsh, E. C., Crossley, P. H., Stainier, D. Y. and Brand, M. (1998). Fgf8 is mutated in zebrafish acerebellar (ace) mutants and is required for maintenance of midbrain-hindbrain boundary development and somitogenesis. *Development* **125**, 2381-95.

Riddle, R. D., Johnson, R. L., Laufer, E. and Tabin, C. (1993). Sonic hedgehog mediates the polarizing activity of the ZPA. *Cell* **75**, 1401-16.

Roelink, H., Porter, J. A., Chiang, C., Tanabe, Y., Chang, D. T., Beachy, P. A. and Jessell, T. M. (1995). Floor plate and motor neuron induction by different concentrations of the amino-terminal cleavage product of sonic hedgehog autoproteolysis. *Cell* **81**, 445-55.

Rohr, K. B. and Concha, M. L. (2000). Expression of nk2.1a during early development of the thyroid gland in zebrafish. *Mech Dev* **95**, 267-70.

Rohr, K., Barth , K. A., Varga, Z. M. and Wilson, S. W. (2001). The Nodal pathway acts upstream of Hedgehog signaling to specify ventral telencephalic identity. *Neuron*, in press.

Rubenstein, J. L., Shimamura, K., Martinez, S. and Puelles, L. (1998). Regionalization of the prosencephalic neural plate. *Annu Rev Neurosci* **21**, 445-77.

Rupp, R. A., Snider, L. and Weintraub, H. (1994). Xenopus embryos regulate the nuclear localization of XMyoD. *Genes Dev* **8**, 1311-23.

Sagerstrom, C. G., Grinbalt, Y. and Sive, H. (1996). Anteroposterior patterning in the zebrafish, Danio rerio: an explant assay reveals inductive and suppressive cell interactions. *Development* **122**, 1873-83.

Sambrook, S., Fritsch, E. F. and Maniatis, T. (1989). Molecular Cloning: A Laboratory Manual. Cold Spring Harbor, New York: Cold Spring Harbor Laboratory Press.

Sampath, K., Rubinstein, A. L., Cheng, A. M., Liang, J. O., Fekany, K., Solnica, K. L., Korzh, V., Halpern, M. E. and Wright, C. V. (1998). Induction of the zebrafish ventral brain and floorplate requires cyclops/nodal signalling. *Nature* **395**, 185-9.

Sasaki, H., Hui, C., Nakafuku, M. and Kondoh, H. (1997). A binding site for Gli proteins is essential for HNF-3beta floor plate enhancer activity in transgenics and can respond to Shh in vitro. *Development* **124**, 1313-22.

Schauerte, H. E., van Eeden, F. J., Fricke, C., Odenthal, J., Strahle, U. and Haffter, P. (1998). Sonic hedgehog is not required for the induction of medial floor plate cells in the zebrafish. *Development* **125**, 2983-93.

Schier, A. F., Neuhauss, S. C., Harvey, M., Malicki, J., Solnica, K. L., Stainier, D. Y., Zwartkruis, F., Abdelilah, S., Stemple, D. L., Rangini, Z. et al. (1996). Mutations affecting the development of the embryonic zebrafish brain. *Development* **123**, 165-78.

Schier, A. F., Neuhauss, S. C., Helde, K. A., Talbot, W. S. and Driever, W. (1997). The one-eyed pinhead gene functions in mesoderm and endoderm formation in zebrafish and interacts with no tail. *Development* **124**, 327-42.

Schulte-Merker, S., Ho, R. K., Herrmann, B. G. and Nusslein, V. C. (1992). The protein product of the zebrafish homologue of the mouse T gene is expressed in nuclei of the germ ring and the notochord of the early embryo. *Development* **116**, 1021-32.

Schulte-Merker, S., Hammerschmidt, M., Beuchle, D., Cho, K. W., De, R. E. and Nusslein, V. C. (1994). Expression of zebrafish goosecoid and no tail gene products in wild- type and mutant no tail embryos. *Development* **120**, 843-52.

Schulte-Merker, S., Lee, K. J., McMahon, A. P. and Hammerschmidt, M. (1997). The zebrafish organizer requires chordino. *Nature* **387**, 862-3.

Shanmugalingam, S., Houart, C., Picker, A., Reifers, F., Macdonald, R., Barth, A., Griffin, K., Brand, M. and Wilson, S. W. (2000). Ace/Fgf8 is required for forebrain commissure formation and patterning of the telencephalon. *Development* **127**, 2549-61.

Shih, J. and Fraser, S. E. (1995). Distribution of tissue progenitors within the shield region of the

zebrafish gastrula. *Development* **121**, 2755-65.

Shih, J. and Fraser, S. E. (1996). Characterizing the zebrafish organizer: microsurgical analysis at the early-shield stage. *Development* **122**, 1313-22.

Shimamura, K., Hartigan, D. J., Martinez, S., Puelles, L. and Rubenstein, J. L. (1995). Longitudinal organization of the anterior neural plate and neural tube. *Development* **121**, 3923-33.

Shimamura, K. and Rubenstein, J. L. (1997). Inductive interactions direct early regionalization of the mouse forebrain. *Development* **124**, 2709-18.

Simeone, A. (2000). Positioning the isthmic organizer where Otx2 and Gbx2meet. *Trends Genet* **16**, 237-40.

Spemann, H. (1938). Embryonic Development and Induction: Yale University Press, New Haven.

Stachel, S. E., Grunwald, D. J. and Myers, P. Z. (1993). Lithium perturbation and goosecoid expression identify a dorsal specification pathway in the pregastrula zebrafish. *Development* **117**, 1261-74.

Strahle, U., Blader, P., Henrique, D. and Ingham, P. W. (1993). Axial, a zebrafish gene expressed along the developing body axis, shows altered expression in cyclops mutant embryos. *Genes Dev* **7**, 1436-46.

Strahle, U., Jesuthasan, S., Blader, P., Garcia-Villalba, P., Hatta, K. and Ingham, P. W. (1998). one-eyed pinhead is required for development of the ventral midline of the zebrafish (Danio rerio) neural tube. *Genes and Function* **1**, 131-148.

Takeda, H., Matsuzaki, T., Oki, T., Miyagawa, T. and Amanuma, H. (1994). A novel POU domain gene, zebrafish pou2: expression and roles of two alternatively spliced twin products in early development. *Genes Dev* **8**, 45-59.

Tanabe, Y. and Jessell, T. M. (1996). Diversity and pattern in the developing spinal cord. *Science* **274**, 1115-23.

Thisse, C., Thisse, B., Halpern, M. E. and Postlethwait, J. H. (1994). Goosecoid expression in neurectoderm and mesendoderm is disrupted in zebrafish cyclops gastrulas. *Dev Biol* **164**, 420-9.

Thisse, C. and Thisse, B. (1998). Antivin, a novel and divergent member of the TGFbeta superfamily, negatively regulates mesoderm induction. *Development*, 229-240.

Thomas, P. and Beddington, R. (1996). Anterior primitive endoderm may be responsible for patterning the anterior neural plate in the mouse embryo. *Curr Biol* **6**, 1487-96.

Toivonen, S. and Saxen, L. (1968). Morphogenetic interaction of presumptive neural and mesodermal cells mixed in different ratios. *Science* **159**, 539-40.

Toresson, H., Martinez-Barbera, J. P., Bardsley, A., Caubit, X. and Krauss, S. (1998). Conservation of BF-1 expression in amphioxus and zebrafish suggests evolutionary ancestry of anterior cell types that contribute to the vertebrate telencephalon. *Dev Genes Evol* **208**, 431-9.

Ungar, A. R. and Moon, R. T. (1996). Inhibition of protein kinase A phenocopies ectopic expression of hedgehog in the CNS of wild-type and cyclops mutant embryos. *Dev Biol* **178**, 186-91.

Wang, S., Krinks, M., Lin, K., Luyten, F. P. and Moos, M. J. (1997a). Frzb, a secreted protein expressed in the Spemann organizer, binds and inhibits Wnt-8. *Cell* **88**, 757-66.

Wang, S., Krinks, M. and Moos, M. J. (1997b). Frzb-1, an antagonist of Wnt-1 and Wnt-8, does not block signaling by Wnts -3A, -5A, or -11. *Biochem Biophys Res Commun* **236**, 502-4.

Weinberg, E. S., Allende, M. L., Kelly, C. S., Abdelhamid, A., Murakami, T., Andermann, P., Doerre, O. G., Grunwald, D. J. and Riggleman, B. (1996). Developmental regulation of zebrafish MyoD in wild-type, no tail and spadetail embryos. *Development* **122**, 271-80.

Weinstein, D. C., Ruiz, i, Altaba, A, Chen, W. S., Hoodless, P., Prezioso, V. R., Jessell, T. M. and Darnell, J. J. (1994). The winged-helix transcription factor HNF-3 beta is required for notochord development in the mouse embryo. *Cell* **78**, 575-88.

Westerfield, M. (1994). The Zebrafish Book: A Guide for the Laboratory use of Zebrafish (Brachydanio rerio): Institute of Nueroscience, University of Oregon.

Whitlock, K. E. and Westerfield, M. (2000). The olfactory placodes of the zebrafish form by convergence of cellular fields at the edge of the neural plate. *Development* **127**, 3645-53.

Wilson, E. T., Cretekos, C. J. and Helde, K. A. (1995). Cell mixing during early epiboly in the zebrafish embryo. *Dev Genet* **17**, 6-15.

Wilson, S. W. and Rubenstein, J. L. R. (2000). Induction and dorsoventral patterning of the telencephalon. *Neuron* **28**, 641-51.

Woo, K. and Fraser, S. E. (1995). Order and coherence in the fate map of the zebrafish nervous system. *Development* **121**, 2595-609.

Woo, K. and Fraser, S. E. (1997). Specification of the zebrafish nervous system by nonaxial signals. *Science* **277**, 254-7.

Xu, J., Lawshe, A., MacArthur, C. A. and Ornitz, D. M. (1999). Genomic structure, mapping, activity and expression of fibroblast growth factor 17. *Mech Dev* **83**, 165-78.

Yamada, T., Placzek, M., Tanaka, H., Dodd, J. and Jessell, T. M. (1991). Control of cell pattern in the developing nervous system: polarizing activity of the floor plate and notochord. *Cell* **64**, 635-47.

Yamanaka, Y., Mizuno, T., Sasai, Y., Kishi, M., Takeda, H., Kim, C. H., Hibi, M. and Hirano, T. (1998). A novel homeobox gene, dharma, can induce the organizer in a non-cell-autonomous manner. *Genes Dev* **12**, 2345-53.

Zhang, J., Talbot, W. S. and Schier, A. F. (1998). Positional cloning identifies zebrafish one-eyed pinhead as a permissive EGF-related ligand required during gastrulation. *Cell* **92**, 241-51.

Table 1. Distribution of donor and host cells in the ventral midline of the chimeric neural tube induced by shield transplantation*

Transplantation Donor/host	Type of transplant† (Composition)	Percentage of each group (%)	Total number of transplants examined (n)
oep /Wild (W)	Group I (W only)	100	37
Wild (W)/*oep*	Group I (*oep* only)	45.8	59
	Group II (*oep* and W)	40.7	59
	Group III (W only)	13.5	59

*The host embryos transplanted with biotin-labeled shield cells were fixed and examined with floor-plate markers, with biotin-peroxidase staining used to visualize donor cells. Serial sections of the secondary axes were made and examined for the distribution of donor (labeled) and host (unlabeled) cells. Only the cells located at the ventral midline of the neural tube were counted.

†Based on the distribution pattern of donor cells, transplants were divided into three classes: ventral midline of the neural tube made up of only host cells (Group I), of both host and donor cells (Group II), and of only donor cells (Group III).

Table 2. Inhibition of Wnt signaling by Zfdkk-1*

Injected mRNA (pg)	Phenotypes (%)							
	I	II	III	IV	V	VI	VII	*N*
wnt8 +fz2	0	3	5	52	18	4	18	77
wnt8 +fz2 +dkk-1 (6)	45	37	14	0	0	0	5	65
wnt8 +fz2 +dkk-1 (12)	86	2	9	2	2	0	0	66
wnt8 +fz2 +dkk-1 (25)	96	3	1	0	0	0	0	69
wnt8 +fz5	0	8	2	38	2	28	22	50
wnt8 +fz5 +dkk-1 (6)	40	45	0	1	0	0	13	84
wnt8 +fz5 +dkk-1 (12)	72	17	10	0	0	0	0	69
wnt8 +fz5 +dkk-1 (25)	98	0	2	0	0	0	0	54

**zfdkk-1* mRNA was injected with 0.2 pg *zfwnt8* and 25 pg *zffz2* or *5* .

I: Embryos with a big head region which is a phenotype raised by *zfdkk-1* injection. II: Normal embryos. III-VII: Embryos with phenotypes raised by over activation of Wnt signaling; III: Embryos with a short axis, IV: Embryos with forebrain defects, V: Embryos with a short axis and forebrain defects, VI: Bustled or radialized embryos, and VII: Embryos with secondary axis. *N* : Total number of embryos examined.

Table 3. Classification of *zfdkk-1* RNA injected phenotypes*

Phenotype	Injection dose (pg)					
	500	200	100	50	25	12.5
Normal	0	0	0	0	0	8
I	0	16	28	53	86	86
II	28	50	36	28	12	0
III	43	30	31	15	2	0
IV	26	0	0	0	0	0
Others†	3	4	5	4	0	6
Total number	141	164	108	138	150	147

*Numbers in the table represent percentage of injected embryos displaying that class of phenotype.

I: Embryos with a big head but no apparent accompanying axial defects.

II: Embryos with a big head and short axis.

III: Embryos with a big head but no notochord.

IV: Embryos with a big head but no notochord nor somites.

†Embryos with defects attributed to injection artifacts.

Table 4. Alteration of *dlx2* expression in the telencephalon of SU5402 soaked embryos

Treated stages	I	II	III	n
tailbud	46.7%	53.3%	0%	15
5-somite	20.0%	45.0%	35.0%	20
10-somite	0%	0%	100.0%	21
15-somite	0%	0%	100.0%	21

Embryos at each developmental stage were treated with 0.1 or 0.2 mg/ml SU5402 for 10 minutes and analysed *dlx2* expression in the telencephalon at 24 hpf. I: no *dlx2* expression, II: reduced *dlx2* expression, III: normal *dlx2* expression. n indicates the total number of the trearted embryos.

Figure legends

Fig. 1. Floor-plate development in chimeric secondary axes in which donor cells distribute in the notochord. In cross sections (D-K), black arrowheads indicate ventral midline host cells expressing floor-plate markers. Donor cells were stained light brown after biotin-peroxidase reaction. (A) Schematic representation of shield transplantation. Cells (about 100 cells) taken from the shield region of labeled donor embryos (wild-type or *oep*) were inserted into the ventral side of the host embryos (wild-type or *oep*) of the same developmental stage (6 hpf; shield stage). The host embryos were fixed at the 18-somite stage (18 hpf) and examined for *shh* (D-F), *F-spondin* (G-I) and *axial* (J, K) expression. (B) Lateral view of the wild-type host transplanted with wild-type shield, hybridized with *shh* probe. The white arrowhead indicates the secondary axis. Anterior is to the top. (C) The donor embryos (90%-epiboly) hybridized with the *gsc* probe. About one-fourth of the donor embryos were negative for *gsc* expression (two embryos to the right) and determined to be *oep* homozygous mutants. (D, G, J) Cross sections of the induced neural tube in which the donor and host cells were wild-type. Host cells in the ventral midline express the floor-plate markers. (E, H) Cross sections of the induced neural tube in which the host cells were wild-type and the donor cells were *oep* mutants. The wild-type host cells in the ventral midline express floor-plate markers. (F, I, K) Cross sections of the induced neural tube in which the host cells were *oep* mutants and the donor cells were wild-type. Note that no expression of the floor-plate markers was detected in the mutant neural tube overlying the wild-type notochord. es, embryonic shield; n, notochord. Scale bars: 300 μm in B, 400 μm in C and 20 μm in D-K.

Fig. 2. Floor-plate development in chimeric secondary axes in which donor cells distribute in the notochord and ventral neural tube. In cross sections (A-H), arrowheads indicate ventral midline host cells expressing floor-plate markers, while arrows indicate the donor cells expressing floor-plate markers in the ventral midline. Donor cells were stained light brown after biotin-peroxidase reaction. (A, D, G) Cross sections of the induced neural tube in which the donor and host cells were wild-

type. Donor cells distributed in the ventral midline, express floor-plate markers. (B, E) Cross sections of the induced neural tube in which the host cells were wild-type and the donor cells were *oep* mutants. The wild-type host cells in the ventral midline express floor-plate markers. Note that *oep* mutant donor cells (labeled) never contribute to the ventral midline. (C, F, H) Cross sections of the induced neural tube in which the host cells were *oep* mutants and the donor cells were wild-type. Note that no floor-plate markers expressed in the mutant neural tube overlying the wild-type notochord. Dashed lines represent the ventral border of the neural tube. In about half the cases, the wild-type donor cells were incorporated into the ventral midline and expressed floor-plate markers. In (C), *oep* mutant cells around the wild-type donor cells in the ventral midline look light blue. This was artificially achieved during photo processing. n, notochord. Scale bars: 20 μm.

Fig. 3. Serial analysis of floor-plate development in the chimeric secondary axes, in which wild-type donor cells were located at the ventral midline of *oep* mutant hosts. Arrowheads indicate the cells expressing floor-plate markers at the ventral midline, while arrows indicate those negative for the markers. Donor cells were stained light brown. Dashed lines represent the ventral border of the neural tube. All pictures were taken from sections at the level of anterior hindbrain. I obtained essentially the same results in the spinal cord region. (A-C, D-F) Serial cross sections (7 μm) taken from the *oep* host in which a group of wild-type donor cells was present in the ventral midline. The hosts were hybridized with *shh* (A-C; at 18-somite stage) or *axial* (D-F; at 8-somite stage) probe. The pictures are arranged rostral (A, D) to caudal (C, F), showing that wild-type (donor) cells adjacent to mutant (host) cells were negative for either *shh* (arrow in B) or *axial* (arrow in E), while those located inside (more caudally) were positive (arrowheads in C, F). In (C), *oep* mutant cells around the wild-type donor cells in the ventral midline look light blue. This was artificially achieved during photo processing. Two serial sections between (A) and (B) showing the same tendency as (B), and one section between (E) and (F) showing the same tendency as (E) were omitted. (G) Schematic drawing showing a lateral view of the secondary axis in which the above data are summarized. Lines connect midline cells to their corresponding pictures. Scale bar: 20 μm

Fig. 4. Floor-plate development of the donor cells in the primary axis of genetic chimeras, obtained by cell transplantation. In cross sections (B-G), black arrowheads indicate the cells expressing *shh* at the ventral midline, while black arrows indicate those negative for *shh*. Donor cells were stained light brown. Dashed line represents the ventral border of the neural tube. (A) Schematic representation of cell transplantation. Cells (about 100 cells) from labeled embryos (wild-type) were injected into unlabeled hosts (wild-type or *oep*) of the same developmental stage (4 hpf; sphere stage). The host embryos were fixed at the 18-somite stage (18 hpf) and examined for *shh* expression. (B, C) Sections from the hosts in which the donor and host cells were wild-type. Both host (B) and donor (C) cells in the ventral midline were positive for *shh*. (D-G) Serial sections (7 μm) taken from the *oep* host in which a group of wild-type donor cells were present in the ventral midline. Four pictures are arranged in a rostral (D) to caudal (G) order, showing that wild-type (donor) cells adjacent to mutant (host) cells were negative for *shh* (arrows in E and F), while those located inside (more rostrally) were positive (arrowhead in D). The mutant cell next to a wild-type donor was negative for *shh* (G). n, notochord. Scale bar: 20 μm.

Fig. 5. Cross sections showing the expression of ventral markers in the neural tube. (A, B) Expression of *nk2.2* in the caudal hindbrain. Arrowhead indicates a floor-plate cell which does not express *nk2.2* in the wild-type embryo (A). In the *oep* mutant embryo (B), cells located at the ventral midline are positive for the transcripts. (C, D) Expression of *islet-1* in the spinal cord of wild-type (C) and *oep* (D) embryos. The expression of *islet-1* is observed in the motor neuron (mn) on both side of the ventral midline. Note that the expression domains in *oep* mutants are ventrally displaced as compared with those in wild-type. n, notochord; RB, Rohon-Beard neuron. Scale bar: 20 μm.

Fig. 6. (A) Sequence comparison of Zfdkk-1 protein with that of mouse and *Xenopus* Dkk-1 protein. Conserved amino acids are in shadowed boxes. Two cysteine-rich domains (Cys 1 and Cys 2) are

underlined. (B) Western blot analysis of Zfdkk-1 transfected COS7 cell culture supernatant. FLAG-tagged *ß-galactosidase* and *zfdkk-1* construct were transfected into COS7 cells. Zfdkk-1 was detected in both cell extraction (c) and culture supernatant (m). (C) Temporal expression of *zfdkk-1* during development. Total RNAs from different stages were separated and probed with *zfdkk-1* in the upper panel. The bottom panel shows bands of 18S ribosomal RNA of the gel from which RNAs were blotted on the filter.

Fig. 7. In situ hybridization analysis of *zfdkk-1* during embryogenesis. In lateral views, dorsal is to the right. (A, B) *zfdkk-1* transcripts are first detected at the high stage (3.5 hpf), with the anti-sense probe (B), but not with the sense probe (A). (C, D) The sphere stage (4 hpf), in lateral view (C) and sagittal section of the same preparation at the dorsal blastoderm margin (D), *zfdkk-1* is expressed in the YSL (arrowhead) and in the overlying blastoderm margin. (E) At 50%-epiboly (5.25 hpf) in animal-pole view, *zfdkk-1* is expressed in the circumference of the blastoderm margin. (F, G) At the shield stage (6 hpf) in lateral view, involuting cells at the dorsal side (arrow) express *zfdkk-1,* but the YSL (arrowhead) no longer expresses *zfdkk-1* transcripts. (H) At 75%-epiboly (8 hpf) in dorsal view, cells in the hypoblast margin express *zfdkk-1.* (I, J) At 90%-epiboly (9 hpf) in lateral view (I), and in dorsal view (J). (K, L) At the 3-somite stage (11 hpf) in lateral view (K), and dorsal view (L); the anterior edge of the *zfdkk-1* expression is indicated by an arrowhead. Scale bar: 150 µm in A-C, E, F, H-L, 50 µm in D and 80 µm in G.

Fig. 8. Zfdkk-1 inhibits the Wnt signaling. (A) An embryo with a secondary axis (arrow) formed by co-injection of *zfwnt8* and *zffz* RNA. (B) 0.1 pg of *zfwnt8* RNA, 25 pg of *zffrizzled2* or *5* RNA and 6, 12, or 25 pg of *zfdkk-1* RNA were injected into 1-2 cell stage embryos. None of the *zfwnt8* injected embryos shows a secondary axis (0/259) and *zffz* injection rarely induces secondary axes (*zffz2*; 0/128, *zffz5*; 1/122). Co-injection of *zfwnt8* and *zffz* only induces secondary axes at high efficiency (*zfwnt8*+*zffz2*; 32/117, *zfwnt8*+*zffz5*; 33/118). Co-injection of *zfwnt8*, *zffz* and *zfdkk-1* inhibited induction of secondary axes in a dose dependent manner (6 pg *zfdkk-1* with *zffz2*; 3/126 and *zffz5*; 1/161, 12 pg *zfdkk-1* with *zffz2*; 0/135 and *zffz5*; 0/143, 25 pg *zfdkk-1* with *zffz2*; 0/114 and *zffz5*; 0/121). Scale bar: 100 µm.

Fig. 9. Zfdkk-1 ubiquitous overexpression anteriorizes embryos. (A) Wild-type control at the bottom and *zfdkk-1* injected embryos classified into four classes that correspond to class I-IV in Table 3. *zfdkk-1* RNA injection induces expansion of head structures including eyes and graded truncation of trunk region. (B-D) Lateral view of the head region, control injection (B), 25 pg *zfdkk-1* RNA injection (C) and 200 pg injection (D). Eyes and the telencephalon expands and otic vesicles are reduced in a dose dependent manner. Arrowheads in B-D indicate the MHB. ov, otic vesicles; tec, tectum; tel, telencephalon. Scale bar: 250 µm in A and 100 µm in B-D.

Fig. 10. Zfdkk-1 overexpression dorsalizes mesoderm. (A, C, E, G, I, K, M, O, Q, S, U, W) Controls and (B, D, F, H, J, L, N, P, R, T, V, X) 25 pg *zfdkk-1* mRNA injected embryos. (A, B) *gsc* expression at 90%-epiboly, animal pole view, dorsal to the bottom. (C, D) *hlx-1* expression at 90%-epiboly, dorsal view, animal pole to the top. (E, F) *twist* expression at 90%-epiboly, dorsal view, animal pole to the top. (G, H) *ntl* expression at 90%-epiboly, dorsal view, animal pole to the top. (I, J) *ntl* expression at the shield stage, lateral view, animal pole to the top. (K, L) *wnt8* expression at 75%-epiboly, dorsal view, animal pole to the top. (M, N) *myoD* expression at 75%-epiboly, dorsal view, animal pole to the top. (O, P) *myoD* expression at 12-somite, dorsal view, anterior to the top. (Q, R) *pax2* expression at the 10-somite stage, dorsal view of flattened embryos, anterior to the left. (S, T) *gata-1* expression at 10-somite stage, dorsoposterior view. (U, V) *gsc* expression at the shield stage, dorsal view, animal pole to the top. (W, X) *chd* expression at the shield stage, dorsal view, animal pole to the top. Arrowheads in I, J indicate *pax2* expression in the pronephros. Scale bar: 150 µm.

Fig. 11. Zfdkk-1 overexpression expands the anterior head at the expense of the posterior head. (A-I) At the 20-somite stage, the *emx1* domain expands and the *krx-20* domain reduces dose

dependently in *zfdkk-1* injected embryos (A-C); the posterior head region, defined dorsally by *wnt-1* expression (D-F) and ventrally by *axial* expression (G-I), reduces dose dependently. This effect already occurs during gastrulation. (J, K) At the bud stage, the *emx1* domain (open arrowhead) extends posteriorly; the MHB domain stained with *pax2* (open circle) is positioned posteriorly. (L-T) At 90%-epiboly, the *anf-1* domain expands posteriorly (L, M); the *otx2* domain expands and the *hoxa-1* domain reduces (N, O); the *her-5* domain positions posteriorly and reduces (P, Q); *otx2* fluorescent and *anf-1* normal blue double staining leave the fluorescent domain expressing only *otx2* but not *anf-1*, which corresponds to the future posterior head and the part of midline (R); the lateral wing domain (arrow heads) compared to the midline domain of this double staining is reduced in injected embryos (S, T). Scale bar: 100 µm in A-I and 150 µm in J-Q, S, T.

Fig. 12. The effect of overexpression of Zfdkk-1 on the anterior neuroectoderm in wild-type and *oep* mutant embryos. (A) COS7 cells transfected with FLAG-tagged *zfdkk-1* (Dkk-1 COS7) or *β-galactosidase* as a control (ß-gal COS7) were transplanted near the animal pole (1) or the shield (2) region (es) of the shield stage embryos. (B-E) At 24 hpf, transplanted Dkk-1 COS7 cells detected by anti-FLAG antibody (arrow in E) expand the head in the live embryo (C). *emx1*, *her-5*, *krx-20* in situ staining shows that the dorsal telencephalon is expanded (arrowhead in E). (F, G) Lateral view at 90%-epiboly. Dkk-1 COS7 (G) does not affect the expression patterns of *otx2* and *hoxa-1*. (H-K) Dorsoanterior view at 90%-epiboly. Dkk-1 COS7 (demarcated by dots) expands the *anf-1* expressing domain (G) and reduces the domain that expresses *otx2* but not *anf-1* (I). (L-O) Dorsoanterior view (L, M) and dorsal view (N, O) at 90%-epiboly. Neither *gsc* or *ntl* expression in the axial mesoderm was affected by Dkk-1 COS7. (P-U) Dkk-1 COS7 cells expand the head in *oep* mutants that lack the prechordal plate, identified by the absence of the floor plate stained with *shh*. Lateral view (P, Q, T, U) and dorsoanterior view (R, S). Eyes are expanded but still fused (arrowheads in Q, S). *emx1* staining (arrowhead in U) is strongly expanded by transplanted Dkk-1 COS7 cells (arrow in U). Scale bar: 200 µm in B, C, F-I, 100 µm in D, E, L, M and 150 µm in J, K, N, O.

Fig. 13. ERK activation detected by anti-dpERK antibody in wild-type embryos. (A-C, E) Lateral view, dorsal to the right. (F) Dorsal view of the head region. (A) 75%-epiboly stage; ERK activation is seen in the marginal mesoderm. (B) 3-somite stage; ERK activation is seen in the MHB and tailbud, and weakly in the ANB. (C) 5-somite stage; ERK activation in the ANB becomes strong. (D) Sagittal section of the embryo shown in C. ERK is strongly activated in the ANB (C, D). (E, F) 8-somite stage; staining in the ANB is faint. Asterisks indicate the staining in the ANB and arrowheads indicate the staining in the MHB. Scale bar: 100 µm in A-C, E, F and 30 µm in D.

Fig. 14. ERK activation in embryos treated with inhibitors to Fgf signaling. All embryos were analyzed at the 5-somite stage. (A-C) Lateral view, dorsal to the right; ERK activation observed in *GFP*-injected embryo (A) is suppressed by injection of Ras^{N17} (B) and *bΔFR4* (C) RNAs. (D) Schematic representation of the SU5402 injection; SU5402 (F) or DMSO as a control (E) was injected into the head region at the tailbud stage. (E, F) Dorsal view of the head region; ERK activation in the ANB is suppressed by the injection of SU5402 (F). (G, H) Lateral view of the head region; BSA (G) or Fgf8b (H)-soaked beads were transplanted in the thick head region at tailbud stage. Ectopic ERK activation is found around the Fgf8b-beads (H). Asterisks indicate endogenous staining in the ANB and arrows indicate the transplanted beads. Scale bar: 100 µm in A-F and 50 µm in G, H.

Fig. 15. Immunostaining and Western blot for activated ERK in *ace* mutants. (A, B) Dorsal views of the head region at the 5-somite embryos stained with anti-dpERK antibody. ERK activation in the ANB is detected in both the wild-type (A) and *ace* homozygous mutant (B). Asterisks indicate the anterior edge of the neural plate. (C) Western blot analysis of activated ERK; the equal amount of homogenates prepared from wild-type, *ace* mutant, DMSO treated and SU5402 treated embryos at the 6- to 7-somite stage, loaded in each lane. Western blot detects one major band of about 50 kDa (arrow), which is reduced in *ace* mutants and sensitive to SU5402. Relative intensity of the

major band is shown at the bottom of each lane. Relative intensity was normalized by non-specific minor band (data not shown) that is insensitive to SU5402. Scale bar: 50 μm in A, B.

Fig. 16. Expression pattern and the activity of zebrafish *fgf3*. (A-E) Expression pattern of *fgf3*. (A, C, E) Dorsal view of the head region. (A, B, E) Tailbud stage, (C, D) 5-somite stage, (F) 6-7-somite stage, wild-type embryos (A-D) and *ace* mutant embryo (E, F). *ace* homozygous mutants at the tailbud stage were recognized by fragmented *myoD* staining in adaxial cells. (B, D) Sagittal sections taken from the embryo shown in A and C, respectively. *fgf3* expression in the ANB is maintained normally in *ace* mutant embryo. (G, H) Lateral view, dorsal to the right; ERK is activated in the whole embryo injected *fgf3* (G) and the effect is cancelled by co-injection of Ras^{N17} RNAs (H). Asterisks indicate positive staining in the ANB and arrowheads indicate that in the MHB. Scale bar: 100 μm in A, C, E-G and 30 μm in B, D.

Fig. 17. Patterning and neurogenesis in the telencephalon in Ras^{N17}-injected embryos. Injected RNA is shown in the upper right and the probe used is indicated at the bottom. (A, B) Lateral view of the head region; Ras^{N17}-injected embryo exhibits the turbid telencephalon, truncation of a part of the eye and no MHB (arrowheads in A and B) in the head region. A' and B' are high magnification views of the telencephalic region of A, B respectively. (C-F) Sagittal section of the embryos detected for DNA fragmentation at 33 hpf (C, D) and 26 hpf (E, F); apoptotic cells are detected in the telencephalon of the Ras^{N17}-injected embryo at 33 hpf (arrows in D) but not at 26 hpf (F). (G-Z) Lateral view (G-T, W-Z) and dorsal view (U, V) of the head region; whole-mount in situ hybridization was performed at the 26 hpf (G-P, W, X), 14-somite (Q-T), 15-somite (U, V) and 12-somite (Y, Z). Subpallial telencephalic expressions of *dlx2* (G, H, S, T), *nk2.1b* (I, J, Q, R), *islet-1* (W, X) and *zash1a* (Y, Z) are lost in the Ras^{N17}-injected embryo while the pallial telencephalic markers, *emx1* (K, L, U, V), *eom* (M, N) and *tbr1* (O, P) covers the entire telencephalon. Arrows in A, B, G, I, Q, S, W and Y indicate the subpallial telencephalon, arrowhead in K, M, O and U indicate the subpallial telencephalon which is negative for *emx1*, *eom* or *tbr1*. Dots indicate the

boundary between the telencephalon and ventral diencephalon. di, diencephalon; tel, telencephalon. Scale bar: 50 μm in A, B, Q, R, U, V, 10 μm in C-F and 30 μm in G-P, S, T, W-Z.

Fig. 18. Telencephalic territory is normally specified in Ras^{N17}-injected embryo. Injected mRNA is shown in the upper right and the probe used is indicated at the bottom. (A, B) Dorsal views of the head region at tailbud stage; *emx1* expression in the prospective telencephalon is not altered by Ras^{N17} injection. (C-F) Lateral views of the head region at 5-somite stage (C, D) and 26 hpf (E, F), anterior to the left; *bf-1* expression in the telencephalon is normally seen in Ras^{N17}-injected embryo. (G, H) Lateral views of the head region at 15-somite stage, anterior to the left; *otx2* expression in the anterior forebrain is normally down-regulated in Ras^{N17}-injected embryos. Arrows indicate the mid-diencephalon. (I, J) Lateral views of the head region at 26 hpf, anterior to the left; *shh* expression in the diencephalon is normal. Scale bar: 75 μm in A, B and 50 μm in C-J.

Fig. 19. Patterning and neurogenesis in the telencephalon in the *bΔFR4* -injected embryos. Injected mRNA is shown in the upper right and the probe used is indicated at the bottom. (A-V) Lateral view (A-N, S-V) and dorsal view (O-R) of the head region; whole-mount in situ hybridization was performed at the 26 hpf (A-L), 14-somite (M, N), 15-somite (O, P, U, V), tailbud (Q, R) and 5-somite (S, T). Subpallial telencephalic expressions of *dlx2* (A, B), *nk2.1b* (C, D, M, N) and *islet-1* (E, F) are suppressed in the *bΔFR4*-injected embryo while the pallial telencephalic markers, *emx1* (G, H, O, P), *eom* (I, J) and *tbr1* (K, L) covers the entire telencephalon. (Q-V) Expression of *emx1* (Q, R), *bf-1* (S, T) and *otx2* (U, V) were normal. Arrows indicate the subpallial telencephalon, and arrowheads indicate the subpallial telencephalon, in which is negative for *emx1*, *eom* or *tbr1*. Dots indicate the boundary between the telencephalon and ventral diencephalon. Scale bar: 30 μm in A-L, O-R and 50 μm in M, N, S-V.

Fig. 20. Patterning and neurogenesis in the telencephalon after treatment of SU5402. The probe used is indicated at the bottom. All embryos are lateral view of the head region at 26 hpf. Embryos

were injected with SU5402 (B, D, F) or DMSO (A, C, E) in the head region at tailbud stage (A-F). For (G) and (H), the embryos were soaked in medium containing SU5402 at 5-somite and 10-somite stages, respectively. (A-F) *dlx2* expression in the subpallial telencephalon is abolished by SU5402 (A, B), while *emx1* reaches the edge of the telencephalon after SU5402 treatment (C, D). *islet-1* expression in the anterior commissure is down-regulated by SU5402 (E, F). Note the smaller telencephalon is frequently seen in treated embryos (B, D, F). (G, H) *dlx2* expression is greatly reduced when the embryos were treated with SU5402 at 5-somite stage, while the expression is relatively normal when treated at 10-somite stage. Arrows indicate the gene expression in the subpallial telencephalon. Dots indicate the boundary between the telencephalon and ventral diencephalon while arrowheads indicate the ventral region that is negative for *emx1*. Scale bar: 50 μm.

Fig. 21. *nk2.1b* expression in the embryos injected with morpholino-modified (MO) antisense oligonucleotides. Lateral views of the head region at 26 hpf. Embryos were injected with standard control (cont.-MO) (A, F), fgf8-MO (B, G), fgf3-MO (C, H), fgf8-MO and fgf3-MO (D), and fgf3-MO and *fgf3* mRNA (E). (A-E) Wild-type embryos were used. Injection of either fgf8-MO (B) or fgf3-MO (C) reduces *nk2.1b* expression. However, reduction of *nk2.1b* is further enhanced when both fgf8-MO and fgf3-MO was co-injected (D). (A'-C') *en2* expression after fgf8-MO injection (B') and fgf3-MO (C'). *en2* expression is reduced in fgf8-MO injected embryo but remains unchanged in fg3-MO injected embryo. (E) *nk2.1b* expression is rescued by co-injection of fgf3-MO and *fgf3* RNAs. (F-H) Embryos from *ace* heterozygous parents were used; fgf3-MO but not fgf8-MO injection enhances the reduction of *nk2.1b* in some embryos. Dots indicate the boundary between the telencephalon and ventral diencephalon. Scale bar: 50 μm.

Figures

Fig. 1

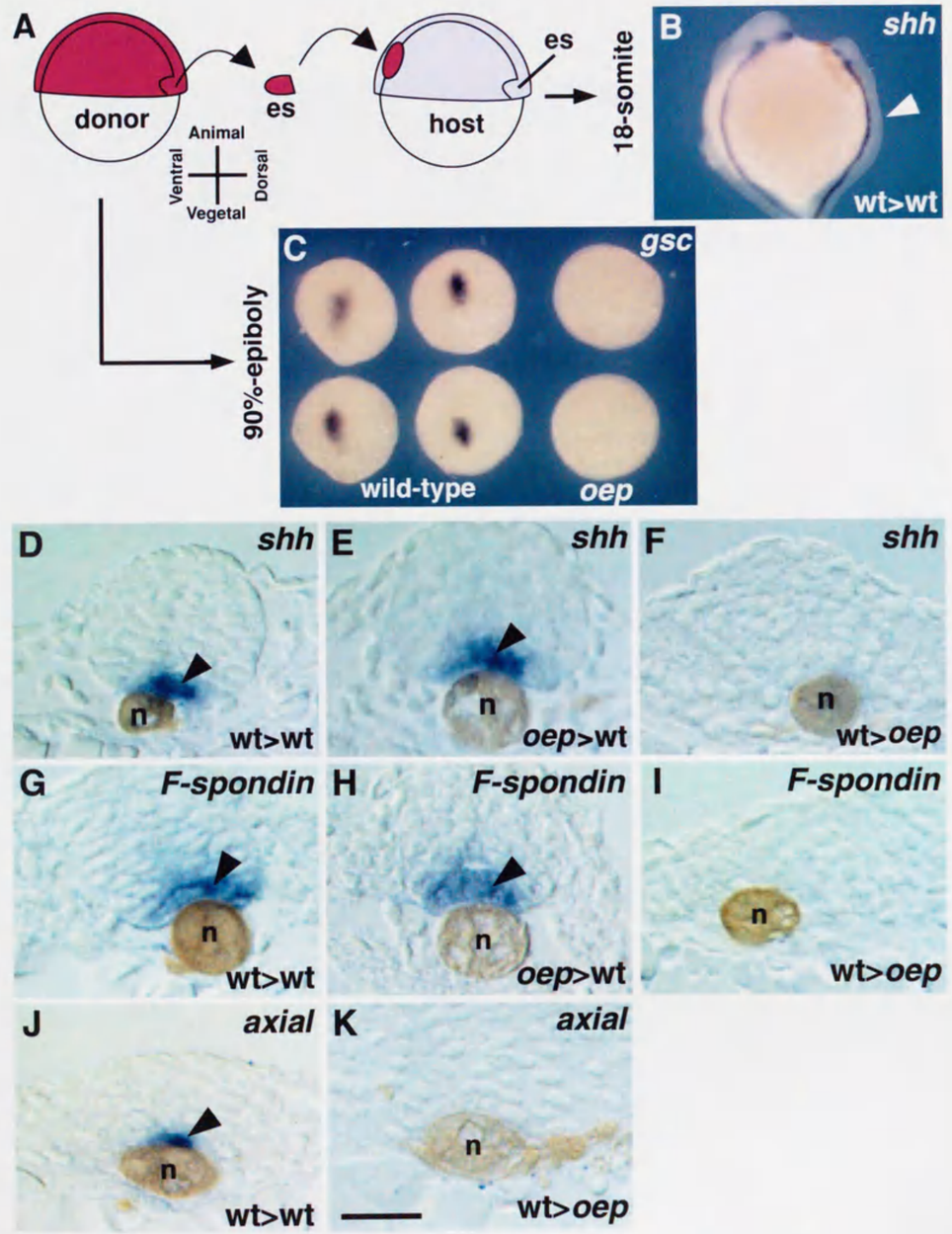
A
donor
es
Animal
Ventral
Dorsal
Vegetal
es
host
18-somite
B
shh
wt>wt
90%-epiboly
C
gsc
wild-type
oep
D
shh
n
wt>wt
E
shh
n
oep>wt
F
shh
n
wt>oep
G
F-spondin
n
wt>wt
H
F-spondin
n
oep>wt
I
F-spondin
n
wt>oep
J
axial
n
wt>wt
K
axial
n
wt>oep

Fig. 2

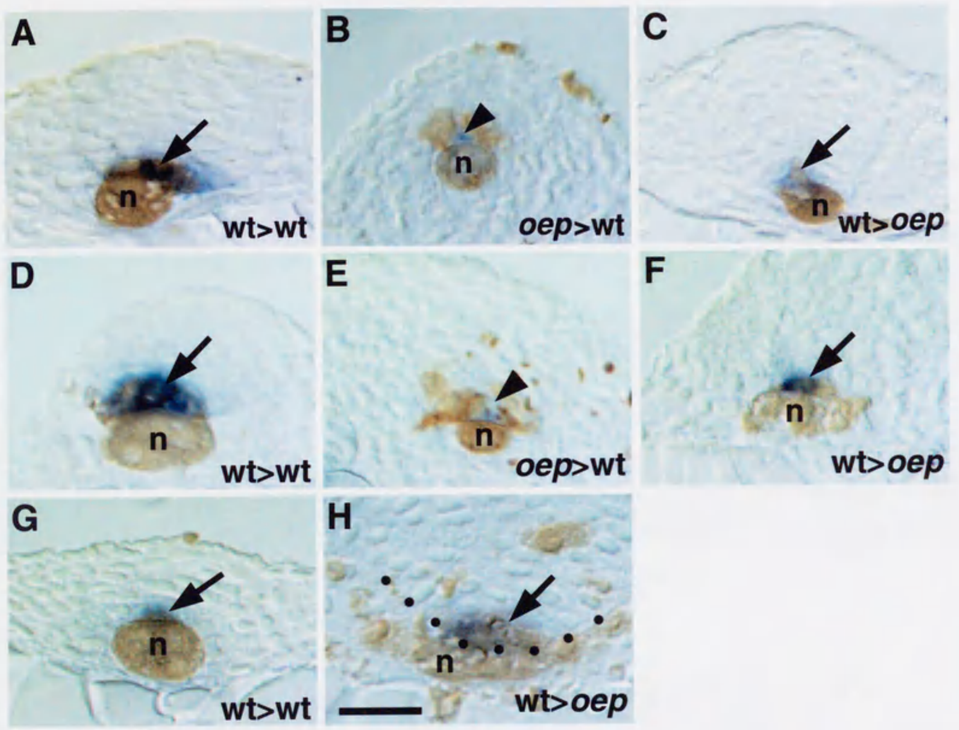
A
n
wt>wt
B
n
oep>wt
C
n
wt>oep
D
n
wt>wt
E
n
oep>wt
F
n
wt>oep
G
n
wt>wt
H
n
wt>oep

Fig. 3

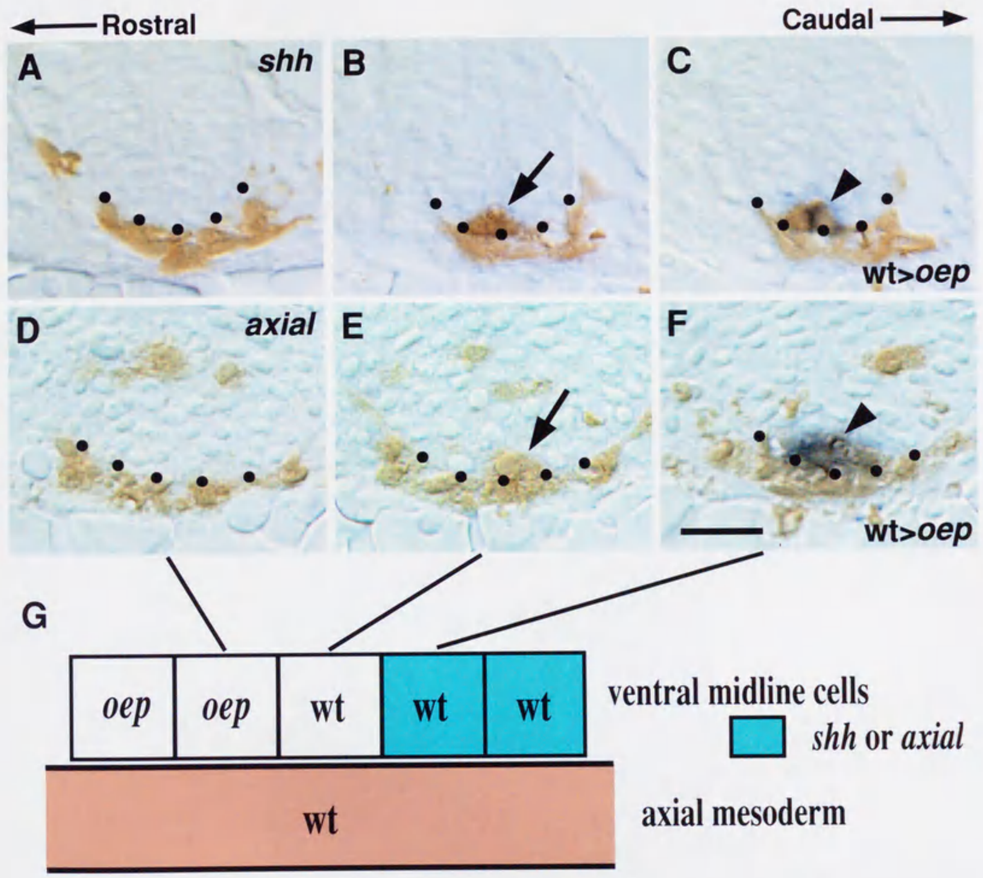
Rostral
Caudal
A
shh
B
C
wt>oep
D
axial
E
F
wt>oep
G
oep
oep
wt
wt
wt
ventral midline cells
shh or axial
wt
axial mesoderm

Fig. 4

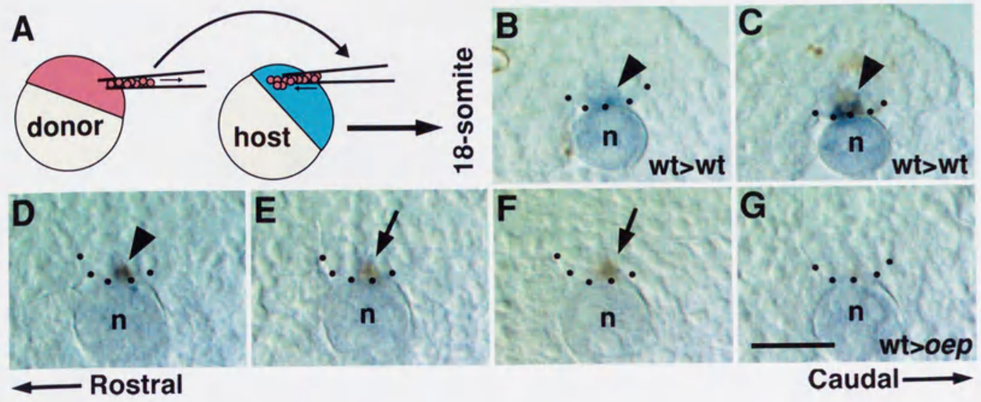
A
donor
host
18-somite
B
n
wt>wt
C
n
wt>wt
D
n
E
n
F
n
G
n
wt>oep
Rostral
Caudal

Fig. 5

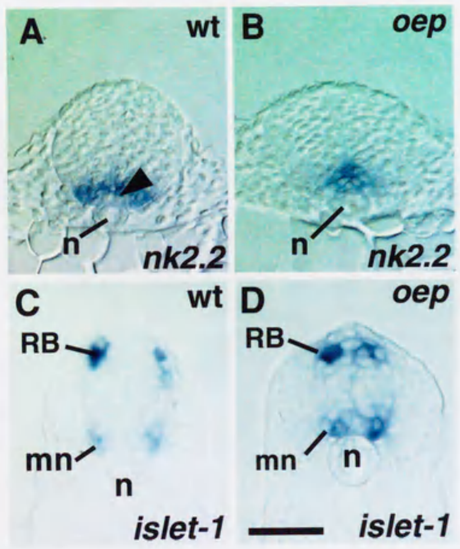
A
wt
n
nk2.2
B
oep
n
nk2.2
C
wt
RB
mn
n
islet-1
D
oep
RB
mn
n
islet-1

Fig. 6

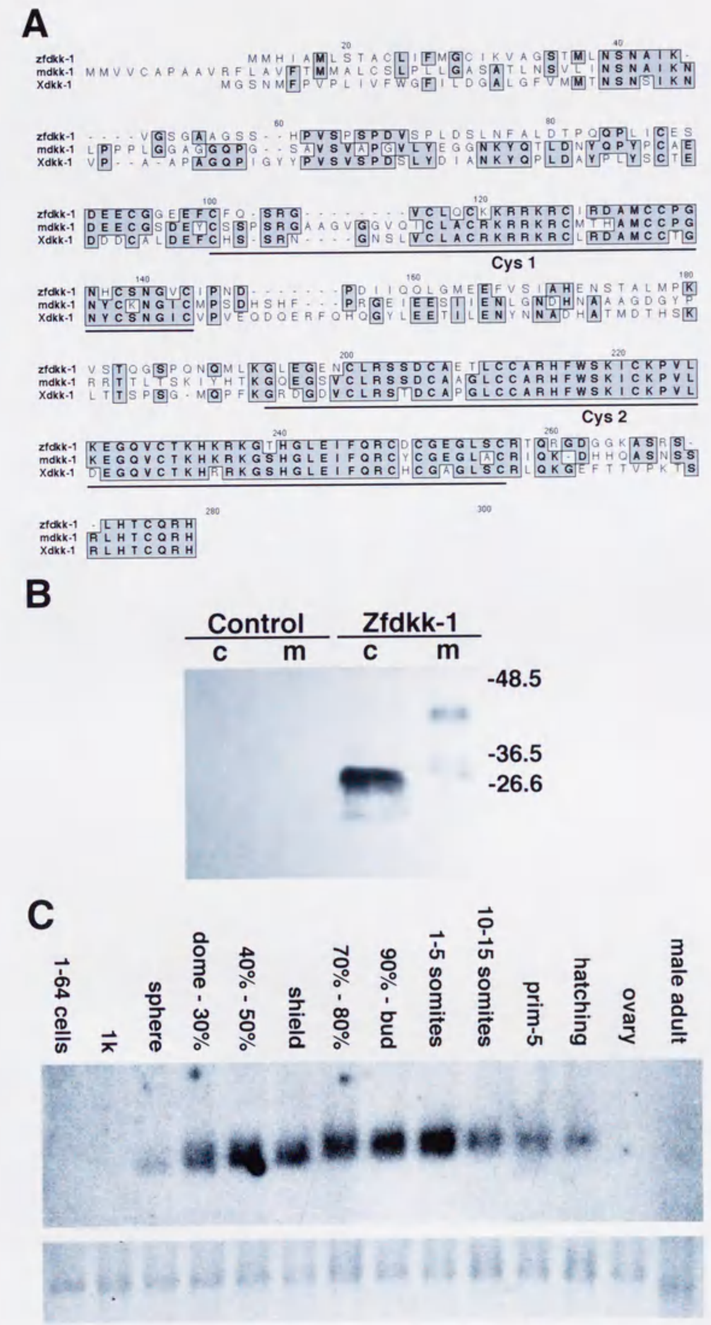
A
zfdkk-1
mdkk-1
Xdkk-1
Cys 1
Cys 2
B
Control
Zfdkk-1
c
m
c
m
-48.5
-36.5
-26.6
C
1-64 cells
1k
sphere
dome - 30%
40% - 50%
shield
70% - 80%
90% - bud
1-5 somites
10-15 somites
prim-5
hatching
ovary
male adult

Fig. 7

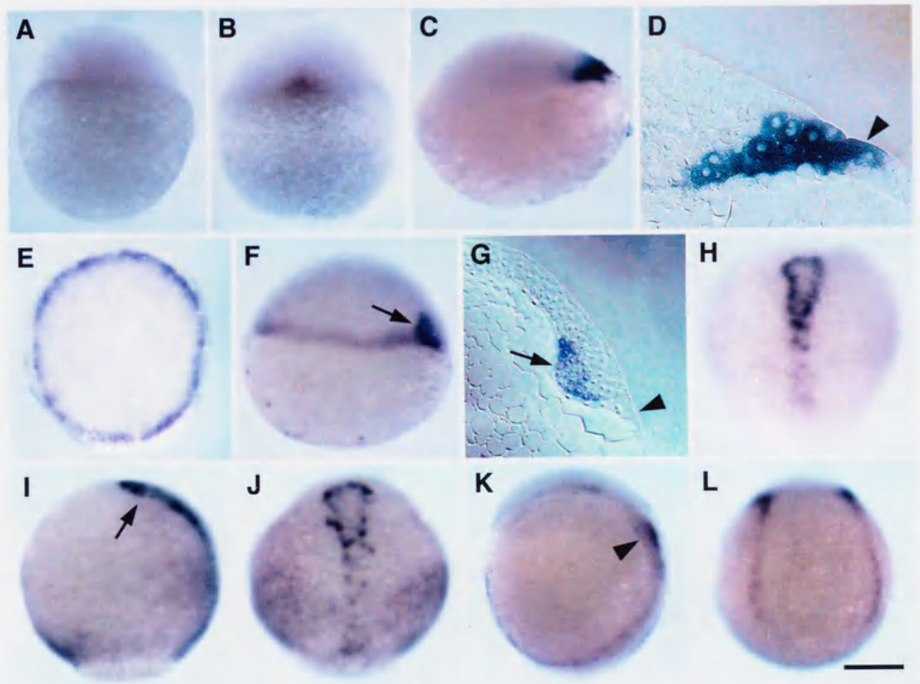
A
B
C
D
E
F
G
H
I
J
K
L

Fig. 8

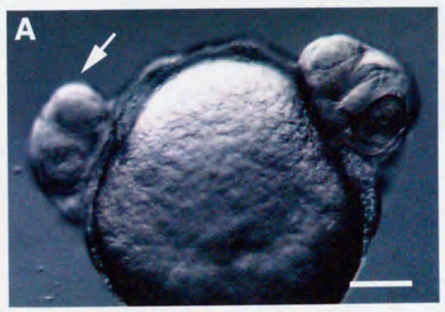
A

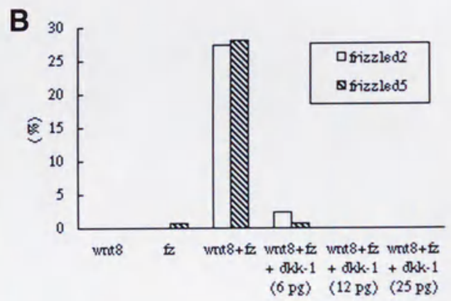
B
30
25
20
15
10
5
0
(%)
frizzled2
frizzled5
wnt8
fz
wnt8+fz
wnt8+fz + dkk-1 (6 pg)
wnt8+fz + dkk-1 (12 pg)
wnt8+fz + dkk-1 (25 pg)

Fig. 9

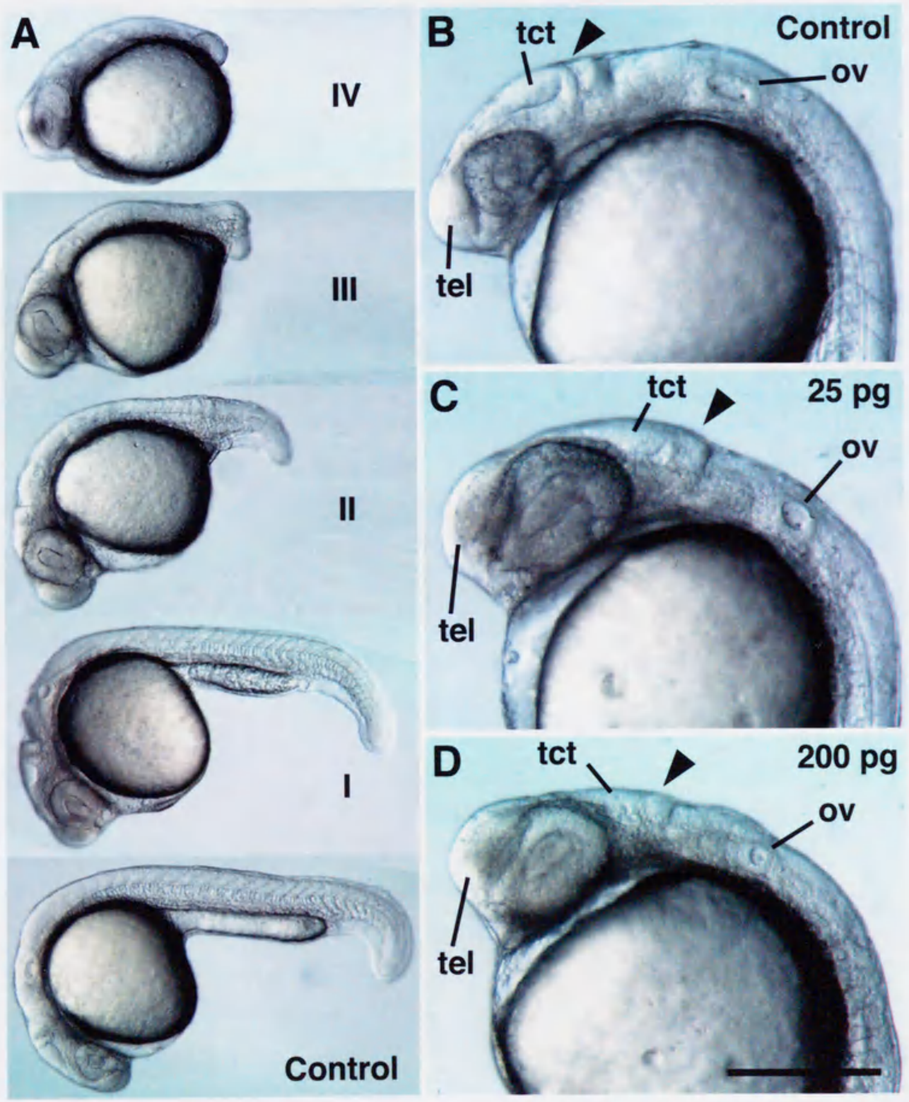
A
IV
III
II
I
Control
B
tct
Control
ov
tel
C
tct
25 pg
ov
tel
D
tct
200 pg
ov
tel

Fig. 10

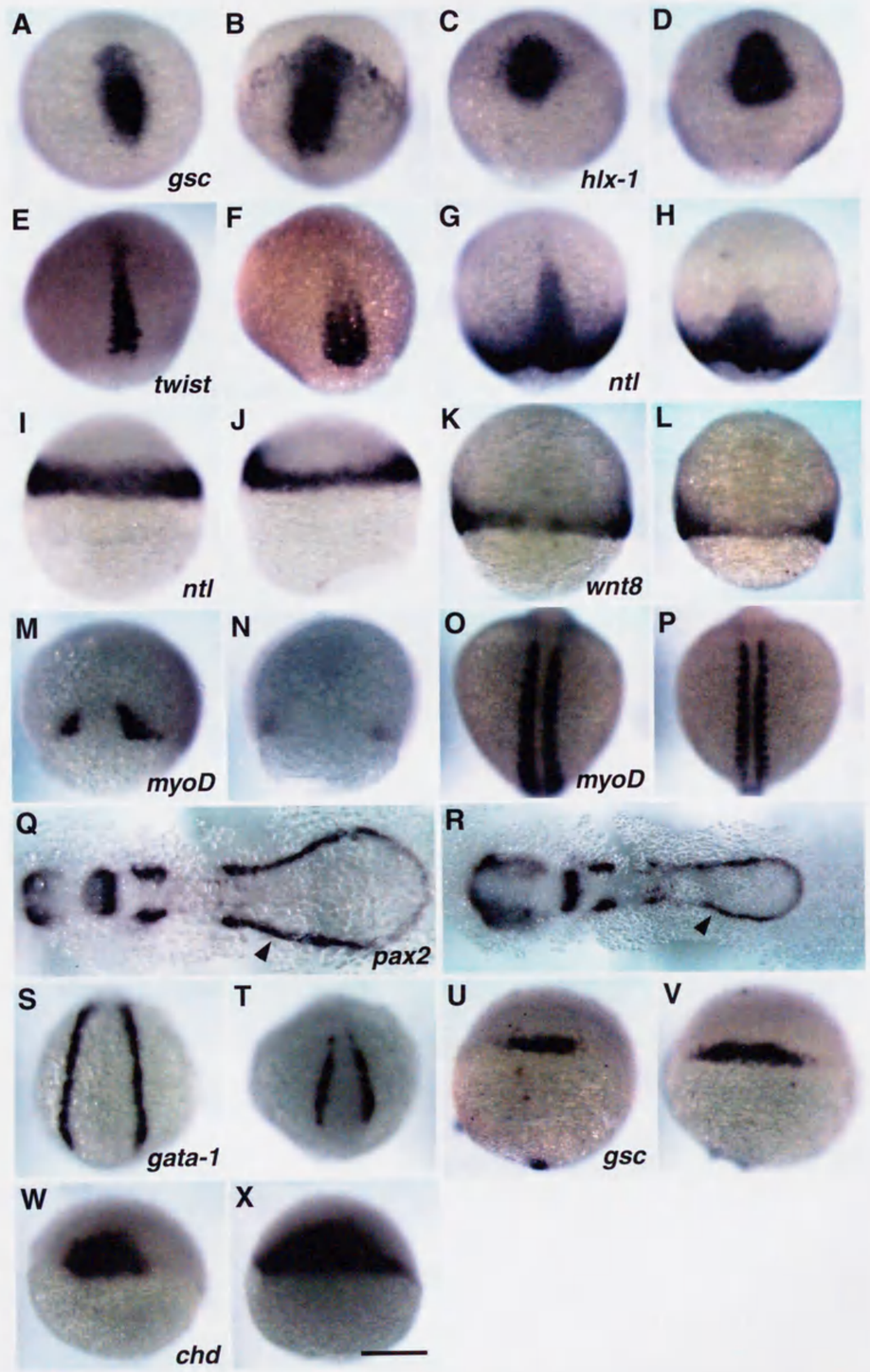
A
gsc
B
C
hlx-1
D
E
twist
F
G
ntl
H
I
ntl
J
K
wnt8
L
M
myoD
N
O
myoD
P
Q
pax2
R
S
gata-1
T
U
gsc
V
W
chd
X

Fig. 11

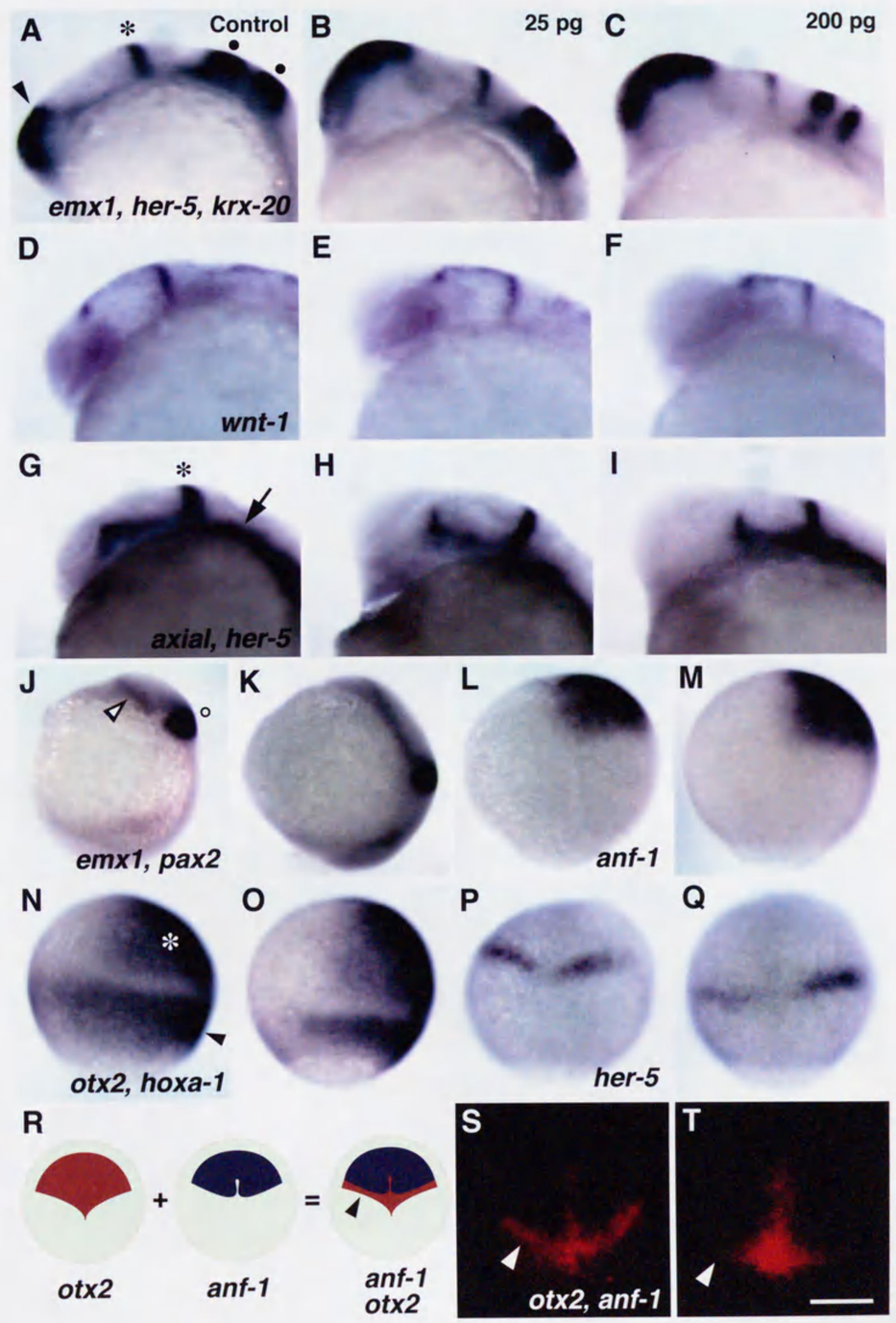
A
Control
B
25 pg
C
200 pg
emx1, her-5, krx-20
D
E
F
wnt-1
G
H
I
axial, her-5
J
K
L
M
emx1, pax2
anf-1
N
O
P
Q
otx2, hoxa-1
her-5
R
otx2
anf-1
anf-1
otx2
S
T
otx2, anf-1

Fig. 12

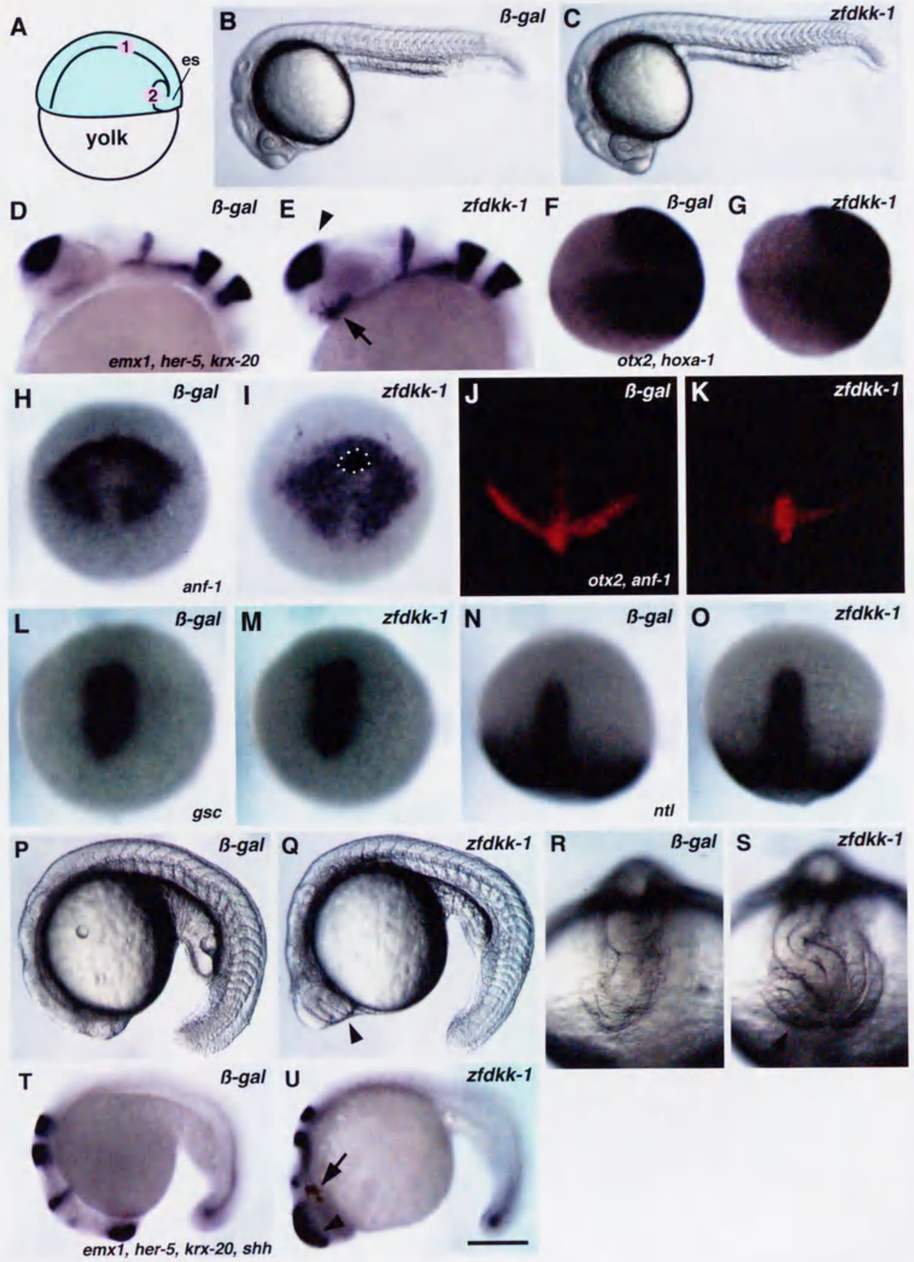
A
1
2
es
yolk
B
ß-gal
C
zfdkk-1
D
ß-gal
emx1, her-5, krx-20
E
zfdkk-1
F
ß-gal
otx2, hoxa-1
G
zfdkk-1
H
ß-gal
anf-1
I
zfdkk-1
J
ß-gal
otx2, anf-1
K
zfdkk-1
L
ß-gal
gsc
M
zfdkk-1
N
ß-gal
ntl
O
zfdkk-1
P
ß-gal
Q
zfdkk-1
R
ß-gal
S
zfdkk-1
T
ß-gal
emx1, her-5, krx-20, shh
U
zfdkk-1

Fig. 13

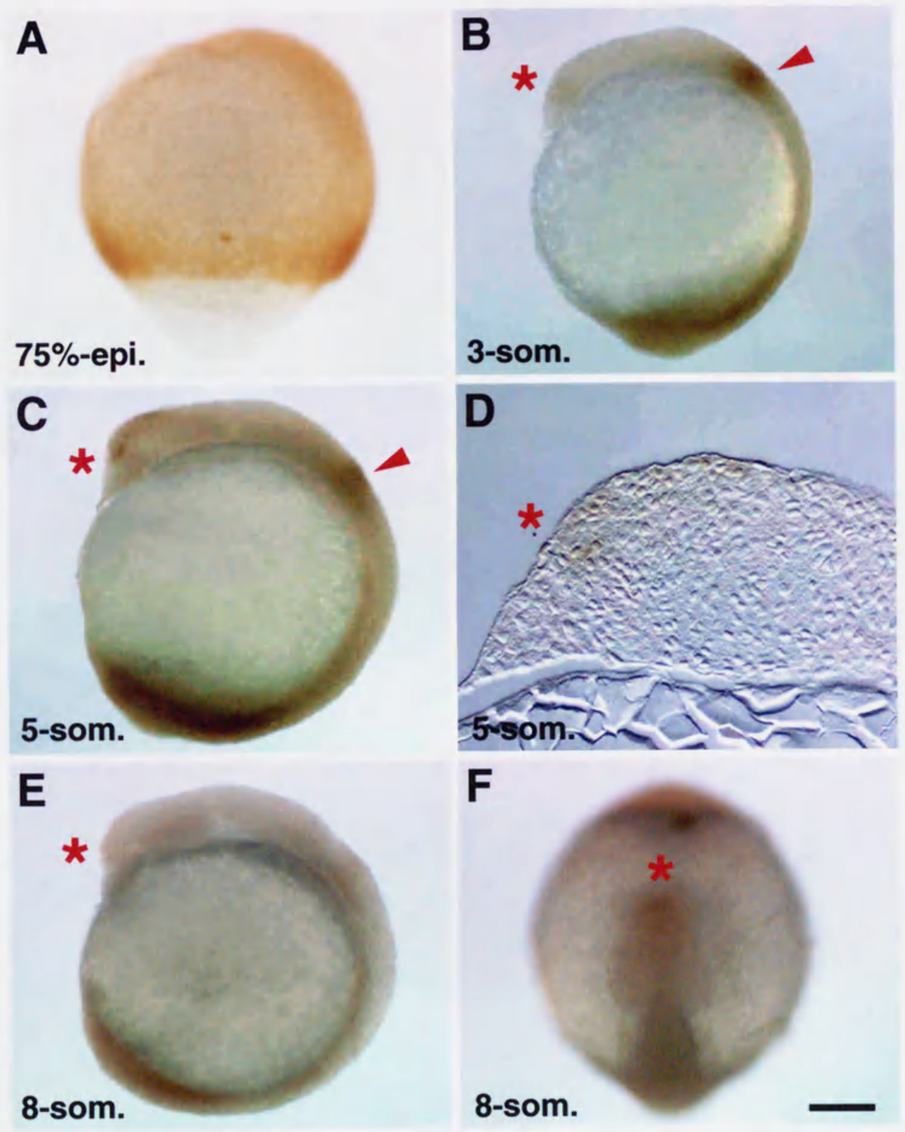

Fig. 14

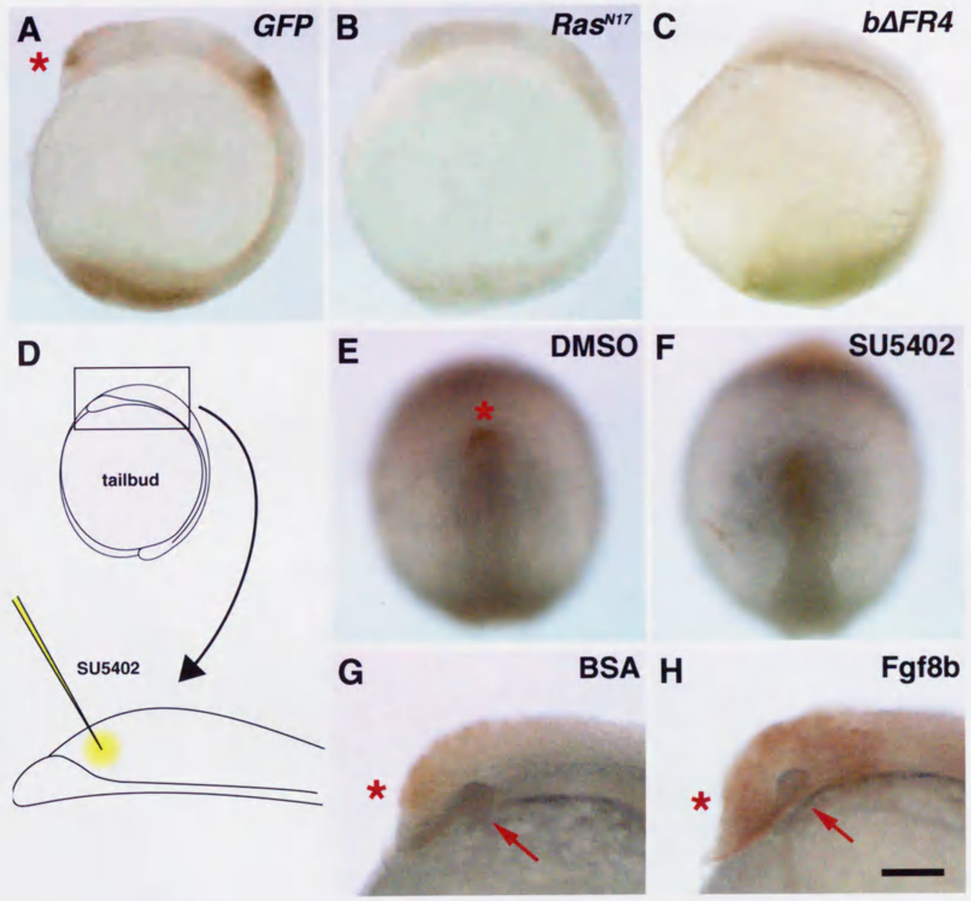
A
GFP
B
Ras^N17
C
bΔFR4
D
tailbud
SU5402
E
DMSO
F
SU5402
G
BSA
H
Fgf8b

Fig. 15

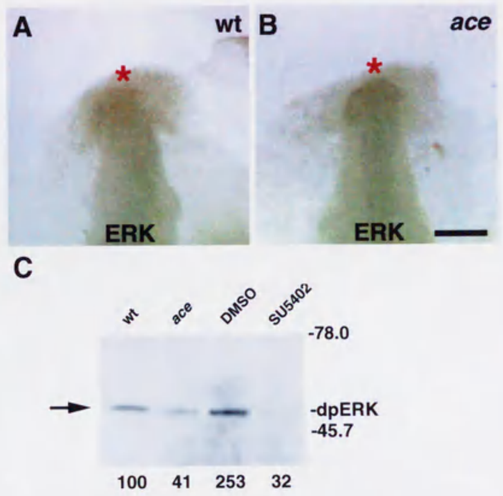
A
wt
ERK
B
ace
ERK
C
wt
ace
DMSO
SU5402
-78.0
-dpERK
-45.7
100
41
253
32

Fig. 16

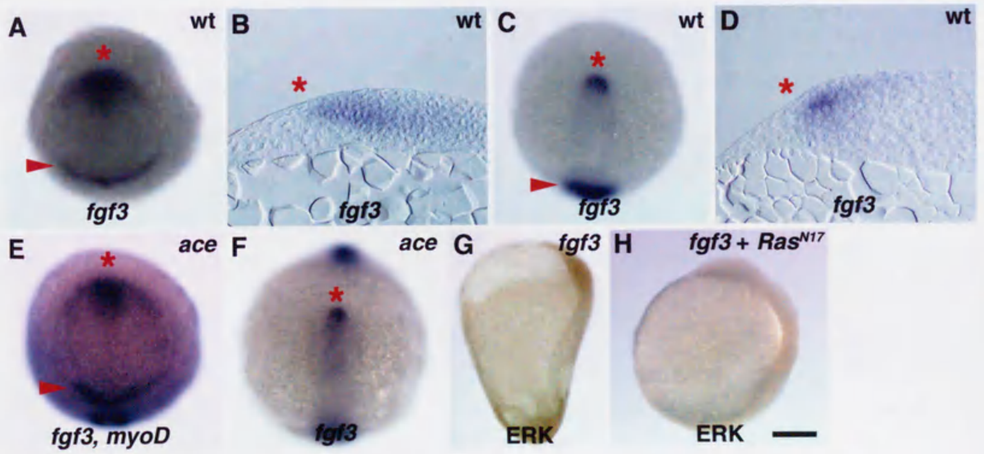
A
wt
fgf3
B
wt
fgf3
C
wt
fgf3
D
wt
fgf3
E
ace
fgf3, myoD
F
ace
fgf3
G
fgf3
ERK
H
fgf3 + RasN17
ERK

Fig. 17

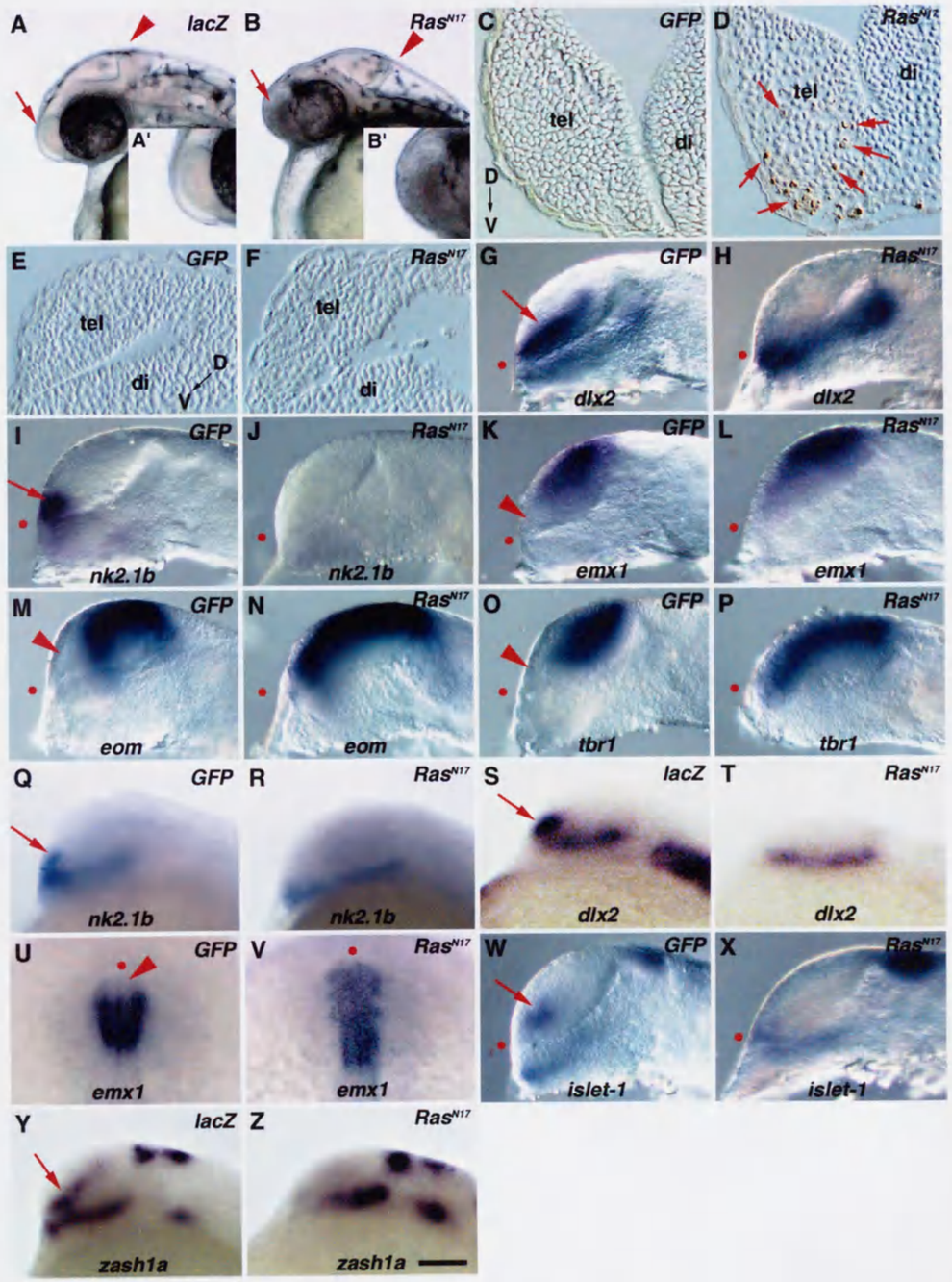
A
lacZ
A'
B
Ras^N17
B'
C
GFP
tel
di
D
V
D
Ras^N17
tel
di
E
GFP
tel
di
D
V
F
Ras^N17
tel
di
G
GFP
dlx2
H
Ras^N17
dlx2
I
GFP
nk2.1b
J
Ras^N17
nk2.1b
K
GFP
emx1
L
Ras^N17
emx1
M
GFP
eom
N
Ras^N17
eom
O
GFP
tbr1
P
Ras^N17
tbr1
Q
GFP
nk2.1b
R
Ras^N17
nk2.1b
S
lacZ
dlx2
T
Ras^N17
dlx2
U
GFP
emx1
V
Ras^N17
emx1
W
GFP
islet-1
X
Ras^N17
islet-1
Y
lacZ
zash1a
Z
Ras^N17
zash1a

Fig. 18

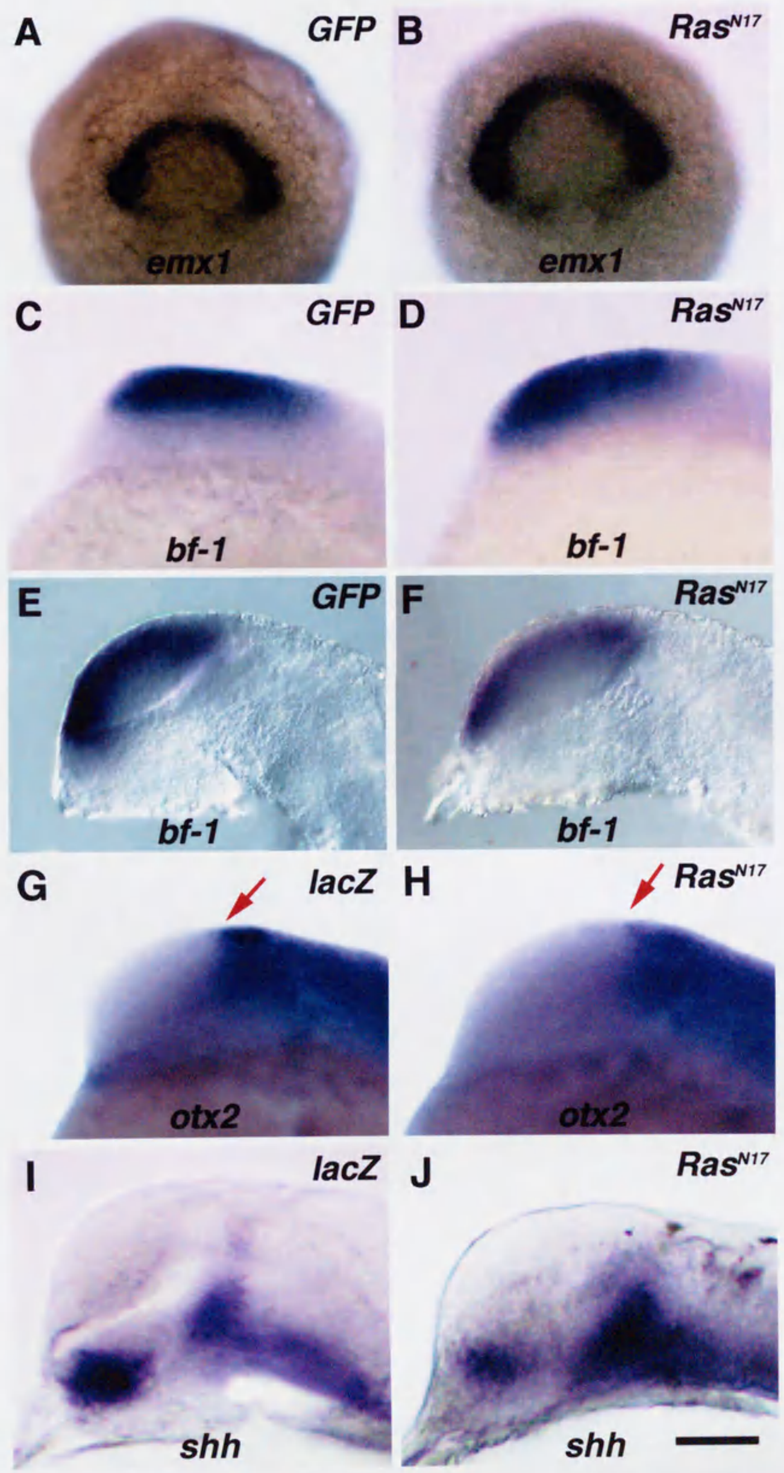
A
GFP
emx1
B
Ras^N17
emx1
C
GFP
bf-1
D
Ras^N17
bf-1
E
GFP
bf-1
F
Ras^N17
bf-1
G
lacZ
otx2
H
Ras^N17
otx2
I
lacZ
shh
J
Ras^N17
shh

Fig. 19

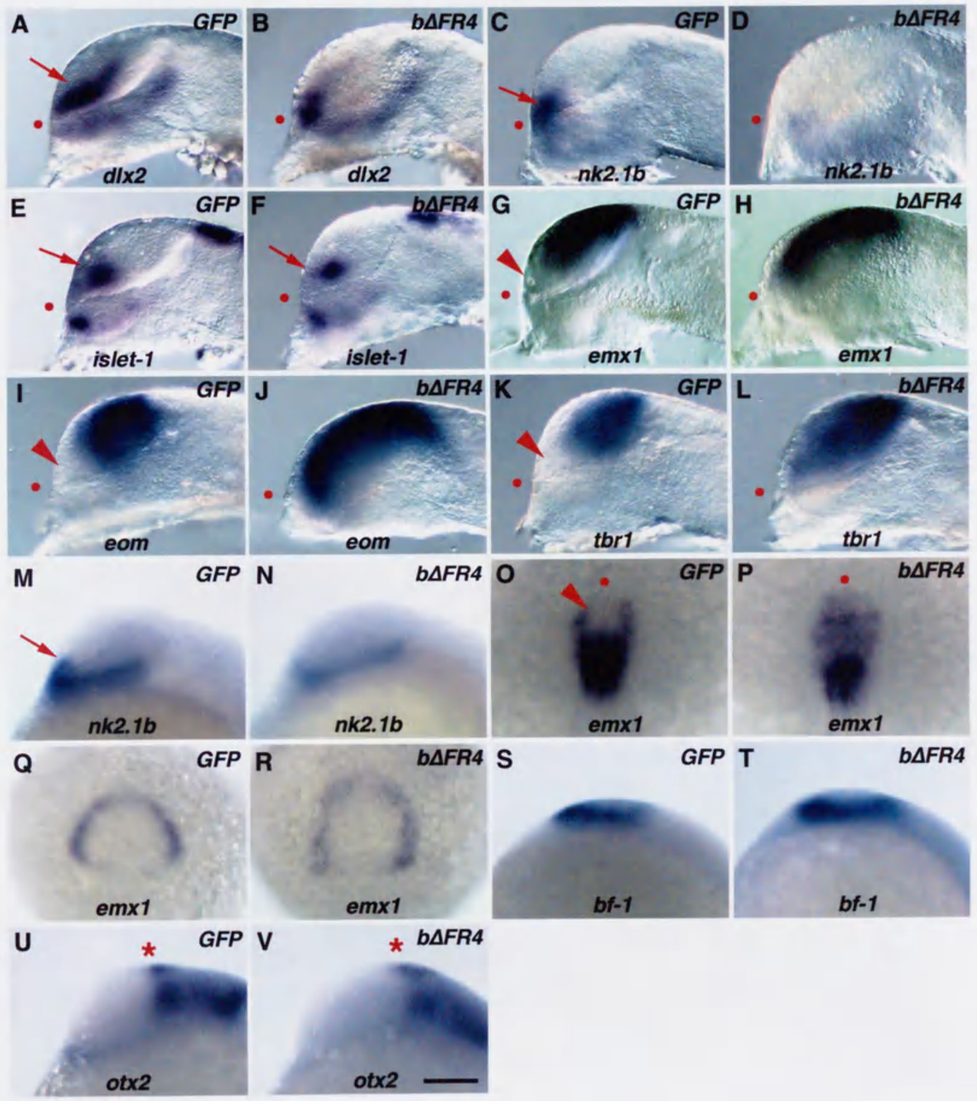
A GFP dlx2
B bΔFR4 dlx2
C GFP nk2.1b
D bΔFR4 nk2.1b
E GFP islet-1
F bΔFR4 islet-1
G GFP emx1
H bΔFR4 emx1
I GFP eom
J bΔFR4 eom
K GFP tbr1
L bΔFR4 tbr1
M GFP nk2.1b
N bΔFR4 nk2.1b
O GFP emx1
P bΔFR4 emx1
Q GFP emx1
R bΔFR4 emx1
S GFP bf-1
T bΔFR4 bf-1
U GFP otx2
V bΔFR4 otx2

Fig. 20

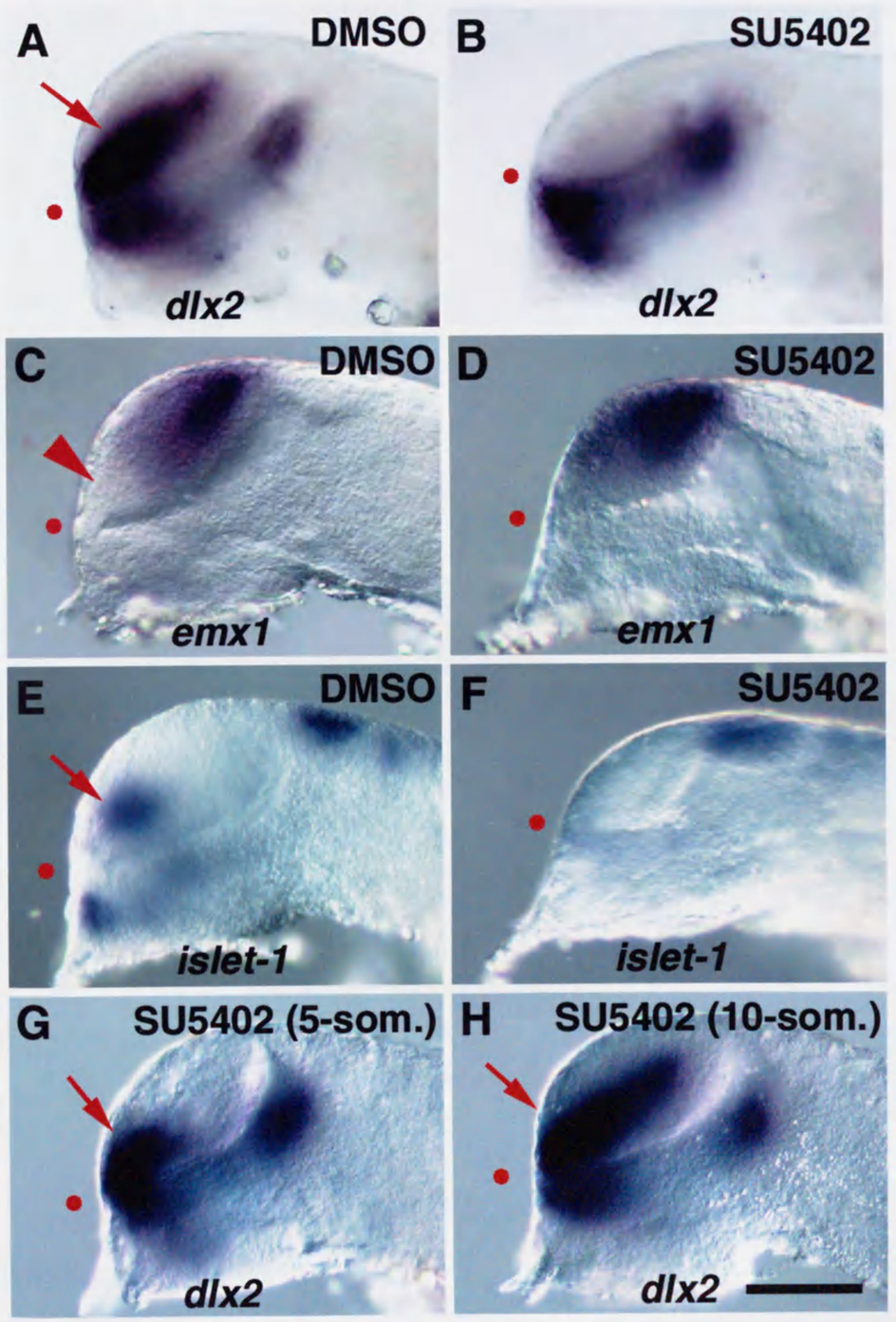
A
DMSO
dlx2
B
SU5402
dlx2
C
DMSO
emx1
D
SU5402
emx1
E
DMSO
islet-1
F
SU5402
islet-1
G
SU5402 (5-som.)
dlx2
H
SU5402 (10-som.)
dlx2

Fig. 21

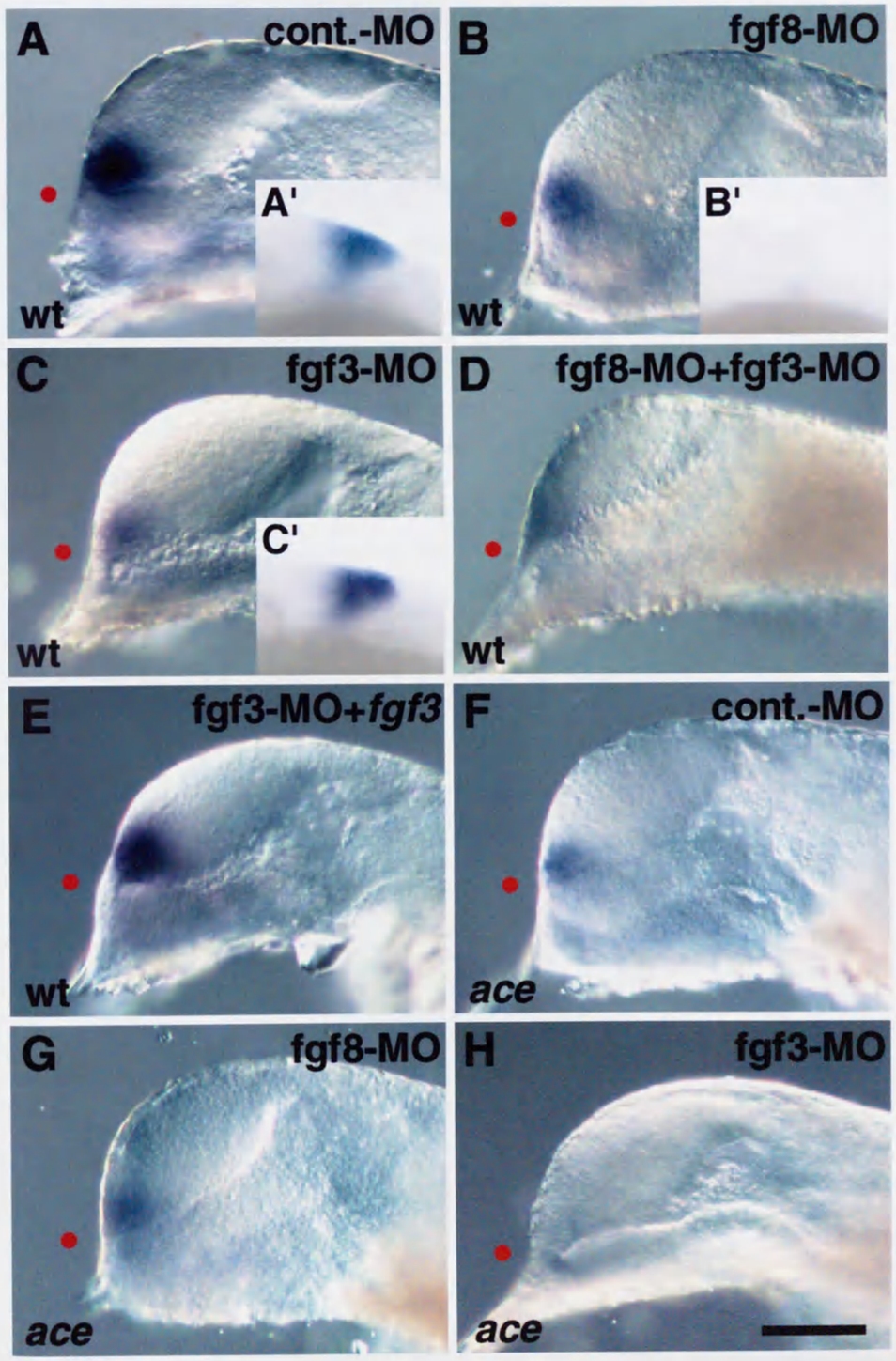
A
cont.-MO
A'
wt
B
fgf8-MO
B'
wt
C
fgf3-MO
C'
wt
D
fgf8-MO+fgf3-MO
wt
E
fgf3-MO+fgf3
wt
F
cont.-MO
ace
G
fgf8-MO
ace
H
fgf3-MO
ace